



저작자표시-비영리-변경금지 2.0 대한민국

이용자는 아래의 조건을 따르는 경우에 한하여 자유롭게

- 이 저작물을 복제, 배포, 전송, 전시, 공연 및 방송할 수 있습니다.

다음과 같은 조건을 따라야 합니다:



저작자표시. 귀하는 원저작자를 표시하여야 합니다.



비영리. 귀하는 이 저작물을 영리 목적으로 이용할 수 없습니다.



변경금지. 귀하는 이 저작물을 개작, 변형 또는 가공할 수 없습니다.

- 귀하는, 이 저작물의 재이용이나 배포의 경우, 이 저작물에 적용된 이용허락조건을 명확하게 나타내어야 합니다.
- 저작권자로부터 별도의 허가를 받으면 이러한 조건들은 적용되지 않습니다.

저작권법에 따른 이용자의 권리는 위의 내용에 의하여 영향을 받지 않습니다.

이것은 [이용허락규약\(Legal Code\)](#)을 이해하기 쉽게 요약한 것입니다.

[Disclaimer](#)

**February 2019**

**Ph.D. Dissertation**

**Structural Basis for a  $\beta$ -lactam  
Resistance by PenL ESBLs from  
*Burkholderia thailandensis***

**Graduate School of Chosun University**

**Department of Biomedical Sciences**

**Thinh-Phat Cao**

**Structural Basis for a  $\beta$ -lactam  
Resistance by PenL ESBLs from  
*Burkholderia thailandensis***

박테리아 *Burkholderia thailandensis* 유래 PenL ESBL 에 의한

beta-lactam 계 항생제 내성의 구조생물학적 성상에 대한 연구

25<sup>th</sup> February 2019

**Graduate School of Chosun University**

**Department of Biomedical Sciences**

**Thin-Phat Cao**

**Structural Basis for a  $\beta$ -lactam  
Resistance by PenL ESBLs from  
*Burkholderia thailandensis***

**Advisor: Prof. Sung Haeng Lee**

*This dissertation is submitted to the Graduate School of  
Chosun University in partial fulfillment of the requirements  
for the degree of Doctor of Philosophy in Science*

**October 2018**

**Graduate School of Chosun University**

**Department of Biomedical Sciences**

**Thinh-Phat Cao**

**This is to certify that the Ph.D.  
dissertation of Tinh-Phat Cao has  
successfully met the dissertation  
requirements of Chosun University**

Chosun Uni.  
School of Dentistry

Prof. Iel Soo Bang



Chosun Uni.  
School of Pharmacy

Prof. Eunae Kim



Uni. of Texas  
at Arlington

Prof. Kwangho Nam



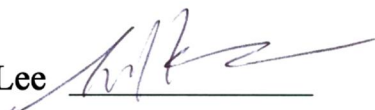
Ulsan National Institute  
of Science and Technology

Prof. Changwook Lee



Chosun Uni.  
School of Medicine

Prof. Sung Haeng Lee



December 2018

**Graduate School of Chosun University**

# Table of Contents

<b>LISTS OF FIGURES</b> .....	<b>iv</b>
<b>LISTS OF TABLES</b> .....	<b>vi</b>
<b>LISTS OF ABBREVIATIONS</b> .....	<b>vii</b>
<b>초록</b> .....	<b>viii</b>
<b>ABSTRACT</b> .....	<b>xi</b>
<b>HIGHLIGHT</b> .....	<b>xiv</b>
<b>I. INTRODUCTION</b> .....	<b>2</b>
1. <i>Burkholderia</i> group.....	2
2. Extended spectrum Pen-type $\beta$ -lactamases (Pen-type ESBLs).....	3
2.1 $\beta$ -lactamase and emergence of extended-spectrum $\beta$ -lactamases (ESBLs).....	3
2.2. Pen-type $\beta$ -lactamase and four novel PenL ESBLs .....	8
Position Cys69 .....	15
Position Asn136 .....	16
Positions Thr171 and Ile173 .....	16
2.3. Objective .....	18
<b>II. MATERIALS AND METHODS</b> .....	<b>20</b>
1. Expression and purification .....	20
2. Crystallization and structure determination .....	21
3. Kinetic parameters determination.....	22
4. Circular dichroism spectra assay .....	25
5. Molecular dynamics simulation.....	25
6. Electrostatic potential calculation.....	26
<b>III. RESULTS AND DISCUSSION</b> .....	<b>28</b>
1. Purification and X-ray crystallography.....	28

1.1. Purification .....	28
1.2. X-ray crystallography .....	29
2. Kinetics study .....	35
2.1. Kinetics property of PenL-WT .....	35
2.2. Biphasic kinetics of PenL-Cys69Tyr and PenL-Asn136Asp.....	37
2.3. Kinetics of PenL-Thr171del and PenL-Ile173del.....	37
2.4. Implication from the distinctions of kinetic property of four PenL ESBL variants .....	38
3. Structural study.....	39
3.1. Circular dichroism (CD) spectra analysis.....	39
3.2. The overall structure of four PenL ESBL variants, Cys69Tyr, Asn136Asp, Thr171del, and Ile173del.....	40
3.3. Structural analysis of PenL-Thr171del and PenLIle173del.....	43
3.3. Structural analysis of PenL-Cys69Tyr.....	50
3.4. Structural analysis of PenL-Asn136Asp.....	54
3.5. Role of Arg104, Tyr105 in substrate recognition .....	61
<b>IV. PERSPECTIVE .....</b>	<b>65</b>
Effects of single mutations on the ceftazidime hydrolysis enhancement of PenL $\beta$ - lactamase .....	65
<i>Single mutations on outside residues influence both <math>\Omega</math>-loop and strands <math>\beta_3\beta_4</math>.....</i>	<i>66</i>
<i>Effect on strand <math>\beta_3\beta_4</math> is more critical than on <math>\Omega</math>-loop in term of CAZ affinity enhancement .....</i>	<i>68</i>
Implication to drug design and medical treatment against <i>Burkholderia</i> pathogens .....	69

<b>V. Appendix 1: Supplementary Data.....</b>	<b>72</b>
<b>VI. Appendix 2: Structural study implies an alternative strategy for the CAZ resistance of <i>Burkholderia thailandensis</i> acquired the PenL variant 165_167delinsPro .....</b>	<b>87</b>
Opinion.....	87
Materials and Methods .....	92
<b>VI. REFERENCES .....</b>	<b>95</b>
<b>ACKNOWLEDGEMENTS .....</b>	<b>122</b>



## LISTS OF FIGURES

Figure 1. Examples of $\beta$ -lactam antibiotics. ....	4
Figure 2. Mechanism for $\beta$ -lactam backbone hydrolysis.....	6
Figure 3. Relationship and similarity of Pen-type with other class A $\beta$ -lactamase families...9	
Figure 4. Diversity at three critical segments of PenL with other class A $\beta$ -lactamases. ....	11
Figure 5. Minimal inhibitory concentration (MIC) of CAZ for <i>B. thailandensis</i> acquired PenL variants.....	13
Figure 6. Positions of four residues Cys69, Asn136, Thr171, and Ile173 on PenL structure .....	14
Figure 7. Stabilization network on $\Omega$ -loop of class A $\beta$ -lactamases represented in PenL. ....	17
Figure 8. Purification of four PenL ESBL variants.....	28
Figure 9. Size-exclusion chromatography of four PenL ESBL variants.....	29
Figure 10. Crystallographic study of four PenL ESBL variants. ....	31
Figure 11. Phasing snapshot for structure determination.....	32
Figure 12. Kinetic study on CAZ hydrolysis of PenL-WT and four ESBL variants. ....	36
Figure 13. CD spectra analysis of PenL-WT and four PenL ESBL variants. ....	40
Figure 14. Essential catalytic ensemble of PenL-WT and four ESBL variants .....	42
Figure 15. Distinction in $\Omega$ -loop of PenL-Thr171del and PenL-Ile173del.....	44
Figure 16. Stabilization network in $\Omega$ -loop of PenL-Thr171del and PenL-Ile173del .....	44
Figure 17. Different conformations of $\Omega$ -loop in PenL-Thr171del upon ligand binding .....	47
Figure 18. Electrostatic property in active site cleft of PenL-WT and PenL-Ile173del.....	48

Figure 19. Modelling dynamic motion of the deletion variants by Ensemble Refinement...	49
Figure 20. Effect of mutation Cys69Tyr on $\Omega$ -loop and strands $\beta 3\beta 4$ .	51
Figure 21. Structural analysis of PenL-Cys69Tyr.	52
Figure 22. Conformational changes in PenL-Cys69Tyr upon ligand binding.	53
Figure 23. Structural analysis of PenL-Asn136Asp.	55
Figure 24. Binding of ligand into active site of PenL-Asn136Asp.	55
Figure 25. Root mean squared deviation (RMSD) of PenL-Asn136Asp during 50 ns simulation	58
Figure 26. Radius of gyration (Rgyr) of PenL-Asn136Asp during 50 ns simulation	59
Figure 27. Root mean squared fluctuation (RMSF) at C $\alpha$ of PenL-Asn136Asp during 50 ns simulation	60
Figure 28. Conformation of PenL-Asn136Asp during 50 ns simulation	60
Figure 29. Role of Arg104 in substrate binding.	63
Figure 30. Appendix: Variation positions in TEM and SHV $\beta$ -lactamases that promote ESBL emergence.	72
Figure 31. Appendix: Minimal inhibitory concentration (MIC) of CAZ for <i>B. thailandensis</i> acquired PenL-165_166delinsPro	88
Figure 32. Appendix: CAZ hydrolysis activity of PenL-165_167delinsPro	89
Figure 33. Appendix: Structural analysis of PenL-165_167delinsPro	90

## LISTS OF TABLES

Table 1. Primary sequence and structural identity of PenL with other class A $\beta$ -lactamases .....	10
Table 2. Crystallization condition for PenL ESBL variants.....	30
Table 3. Data statistics summary for X-ray crystallography of PenL-Cys69Tyr and PenL-Asn136Asp .....	33
Table 4. Data statistics summary for X-ray crystallography of PenL-Thr171del and PenL-Ile73del .....	34
Table 5. Kinetic parameters for CAZ hydrolysis by PenL-WT and four ESBL variants .....	35
Table 6. Appendix: Hotspots of mutation that induce the emergence of ESBLs on TEM and SHV $\beta$ -lactamases.....	73
Table 7. Appendix: Data statistics summary for X-ray crystallography of PenL-165_167delinsPro .....	93

## LISTS OF ABBREVIATIONS

AR	Antibiotic resistance
ESBL	Extended-spectrum $\beta$ -lactamase
CAZ	Ceftazidime, a third-generation cephalosporin
CBA	Ceftazidime-like glyceryl boronic acid
PenL	Pen-type $\beta$ -lactamase from <i>B. thailandensis</i>
PenI	Pen-type $\beta$ -lactamase from <i>B. pseudomallei</i>
MIC	Minimal inhibitory concentration
SEC	Size-exclusion chromatography
CD	Circular dichroism spectra analysis
MD	Molecular dynamics simulation
RMSD	Root mean squared deviation
RMSF	Root mean squared fluctuation
Rgyr	Radius of gyration

## 초록

# 박테리아 *Burkholderia thailandensis* 유래 PenL ESBL 에 의한 Beta-lactam 계 항생제 내성의 구조생물학적 성상에 대한 연구

카오 틴 팻

지도교수: 이성행, Ph.D.

의과대학

조선대학교 대학원

항생제 내성은 병원성 박테리아 감염에 대한 의료 치료에서 가장 심각한 문제이다. 널리 알려진 병원균들은 새로이 개발된 항생제들의 스트레스에서 살아남기 위해 여러 기전들을 발전시켰다. 전 세계적으로 병원균들의 높은 항생제 저항력에 대한 연구는 더욱 효과적인 약물을 개발하기 위한 필요하다. 특히, 세균의 항생제 저항에 대한 분자적메커니즘을 이해 새로운 항생제의 개발과 그에 따른 의료문제 해결에 필수적이라 할 수 있다.

병원균의 항생제 저항성은 흔히 약물 흡수를 줄이고, extended spectrum  $\beta$ -lactamases (ESBL)를 유도하여 약물을 비활성화 시키고, 유출 펌프 작용을 강화하는 등, 대략 세가지 메커니즘을 통해 설명된다. 그러한 메커니즘들 중, ESBL의 출현은 전염병 치료제인  $\beta$ -lactam 항생제와 이 항생제를 분해하는 효소인  $\beta$ -lactamase 의 억제제 때문이다. Penicillin-type, carbapenem-type, and cephalosporin-type 항생제를 포함하는 모든  $\beta$ -lactam 항생제와  $\beta$ -lactamase 억제제는  $\beta$ -lactamases 의 작용을 피하거나 비활성화하도록 설계 되어 있어서,

박테리아 세포벽 생합성을 효과적으로 저해 할 수 있다. 그러나 단일 아미노산의 돌연변이, 즉 단일 아미노산 치환과 삭제에 의해 거대 복합 구조  $\beta$ -lactam 항생제를 가수 분해하는 ESBL 의 출현은 극복해야할 의료적 문제이다. 이러한 단일 돌연변이에 의해 발생한 ESBL 들의 항생제 분해 메커니즘의 원리 연구는 차세대 항생제 개발에 기초적인 지식 기반을 제공할 것이다.

이 논문의 목적은 *Burkholderia* 병원체, 특히 *B. pseudomallei* 유래 ESBL 들의 구조생물학 및 효소동력학 연구를 통해 항생제 내성에 대한 분자적 기전을 규명하는 것이다. *B. pseudomallei* 는 치명적인 전염병인 멜리오이도증 (melioidosis)을 일으키는 그람 음성 병원균이며, *B. pseudomallei* 에 의한 급성 감염은 박테리아의 항생제 저항성 때문에 매우 치명적이다. *B. pseudomallei* 에 대한 치료법은 ceftazidime 와 meropenem 과 같은 몇 가지 강력한  $\beta$ -lactam 항생제로 제한되며 높은 사망률로 유명하다. 따라서 *B. pseudomallei* 에 대한 새로운 약물과 치료 전략을 수립하기 위해서는 세균의 항생제 저항에 대한 메커니즘 이해가 반드시 필요하다. 하지만 이 위험한 병원균에 대한 실험은 또 다른 심각한 문제이다. 다행히 *B. pseudomallei* 의 이상적인 연구 모델로 계놈, 생리학, 면역 반응 특징 면에서 모두 높은 유사성을 지닌 비병원성 *B. thailandensis* 를 이용 할 수 있다. 이와 관련하여 *B. thailandensis* 로부터의 Pen-type  $\beta$ -lactamase, 즉, PenL 이란 단백질이 본 연구에서 조사 대상으로 선택되었다. 4 가지 PenL ESBL 변종 Cys69Tyr, Asn136Asp, Thr171del 및 Ile173del 의 ceftazidime 의 3 세대 cephalosporin 의 가수 분해 능력을 삼차원 PenL ESBL 의 분자구조에 분자동력학 시뮬레이션 및 생체 물리학 데이터와 결합하여 연구 하였다. 본 연구는 이러한 네 가지 돌연변이가 구조적으로 국부적 구조 성분들의 매우 세밀한 변화를 유발하여 기존에 알려진 효소의 기질 결합과 촉매 활성화에 필수적인 세 가지 부분에 영향을 미친다는 것을 발견하였다. 그 결과는 (i) Cys69Tyr 경우, strands  $\beta 3\beta 4$  를 변형시키고 canonical

oxyanion hole 주위의 정전기적 분포를 변경하는 것; (ii) Asn136Asp 돌연변이는  $\Omega$ -loop 유연성을 높임으로써, 연속적인 충돌 효과를 통해  $\beta\beta_4$ 의 유연성을 증폭시킨다; (iii) Thr171del 과 Ile173del 의 경우,  $\Omega$ -loop 를 단축과 유연성을 향상시켜 크기가 큰 기질의 결합을 위한 활성자리의 공간을 확보함을 관찰 하였다. 세 가지 언급 된 영향은 모두 ceftazidime 의 수용을 용이하게 하는 활성 자리의 확대와 그 주위의 아미노산 잔기들의 재배치를 초래한다. 결과적으로, 위 새로운 non-canonical region 에서 일어나는 네 가지 돌연변이에 의하여 생성된 ESBL 효소는, 미세한 내적 구조 성분의 변화를 통하여 돌연변이 효과가 궁극적으로 기질 결합과 촉매반응에 필수적인 부위 ( $\beta\beta_4$ ,  $\Omega$ -loop)에 전해져 3 세대 cephalosporin 인 ceftazidime 에 대한 기질 친화력 증가 및 촉매 효율을 증가시킴을 관찰 하였다.

본 연구결과는 박테리아의 항생제 내성에 대한 메커니즘적 근거를 분자 수준에서 고찰 하였으며,  $\beta$ -lactamase 에 의한 항생제 가수 분해 능력의 증가는 구조상의 미묘한 변화에 의해 촉발될 수 있다. 이러한, 현재까지 보고된 ESBL 의 위치와는 확연히 다른 non-canonical region 및 deletion 에 의한 새로운 ESBL 의 출현은 의학적으로 매우 중요한 의미를 가지며, 다른 병원균에서도 이러한 위치에서의 돌연변이 유래 ESBL 들의 출현이 예상된다. 따라서, 본 연구의 결과는 *Burkholderia* 병원균 및 다른 병원균의  $\beta$ -lactamase 억제제 개발 전략에서 새로이 고려 되어야 할 기초지식을 제공 한다.

## ABSTRACT

### **Structural Basis for a $\beta$ -lactam Resistance by PenL ESBLs from *Burkholderia thailandensis***

Thinh-Phat Cao

Advisor: Prof. Sung Haeng Lee, Ph.D.

Department of Biomedical Sciences

Graduate School of Chosun University

Antibiotic resistance is the most severe problem in medical treatment against the pathogenic infection. Notorious pathogens, e.g. *Klebsiella pneumoniae*, *Acinetobacter baumannii*, *Burkholderia pseudomallei*, etc., have evolved several types of machinery to survive under the pressure of innovative antibiotics. The high rate of antibiotic resistance on the world has required more endeavors to discover effective drugs used in the treatment against those pathogens. Understandings the molecular basis of the resistance have, therefore, emerged as critical first step to address the issue, and ultimately improve the public health care.

Common observed mechanisms of the antibiotic resistance in pathogens include: reduction of drug uptake; modification drug target; inactivation of drug by inducing the extended spectrum  $\beta$ -lactamases (ESBLs); and enhancement of action of efflux pump. Among these mechanisms, the emergence of ESBLs is the most widespread due to the common use of  $\beta$ -lactam antibiotics and  $\beta$ -lactamase inhibitors as the first-line in infectious disease treatment. All of the  $\beta$ -lactam antibiotics and  $\beta$ -lactamase inhibitors, including penicillin-type, carbapenem-type, and cephalosporin-type have been designed to avoid and/or to inactivate the action of  $\beta$ -lactamases, so that the drugs can effectively attack the transpeptidase enzymes which involved in bacterial cell wall biosynthesis.



However, bacteria have evolved their ESBLs, which can hydrolyze the novel  $\beta$ -lactam antibiotics which have large size and complex substituent branches, and escape from antibiotic-like inhibitors. Interestingly, emergence of ESBLs can be triggered by single amino acids mutations on the wild-type  $\beta$ -lactamase, i.e., substitution and deletion. The mechanistic principle for the effect of such single mutations on the enhancement of drug hydrolysis by  $\beta$ -lactamase should be thoroughly investigated to underlie the basis for drug resistance, which is necessary for next-generation drug innovation.

The objective of this thesis is to elaborate the mechanistic basis of antibiotic resistance of *Burkholderia* pathogens, especially *B. pseudomallei*, at the molecular level through structural and kinetic studies. *B. pseudomallei* is a Gram negative pathogen which causes the melioidosis, a fatal infectious disease. Despite being relatively rare among the notorious pathogens, acute infection of *B. pseudomallei* is a significant threat due to its complicated intrinsic resistance to the common  $\beta$ -lactam antibiotics. Therapy for treatment against *B. pseudomallei* is largely restricted to a few strong  $\beta$ -lactam antibiotics such as ceftazidime and meropenem. However, the treatment is very easy to fail with high mortality rate. In order to develop novel drugs and medical treatment strategies against *B. pseudomallei*, the comprehension on the mechanistic basis for the resistance of the bacterium is certainly required. However, experimenting with this dangerous pathogen is another serious problem. For the reason, the non-pathogenic *B. thailandensis* which has high similarity in both genome, physiology, and immune response characteristics has been used as research model for *B. pseudomallei*. With the regards, the Pen-type  $\beta$ -lactamase from *B. thailandensis*, i.e., PenL, is chosen to investigate in this study. The hydrolysis ability of ceftazidime, a third-generation cephalosporin, of four PenL ESBL variants Cys69Tyr, Asn136Asp, Thr171del, and Ile173del is discussed based on their kinetic parameters and high-resolution structures, in combination with molecular dynamics simulation and biophysical characterization. Our researches demonstrate that although the four mutations occurred at non-catalytic and non-substrate-binding sites, they can trigger the subtle rearrangements on the local configuration, which consequently influence the three critical catalytic

segments of the enzyme. These effects include (i) distorting the strands  $\beta 3\beta 4$  and altering the electrostatic distribution around the canonical oxyanion hole (Cys69Tyr); (ii) enhancing the flexibility of  $\Omega$ -loop to boost the fluctuation of strands  $\beta 3\beta 4$  via serial steric conflicts (Asn136Asp); and (iii) shortening the  $\Omega$ -loop to increase both the space for substrate binding and the flexibility of  $\Omega$ -loop *per se* (Thr171del and Ile173del). As a result of these effects, the active site cleft of the enzyme is enlarged and rearranged to facilitate the accommodation of ceftazidime. As a consequence, the affinity toward ceftazidime of the mutated enzymes is augmented to give rise to their catalytic efficiency, thus far explaining for the biological advantage of these ESBLs in term of ceftazidime resistance of *B. thailandensis*.

Our findings underlie the mechanistic basis for the antibiotic resistance of bacteria at the atomic level. The increase in antibiotic hydrolysis ability can be triggered by any subtle change in the structure of  $\beta$ -lactamase that affects the critical segments. The emergence of ESBLs, therefore, can be induced by mutations any unanticipated single amino acids regardless of position, i.e. single the mutations occur at non-canonical regions. Our data also provide insights that may implicate the strategy for the development of a novel  $\beta$ -lactamase inhibitor, e.g. an inhibitor with extra negative branches, which can be used in combination with ceftazidime to improve the effectiveness of treatment against *Burkholderia* pathogens.

## HIGHLIGHT

*B. thailandensis* is the research model for pathogens in *Burkholderia* groups (*B. pseudomallei*, *B. mallei*, *B. cenocepacia*, etc.) that cause melioidosis, glanders, respiratory infection, etc.

*Purposes of this thesis:* To understand the effect of single mutations at non-catalytic and non-substrate binding residues that promote the substrate spectrum extension of PenL  $\beta$ -lactamase: Cys69Tyr and Asn136Asp, Thr171del and Ile173del.

# **I. INTRODUCTION**

# I. INTRODUCTION

## 1. *Burkholderia* group

*Burkholderia* group comprises of several opportunistic nosocomial gram-negative pathogens which, for instances, notoriously cause respiratory infections (*B. multivorans*, *B. cenocepacia*), glanders (*B. mallei*), and melioidosis (*B. pseudomallei*) [1, 2]. Specifically, *B. pseudomallei* infects to human through inhalation, ingestion, or skin penetration of contaminated soil or groundwater, leading to a wide range of clinical outcomes including asymptomatic state, or clear symptoms such as pneumonia, skin abscess, and highly fatal bacteremia. Moreover, melioidosis caused by *B. pseudomallei* infection can be in latency state up to decades before outbreak [3]. *B. mallei* and *B. pseudomallei* are also listed as biological weapons [1].

Notably, *Burkholderia* pathogens intrinsically resist to common antibiotics such as ampicillin or carbenicillin [4-6], making it difficult for medical treatment. The drug choice for *Burkholderia* pathogens is thus restricted to a few strong antibiotics such as ceftazidime (third-generation cephalosporin) or meropenem (carbapenem) [6, 7]. The antibiotic resistance factors from those species have been identified to include class A Pen-type  $\beta$ -lactamases, quorum sensing, signal transduction systems [5, 8, 9]. Among these factors, the mutations on Pen-type  $\beta$ -lactamases are reported the most prominent resistance factor.

Because of the risk of infection, experiments that carried out on *B. pseudomallei* and other pathogens in *Burkholderia* groups require stringent protocols, leading to difficulties and limits when studying the treatment and prevention methods. In 1998, Brett *et al.* discovered a soil saprophyte named *B. thailandensis* E264, which has close similarity in 16S rRNA with *B. pseudomallei* [10]. The genomes of both strains conserve in 85% and are highly syntenic [11, 12]. On the other hand, *B.*

*thailandensis* is not an opportunistic pathogen. Therefore, *B. thailandensis* is being considered as a good model for researching in *B. pseudomallei*, as well as other species in *Burkholderia* groups in some specific proteins due to their high similarity [13-15]. Based on these reasons, this thesis is centered on the single mutations on a Pen-type  $\beta$ -lactamase from *B. thailandensis*, PenL, and their biochemical and structural characterization.

## 2. Extended spectrum Pen-type $\beta$ -lactamases (Pen-type ESBLs)

### 2.1 $\beta$ -lactamase and emergence of extended-spectrum $\beta$ -lactamases (ESBLs)

$\beta$ -lactam is one of largest classes of antibiotic (the other classes are aminoglycoside, macrolide, and fluoroquinolone) and encompasses approximately 55% of all antibiotics currently circulated [16].  $\beta$ -lactams target to the bacterial cell wall integrity by inhibiting the biosynthesis of peptidoglycan layer.  $\beta$ -lactam is comprised of three basic types, in which the square  $\beta$ -lactam ring may be fused with another five-member ring, i.e. penicillin and carbapenem, or six-member ring, i.e. cephalosporin (Figure 1). Based on the basis of these types,  $\beta$ -lactam drugs can be developed by varying the substituent groups R, R1, R2, and R3. In addition, Aztreonam is the only one monobactam that is currently circulated (Figure 1). Extensive use of  $\beta$ -lactam antibiotics has accelerated the selective process triggering the evolution of one important class of enzyme in the field of antibiotic resistance:  $\beta$ -lactamase, EC 3.5.2.6. Interestingly, the first  $\beta$ -lactamase, penicillinase in *E. coli*, was discovered in 1940 by Abraham and Chain[17], even before the first  $\beta$ -lactam antibiotic, penicillin, was clinically used two year subsequent[18]. Noted that another class of  $\beta$ -lactam drugs is also invented, namely  $\beta$ -lactamase inhibitor (Figure 1). These drugs act as suicide substrates that can react an stick permanently in the enzyme active site [19].

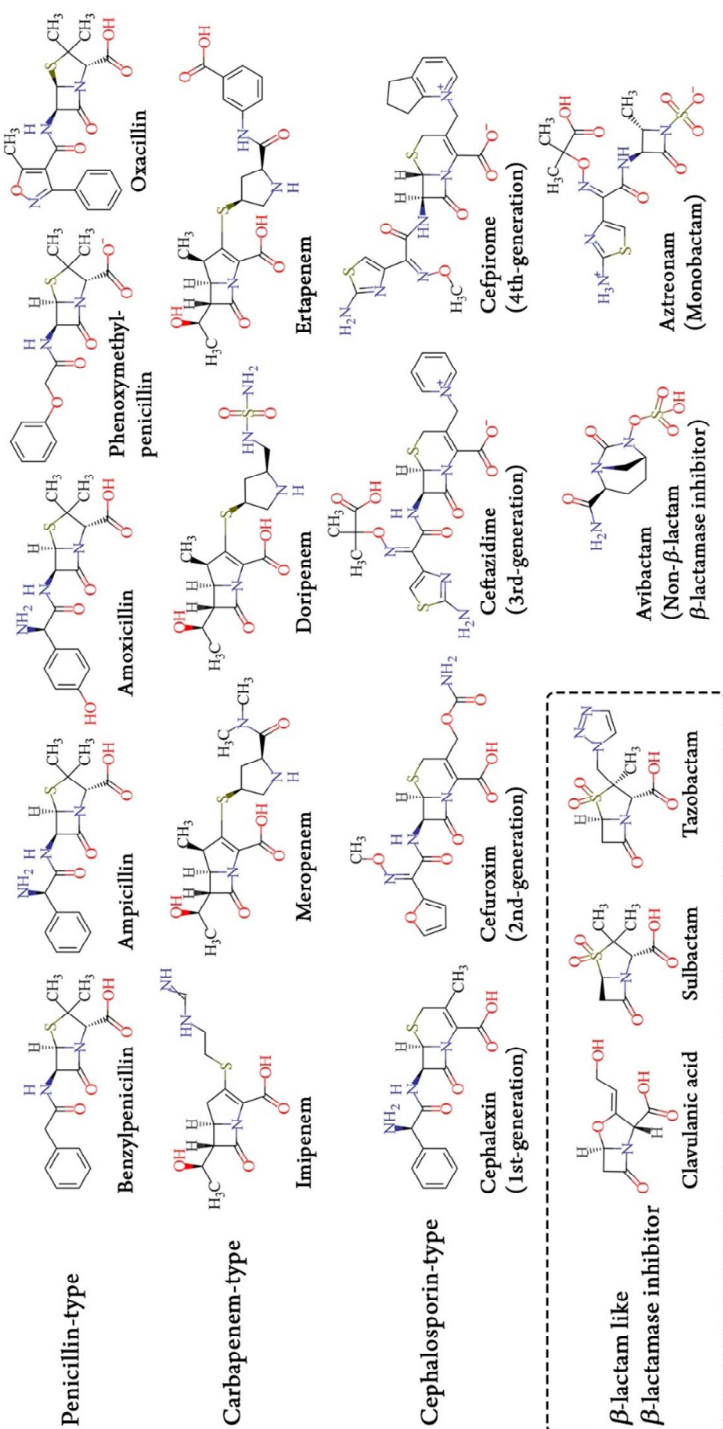


**Figure 1. Examples of  $\beta$ -lactam antibiotics.**

Avibactam, a novel non- $\beta$ -lactam  $\beta$ -lactamase inhibitor is also shown.

The enzyme  $\beta$ -lactamase hydrolyzes the amide bond, opens the  $\beta$ -lactam ring thus inactivates the effect of the drug. In an effort to characterize the enzyme which exclusively emerges in bacteria, several classification strategies for  $\beta$ -lactamase have been suggested. One of them, the functional classification scheme separates  $\beta$ -lactamases into several groups based on their special activity exhibition toward specific substrates and inhibitors [20, 21]. This scheme, however, has not been sufficiently elaborated so far. The most common scheme based on their amino acid sequence was suggested by Ambler *et al.*, 1980 [22, 23]. Originally, Ambler specified two classes: class A or serine  $\beta$ -lactamase which harbors a reactive serine residue in its active site, and class B or metallo- $\beta$ -lactamase which employs divalent metal ion (usually  $Zn^{2+}$ ) for its activity [22]. Later, two new classes of serine  $\beta$ -lactamase, class C and class D, were supplemented [24, 25]. The  $\beta$ -lactam hydrolysis mechanisms catalyzed by four classes are slightly different, yet those of classes B, C, and D are beyond the scope of this thesis.

Structure and functional amino acids of class A  $\beta$ -lactamases were well described for more than 30 years. Originated from the same ancestral protein with penicillin-binding protein, serine  $\beta$ -lactamases possess the catalytic mechanism that is similar to the serine protease. Within class A, three subclasses dominate as TEM/SHV (penicillinase), PER/OXA/TOHO (cephalosporinase), and CTX-M (carbapenamase). While sharing high structural similarity, those subclasses are slightly diverse in active site cleft to adapt their preferential substrates (see more in Figure 3, next section).

The overall structure of class A  $\beta$ -lactamases can be separated into two major compartments: the conserved catalytic ensemble and the variable recognition ensemble. The conserved catalytic ensemble consists of the reactive Ser70 which attacks the  $\beta$ -lactam amide bond; two general bases Lys73 and Glu166 which electrostatically activate the nucleophilic Ser70; the typical oxyanion hole formed by N atoms of Ser70 and Thr237 which stabilizes the negative transient acyl-intermediate;



the hydrolytic water coordinated to Glu166 and Asn170 which disrupts the acyl-bond; and several of amino acids involved in the  $\beta$ -lactam backbone orientation and proton shuttle including Asn132, Thr235, Gly236, Thr237, and Ser130 (Figure 2, and see more in Figure 10A, *Results and Discussion*) [19, 26, 27]. The catalytic ensemble is strictly conserved.

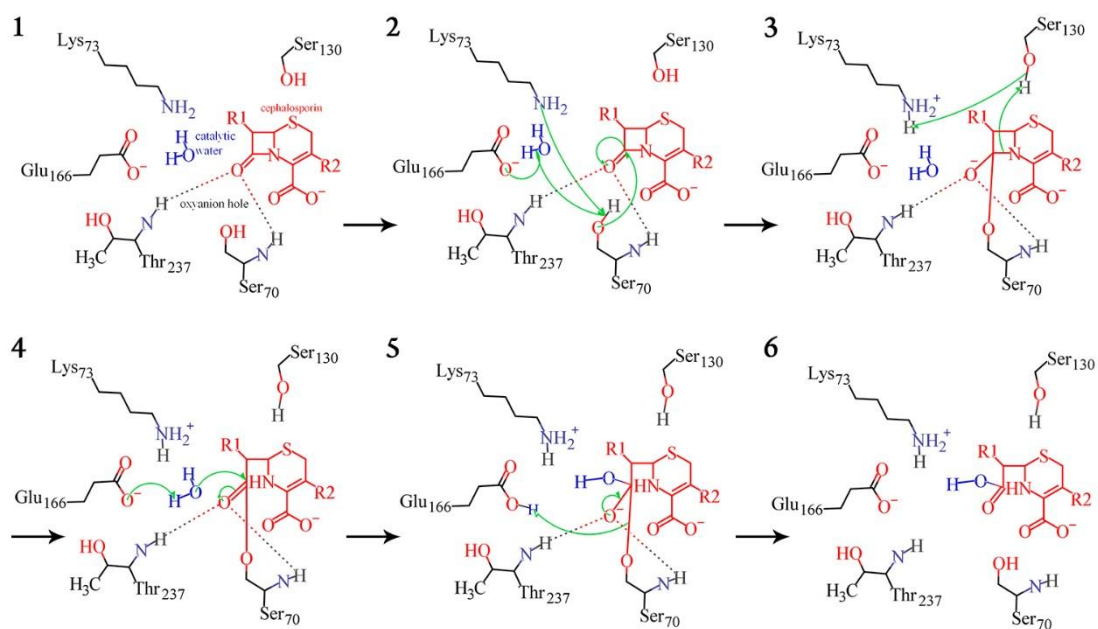


**Figure 2. Mechanism for  $\beta$ -lactam backbone hydrolysis**

(1) The carbonyl of  $\beta$ -lactam is stabilized by the typical oxyanion hole formed by the N atoms of Ser70 and Thr237. (2) Ser70 can be either activated by two ways: (i) by Lys73 or (ii) by the catalytic water which is formerly activated by Glu166; in turn, the nucleophilic Ser70 attacks the amide bond of  $\beta$ -lactam forming the acyl-enzyme complex. (3) A proton shuttle is initiated starting from  $\beta$ -lactam to Ser130 then to Lys73. (4) Glu166 abstracts a proton from the catalytic water, which in turn interrupts the acyl bond. (5) The activated catalytic water is added across the acyl-bond, the deacylation is finally carried out by Glu166. (6) The inactivated  $\beta$ -lactam is released from the enzyme active site.

On the other hand, the recognition ensemble is responsible for the adaptability toward different substrate types. Upon the innovation of drugs, the residues in this ensemble are further varied to adopt alternative recognition modes that facilitate the accommodation of novel substrates with extra complex substituent groups. Extensive use of  $\beta$ -lactam antibiotics has accelerated the selective process triggering the evolution of one important class of enzyme in the field of antibiotic resistance:  $\beta$ -lactamase, EC 3.5.2.6. Interestingly, the first  $\beta$ -lactamase, penicillinase in *E. coli*, was discovered in 1940 by Abraham and Chain [17], even before the first  $\beta$ -lactam antibiotic, penicillin, was circulated in clinical use two year subsequent [18]. Through these alterations, the extended-spectrum  $\beta$ -lactamases (ESBLs) were emerged. In most cases, the variations took place in three critical regions, which are placed surrounding, or a part of the catalytic ensemble: lid (92-118),  $\Omega$ -loop (160-180), and strands  $\beta$ 3- $\beta$ 4 (230-251) [14, 28-32] (the summary of ESBL variations found in the two most popular types of class A  $\beta$ -lactamase, TEM and SHV, is available at <https://www.lahey.org/Studies/> and is also tabulated in Appendix 1 Table 6).

The first ESBL was reported in 1979 by Sander and Sander Jr. which described a case of cefamandole resistance, a second-generation cephalosporin, in *Enterobacteriaceae* species [33]. Afterward, a number of cases of ESBL emergence cases have been reported and have become the most serious problem in medical treatment against pathogenic infectious diseases due to their major responsibility in the resistance against the latest innovative antibiotics. Up until now, although the categorical system has yet developed for their thorough clarification, two types of the “historical term” ESBL have commonly discussed based on the type of drug they confer the resistance. The first type is the mutated  $\beta$ -lactamases that are able to hydrolyze the broad- to extended-spectrum  $\beta$ -lactam antibiotics such as amoxicillin, ceftazidime, cefotaxime, imipenem, etc. The second type, of which the mutations occur to reduce the ligand binding affinity of  $\beta$ -lactamase, can preclude the inactivation effect of  $\beta$ -lactamase inhibitor drugs such as clavulanic acid, tazobactam, avibactam, etc. The

emergence of these ESBL types has led to the idea for the efficient recipe in the treatment: a combination of a  $\beta$ -lactam antibiotic and a  $\beta$ -lactamase inhibitor. A famous example for this recipe is amoxicillin-clavulanic acid, also known as Augmentin which was invented from 1979 by British pharmaceutical company Beecham (now part of GlaxoSmithKline), has been being prevalently used around the world as the first-line in regimen of treatment against a wide range of bacterial infection. In 2015, another combination has been circulated, i.e. ceftazidime-avibactam (Figure 1), approved by US Food and Drug Administration under brand the name Avycaz and by European Medicines Agency with the name Zavicefta, to treat the infection from the multi-drug resistance gram-negative pathogens [34-37]. Unfortunately, the resistance against the combination ceftazidime-avibactam has already been reported even while the efficacy and effectiveness of the drugs are still under examination [38-40]. The rapid evolution of bacteria is therefore an enormous challenge for the scientists on the race to combat the infectious diseases.

## **2.2. Pen-type $\beta$ -lactamase and four novel PenL ESBLs**

Pen-type  $\beta$ -lactamase is less common than the other three dominant class A family enzymes. The term “Pen” was named for this family because of its natural penicillinase activity. Pen-type  $\beta$ -lactamase is the major factor for the resistance of *Burkholderia* pathogens. Phylogenetic diversity of Pen-type respect to the other class A family has not been profoundly analyzed so far. In an attempt to clarify the locus of Pen-type among class A  $\beta$ -lactamases, amino acid sequences of several Pens from *Burkholderia* pathogens and PenL (*B. thailandensis*) were aligned to the representatives from the other subclasses. The phylogenetic tree portrayed in Figure 3 demonstrates the utmost close distance of PenL with other Pens, especially with PenI (*B. pseudomallei*, 89% identity) and PenK (*B. mallei*, 89% identity), which has two implications for the present thesis. First, the high similarity of PenL to other Pen family enzymes implied the high relevance of this study to the understanding of

other Pen-type  $\beta$ -lactamases. Particularly, the vicinity of Pens with the notorious ESBLs such as Toho-1, CTX-M-15 asserts their structural and functional kinship. Second, the relative apart distance of Pens in respect to TEM-1 and SHV-1 suggests that Pens is possibly classified in an independent family.

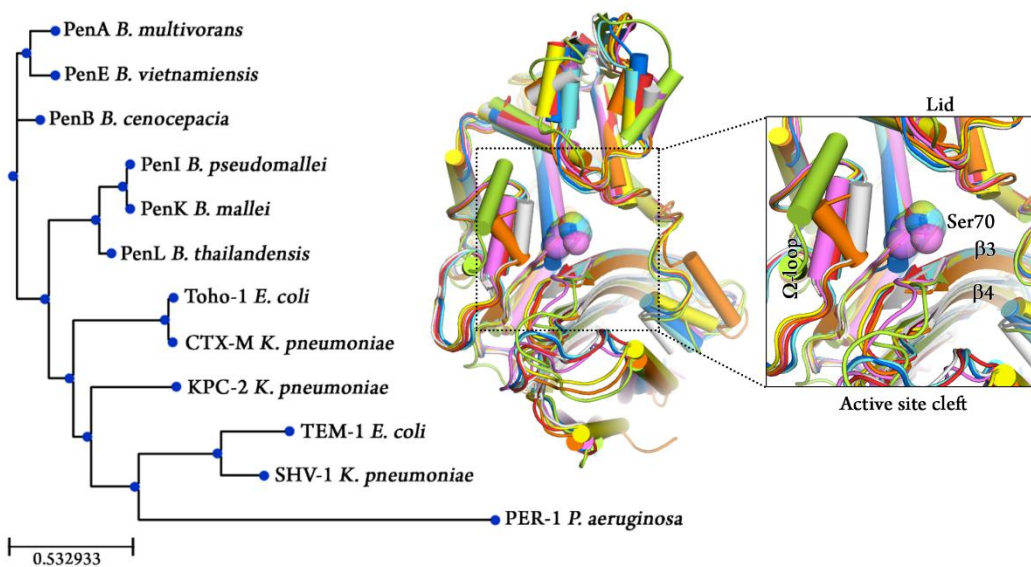


**Figure 3. Relationship and similarity of Pen-type with other class A  $\beta$ -lactamase families.**

LEFT, phylogenetic tree demonstrates the relationship of Pen-type with SHV, TEM, CTX-M, TOHO, KPC-2, and PER-1 types of class A  $\beta$ -lactamase. RIGHT, superposition of PenL (white, PDB ID: 5GL9[41]) and PenI (red, 3W4P[27]) with other class A  $\beta$ -lactamases including SHV-1 (orange, 1SHV[42]), TEM-1 (yellow, 1M40[43]), CTX-M-15 (cyan, 4S2I[44]), Toho-1 (blue, 1IYO[45]), KPC-2 (pink, 5UJ3[46]), and PER-1 (green, 1E25[47]). The reactive Ser70 is depicted with spheres. The inset shows the magnified active site cleft of the enzymes in which the position of three critical segments are indicated.

The structures of PenL[41], PenI[27], as well as other class A  $\beta$ -lactamase representatives such as TEM-1[43], SHV-1[42], CTX-M-15[44], Toho-1[45], KPC-2[46], and PER-1[47] have been determined. To portray an overall picture in term of structural similarity of Pen-type with the others, those class A  $\beta$ -lactamases are superimposed (Figure 3, Right panel). The structural alignment shows that PenL is almost identical with the others, expressed by the RMSD at C $\alpha$  atoms that shown in Table 1 below.

**Table 1. Primary sequence and structural identity of PenL with other class A  $\beta$ -lactamases**

	PDB ID	Primary sequence identity (%)	Root mean square deviation (RMSD) (Å)
PenI	3W4P	89	0.294
SHV-1	1SHV	81	0.723
TEM-1	1M40	81	0.379
CTX-M-15	4S2I	54	0.563
Toho-1	1IYO	54	0.473
KPC-2	5UJ3	55	0.594
PER-1	1E25	26	0.956

Despite the overall similarity of the structure, the active site cleft is marginally different among the enzymes (Figure 3), suggesting that the functionality and substrate specificity of the class A  $\beta$ -lactamases are varied by subtle changes in the space of binding cleft. In particular, as demonstrated in the same figure, the variations are pronounced at  $\Omega$ -loop, lid, and strands  $\beta_3\beta_4$ , where the C $\alpha$  backbones fluctuate conspicuously. These fluctuations may alter the binding cavity, which in turn alter the ability of the enzyme for the accommodation of different types of substrate. This structural aspect has been discussed previously [48, 49]. In case of PenL, the amino acid motif on strand  $\beta_3$  is

235-TGTG\_D-240, where the position 237 is occupied by a threonine while no amino acid dwells in position 239, according to the Ambler numbering system. Since the N atom of the residue Xaa237 constitutes oxyanion hole that stabilizes the tetrahedral intermediate of the substrate, the diversity in side chain at this position and its neighbor, position 236, may correlate with the variation in substrate specificity of class A  $\beta$ -lactamase [50-52]. These two positions are thus prominently varied (Figure 4). Another distinctive features are the acidic residue at Ambler position 104 on TEM-1 and SHV-1, which is displaced by a basic residue, i.e., arginine, on Pens (Figure 4). This basic residue provides the inherent recognition for the enzyme toward oxymino-cephalosporin like ceftazidime (CAZ), apparently contributes to the intrinsic resistance to CAZ of *Burkholderia* bacteria. The role of Arg104 in PenL will be discussed further in *the Results and Discussion* section.

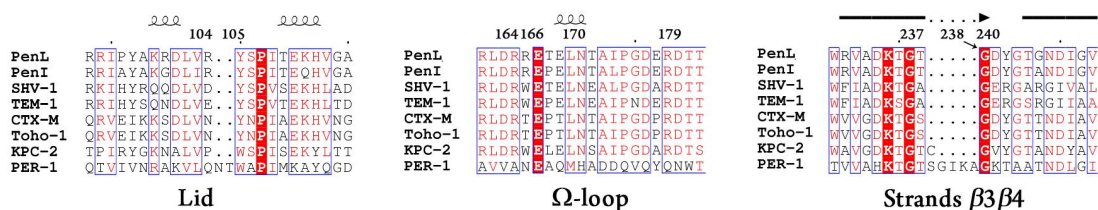


**Figure 4. Diversity at three critical segments of PenL with other class A  $\beta$ -lactamases.**

LEFT, the lid contains two important residues involved in substrate recognition and binding, 104 and 105. Position 105 is always occupied by an aromatic residue that stabilizes the substrate *via*  $\pi$ -anion interaction, whereas position 104 is considerably variable to alter substrate specificity. CENTER, two positions Glu166 and Asn170 on  $\Omega$ -loop are strictly conserved among class A  $\beta$ -lactamases, except for the role of Asn170 is displaced by Gln176 in PER-1. Position 167, which links to Glu166 by a *cis*-peptide bond (except for PER-1), is also diverse so that the absence of proline at this position may imply the more flexible  $\Omega$ -loop. Two positions Arg164 and Asp179 form the interaction network that stabilizes the  $\Omega$ -loop, so that these are two hotspots for the emergence of ESBLs. RIGHT, position 237, of which the N atom contributes to the typical oxyanion hole formation, is adaptable in the side chain to confer the substrate specificity alteration. Mutation at position 240 also grants the cephalosporin hydrolysis capacity to CTX-M-type  $\beta$ -lactamases. Position 239 is lacked in all the representative enzymes.

As described above, the medical treatment against *Burkholderia* pathogens is restricted to a few antibiotics, in which the first-line of treatment regime may be immediately prescribed with the third-generation cephalosporin, ceftazidime (CAZ) [5, 6, 53]. However, upon the CAZ treatment, the primitive Pens have been selectively modified to improve the hydrolysis capacity. For instance, PenI variant Cys69Tyr is frequently isolated from the melioidosis patients infected by *B. pseudomallei* [54, 55]. Alternatively, the simulated selection experiment on *B. thailandensis* also gave some mutations on PenL that confer CAZ hydrolysis augmentation, most of them occurred at  $\Omega$ -loop, including tandem repeats [15], substitutions [14], and deletions [14, 56]. The structural basis for CAZ hydrolysis capacity of PenL by tandem repeat mutations on  $\Omega$ -loop was studied previously underlying the role of increased flexibility of  $\Omega$ -loop in substrate spectrum extension of PenL [41]. Nonetheless, the molecular effects of single substitutions and deletions at non-catalytic residues, i.e., Cys69Tyr/Phe, Asn136Asp/Lys, Thr171del and Ile173del, are not disclosed, even if Cys69Tyr variant is well-known. Figure 5 shows the extremely high minimal inhibition concentration (MIC) values of CAZ treated on *B. thailandensis* which acquired single mutations on PenL at four positions: Cys69, Asn136, Thr171, and Ile173.

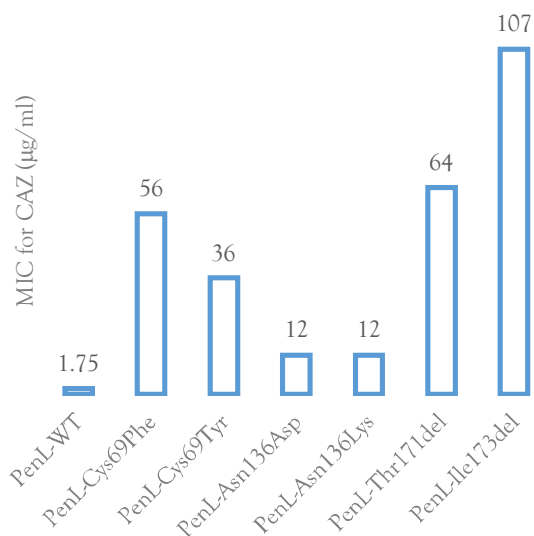


**Figure 5. Minimal inhibitory concentration (MIC) of CAZ for *B. thailandensis* acquired PenL variants**

Data adapted from Yi et al., 2012 [14] and Hwang et al., 2014 [56]

Due to the unusual locations of the mutations and the need to develop new strategy for drug design and medical treatment, the molecular mechanism for the CAZ hydrolysis augmentation by these single mutations has attracted. For the reasons, the four single mutations on PenL, Cys69Tyr, Asn136Asp, Thr171del, and Ile173del, are the focus of this thesis. In what follows, the structural basis for those single mutations in the enhancement of CAZ hydrolysis of PenL is discussed in details.



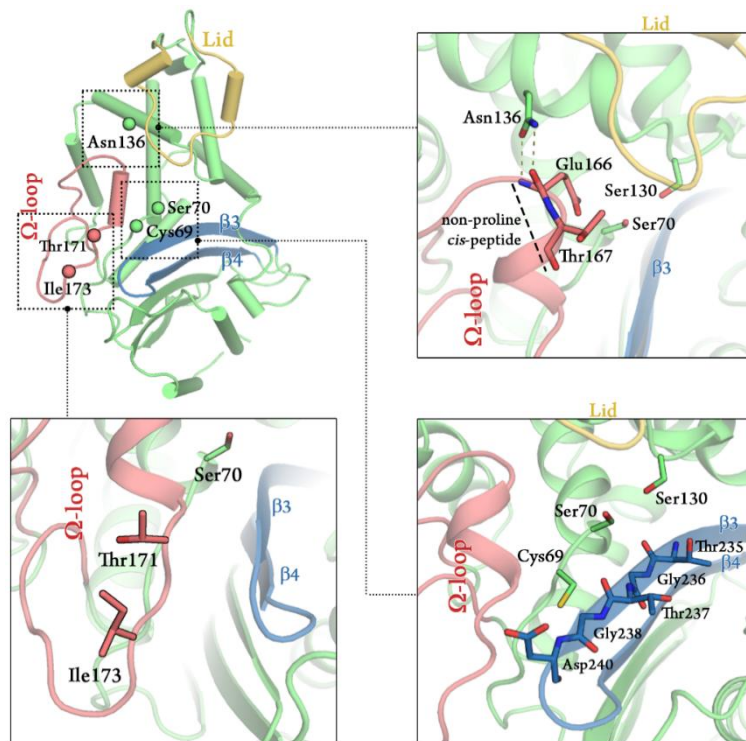


**Figure 6. Positions of four residues Cys69, Asn136, Thr171, and Ile173 on PenL structure**  
 UP LEFT, overall structure of PenL  $\beta$ -lactamase (wild-type). Three critical segments are colored in deep-salmon ( $\Omega$ -loop), yellow-orange (lid), and sky-blue (strands  $\beta_3\beta_4$ ). Four positions Cys69, Asn136, Thr171, and Ile173, are depicted with spheres. UPPER RIGHT, residue Asn136 stabilizes the energetically unfavorable non-proline *cis*-peptide Glu166-Thr167. DOWN LEFT, residues Thr171 and Ile173 are located on  $\Omega$ -loop but direct out from active site cleft. LOWER RIGHT, residue Cys69 situates adjacently to the reactive Ser70 but confronts the strands  $\beta_3\beta_4$  and does not directly participate in substrate binding or catalysis.

## **Position Cys69**

Being adjacent to the reactive Ser70, the Ambler position 69 plays a vital role in substrate specificity of class A  $\beta$ -lactamase families. In 2009, the first case of the variant Cys69Tyr on PenI  $\beta$ -lactamase was reported to be responsible for the resistance to CAZ of *B. pseudomallei* that infected to a male patient [54]. Soon after, the same mutation was once again isolated in a representative melioidosis patient who was also treated with CAZ [55]. Even before, many reports on other class A  $\beta$ -lactamase families, including, SHV- and TEM-types have already pointed out the potential role of position 69 in substrate specificity. Wherein, the substitution of Met69 into Tyr, Phe, or Lys in those  $\beta$ -lactamases has increased their CAZ hydrolysis activity, while the replacement with Ile, Leu, or Val has resulted in  $\beta$ -lactamase inhibitor resistance [57-60]. It should be emphasized that the position 69 is never directly involved in substrate binding or recognition, due to the inherent geometry of this residue on the peptide sequence. In other words, because the reactive Ser70 has to confront the substrate, the adjacent residue at position 69 must face to another direction. Indeed, in all structures of class A  $\beta$ -lactamases determined so far, the residue at position 69 faced toward the strands  $\beta 3\beta 4$  (Figure 6, lower right panel). While this is true, several structural and kinetics studies suggested that such substitutions on Met69 may disrupt, or perturb the oxyanion hole of active site [58, 61, 62].

Nevertheless, this suggestion is not fully confirmed and remain controversial. Notably, those studies were unable to address the effect of substitution from Cys69 into bulky Tyr or Phe in case of Pen-type  $\beta$ -lactamase, in both physical (size) and chemical (the displacement of functional group in side chain) properties. Most importantly, the lack of high-resolution structure restricted the full explanation of the mechanistic basis for the mutation in this position.

### ***Position Asn136***

Until now, Asn136 has not been reported as a potential target for the emergence of ESBLs in class A  $\beta$ -lactamase. Located on helix  $\alpha_4$ , Asn136 plays its role in the stabilization of  $\Omega$ -loop by forming hydrogen bonds with the backbone of Glu166 (Figure 6, upright panel). Notice that on the one hand, Glu166 is the critical catalytic residue (Figure 2), on the other hand in many cases of class A  $\beta$ -lactamases, the backbone linkage between Glu166 and Xaa167 (Thr167 in PenL) is an energetically unfavorable non-proline *cis*-peptide (Figure 4). Asn136 is thus crucial for the proper functional orientation of Glu166. The loss of activity of a class A  $\beta$ -lactamase due to the lack of asparagine at position 136 (by replacing with an alanine) was previously reported [63]. Thus far, the increase in CAZ hydrolysis ability by the substitution of Asn136 into aspartate or lysine in PenL is of a particularly interesting question.

### ***Positions Thr171 and Ile173***

Likewise Asn136, the two positions 171 and 173 have not been identified as potential mutation sites for ESBL induction. These two positions are located on  $\Omega$ -loop, which has been mentioned frequently in term of ESBLs due to its critical role in both catalysis and substrate recognition. The enhancement of the flexibility of  $\Omega$ -loop was proved to alter the substrate specificity, therefore, trigger the emergence of ESBLs. The tandem repeat on  $\Omega$ -loop of PenL as was cited above is one of the instances.

Another example is the Pro167Ser substitution, which occurs in CTX-M  $\beta$ -lactamases [64] and PenI [65]. As was also stated, the linkage between Glu166-Xaa167 is always a *cis*-peptide, so that the presence of proline at position 167 certainly alleviates the movement of  $\Omega$ -loop. Hence, the replacement of this proline inevitably results in disruption of this stabilization. Another typical example is the mutation at Arg164, which constitutes a significant part of the interaction network

that stabilizes the  $\Omega$ -loop, including Arg164-Asp179-Xaa171 (Figure 4, 7). Arg164, and sometimes Asp179, are two hotspots for ESBL induction in TEM and SHV  $\beta$ -lactamases (see more at <https://www.lahey.org/Studies/>), in which the single substitution at one of these two sites breaks down the interaction network leading to an increased flexibility of  $\Omega$ -loop. As further shown in Figure 7, Thr171 in PenL is also hydrogen bonded to Arg164, implying that any single substitution at Thr171 which disrupts this interaction may lead to the same outcome.

Nonetheless, the occurrence of PenL ESBL has been acquired by the single deletion of Thr171. In fact, deletion of the amino acid is not a common evolutionary strategy in living things because it may affect the integrity of the protein. In this case, the deletion of Thr171 indeed resulted in the shortening of  $\Omega$ -loop, raising a question on how this mutation leveled up the CAZ hydrolysis activity of the enzyme.

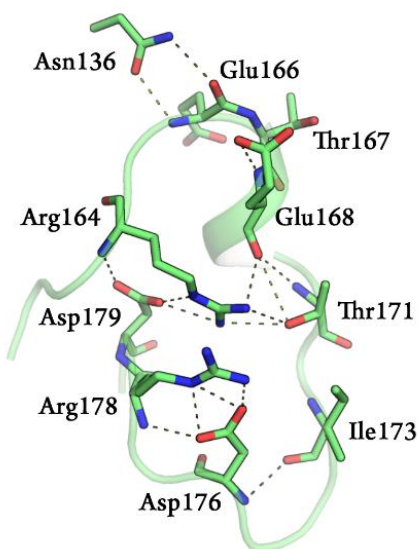


**Figure 7. Stabilization network on  $\Omega$ -loop of class A  $\beta$ -lactamases represented in PenL.**

Position Asn136 stabilizes the non-proline *cis*-peptide between Glu166-Thr167. Arg164 and Asp179 intrinsically play a significant role in maintaining the steadiness of  $\Omega$ -loop thus far are two hotspots for induction of ESBLs in class A  $\beta$ -lactamases.

A similar question also arises in the case of Ile173. This residue, despite being located on  $\Omega$ -loop, is always exposed to the surface and merely interacts with Asp176 *via* a backbone atom hydrogen bond (Figure 7). Moreover, Ile173 never participates to catalysis or substrate recognition. Therefore, the increase in CAZ hydrolysis of PenL-Ile173del is intriguingly and may implicate the intimidation of the ESBL emergence that is triggered by single non-catalytic residue mutations.

### 2.3. Objective

In an attempt to understand the mechanistic basis of CAZ hydrolysis enhancement acquired by mutations on the four residues mentioned above, the PenL variants carrying Cys69Tyr, Asn136Asp, Thr171del, and Ile173del were overexpressed in *E. coli*, purified, and then subjected to kinetic assay and X-ray crystallography. High-resolution structures of the four variants, further in complex with the ligand, revealed the distinctive features with respect to the wild-type enzyme which is also correlated to their kinetic parameters. Understandings from this study may contribute to an improvement of novel antibiotic design as well as in medical treatment strategy against *Burkholderia* pathogens, particularly *B. pseudomallei*.

## **II. MATERIALS AND METHODS**

## II. MATERIALS AND METHODS

### 1. Expression and purification

PenL-Cys69Tyr, PenL-Asn136Asp, PenL-Thr171del, and PenL-Ile173del were isolated as described previously [14, 56] and subcloned into pET28a(+) expression vector. *E. coli* BL21 (DE3) competent cell strain was used to overexpress all of the constructs. Transformed cells were pre-inoculated to grow in 5 ml LB media at 37°C, then were transferred into 1.5 liter LB media supplemented with 100 µg/ml of kanamycin at 37°C until OD<sub>600</sub> reach ~ 0.6, protein overexpression were induced by 0.5 mM of isopropyl-β-D thiogalactopyranoside. After additional 16 hour growing at 18°C, cells were pelleted by centrifugation (5,000×g at 4°C in 20 min). Cell pellets were resuspended in lysis buffer contained 50 mM Tris-HCl, 500 mM NaCl and 10 mM imidazole, pH 7.5, supplemented with 0.1 mM phenylmethane sulfonyl fluoride, 1 mM dithiothreitol, and Dnase I. Resuspension cocktails were disrupted by high intensity sonication at 4°C, then the insoluble fractions were separated using high speed centrifugation (20,000×g at 4°C in 30 min). The soluble fractions, which contained the desired proteins with N-term 6×His-tag were loaded onto Ni-agarose columns. Impure proteins were washed out with excess amount of buffer contained 50 mM Tris-HCl, 500 mM NaCl, and 20 mM imidazole, pH 7.5. Desired proteins were eluted using buffer comprised of 50 mM Tris-HCl, 500 mM NaCl, and 250 mM imidazole, pH 7.5. To remove the N-term 6×His-tag, eluents were firstly exchanged to buffer contained 20 mM Tris-HCl, 150 mM NaCl, and 2 mM CaCl<sub>2</sub>, pH 7.5 to eliminate the imidazole that inhibits the thrombin activity. 10 U of human α-thrombin (HTI, USA) was then treated per 1 mg/ml protein in the presence of 2 mM CaCl<sub>2</sub> as a cofactor. Proteins were then further purified using size-exclusion chromatography employed HiLoad 16/60 Superdex 200 pg column (GE Healthcare, USA) with buffer consisted of 20 mM Tris-HCl,

and 50 mM NaCl, pH 7.5. Purity of protein was examined using 12% SDS-polyacrylamide gel electrophoresis and visualized by Coomassive brilliant blue G250 (Sigma). The final purified protein supplemented with 20% glycerol can be stored for long-term usage up to six month at -80°C.

## **2. Crystallization and structure determination**

The purified PenL ESBL variants were concentrated to 10 µg/µl using 10,000 Da cut-off Vivaspin® centrifugal concentrator (Sartorius). Crystallization was carried out using hanging drop vapor diffusion method by mixing 1.2 µl protein sample with 1.2 µl reservoir solution. Initial screenings were set up using commercial crystallization kits from Hampton (USA) including Index 1-96, SaltxRx 1-2, PEGRx 1-2, PEG/Ion 1-2, Crystal Screens 1-2, Crystal Screen Lite, and Rigaku (Japan) including Wizards I-II-III-IV. Crystallization condition for all PenL ESBL variant crystals are shown in Table 2. Because the quality of the crystals is sufficient to further X-ray diffraction experiment, the crystallization conditions were slightly modified by adding glycerol to assist the sustainability.

Suitable crystals were transferred to the cryo-solutions which is comprised of their growing solution supplemented with 15 – 20% glycerol for 30 s, and then flash-frozen by immersing in liquid nitrogen. In order to determine the complex structure of PenL-Cys69Tyr and PenL-Asn136Asp with ceftazidime-like glycylylboronate (CBA), the cryo-solutions were supplemented with 2 mM of CBA, followed by the soaking crystals overnight at 4°C before flash-freezing. All crystals were diffracted at max ~1.2 Å resolution. X-ray diffraction and data collection were performed at Pohang Light Source (PLS) beamline 5C (Pohang, South Korea) using ADSC Q315r CCD detectors. Collected data were proceeded to index, integrate, and scale using HKL2000 (HKL Research Inc.). Structure of four PenL ESBL variants were determined by molecular replacement method using MolRep [66] and structure of PenL-WT (PDB code 5GL9 [41]) as reference model. The refinement was carried



out by Refmac5 [67] and phenix.refine [68, 69] in which the anisotropic temperature factors was engaged. To prevent the over-refinement at the final round, the highest level of strategy was applied, including individual B-factors, groups B-factors, translation-libration-screw (TLS) rotation parameters, occupancies, NCS restraint, secondary structure restraint, X-ray/stereochemistry weight optimization. The coordination and restraint of CBA was generated by eLBOW [70], then manually fitted to Fo-Fc map employing Coot [71]. Quality of models was validated by MolProbity [72] and wwPDB Validation Service (<https://validate.wwpdb.org>). All the criteria should be in acceptable range, including R-factors, Ramachandran plot, rotamer outliers, bond length, bond angle, bad clashes, C-beta outliers, etc. Details of data diffraction and structural refinement were shown in Tables 3, 4.

### 3. Kinetic parameters determination

Because of its poor spectroscopic property, ceftazidime (CAZ) can only be measured at maximal concentration of ~120  $\mu\text{M}$ . Therefore, appropriate amount of purified enzymes is mixed with various concentration of CAZ from 10 to 100  $\mu\text{M}$  in reaction buffer comprised of 50 mM potassium phosphate pH 7.0 supplemented with 20  $\mu\text{g/ml}$  of bovine serum albumin. The absorbance at 260 nm is immediately monitored with 0.1 s intervals. The temperature was kept at 25°C using thermostats cuvette holder. The initial velocity of PenL-WT, PenL-Thr171del and PenL-Ile173del is measured as common procedure. In case of biphasic reaction of PenL-Cys69Tyr and PenL-Asn136Asp, the velocity at first 10 seconds of each phase (initial phase and final phase) is obtained. Those velocities ( $v$ ) are then fit to Michealis-Menten equation:

$$v = \frac{V_{max}[S]}{K_M + [S]} \quad (1)$$

Where  $V_{max}$  is maximal reaction rate,  $K_M$  is Michaelis constant, and  $[S]$  is substrate concentration. The first-order persistence of reaction by PenL-WT prevents the calculation of  $K_M$  and  $k_{cat}$  individually, however, the catalytic efficiency can be estimated by conventional linear fitting in which the slope of regression curve is  $k_{cat}/K_M$ .

Linear fitting can be done using MS Excel or Scipy [73] module *stats.linregress*. Non-linear fitting was carried out using in-house Python scripts with the power of SciPy [73] library for parameter estimation, and Matplotlib [74] module for data visualization. The script code is written as follows:

```
# Python script code for enzyme kinetic data fitting
# Prerequisite: Numpy and SciPy libraries

# import Numpy and scipy.optimize modules
import numpy as np
from scipy import optimize

### Non-linear fitting:
# define a class to fit data into Michaelis-Menten equation
class Michaelis_Menten_fit():
    """ Fit data into Michaelis-Menten equation,
    x -- substrate concentration
    y -- initial velocity in uM/s, or specific activity in uM/mg/s
    x and y can be list of float, Numpy array or pandas Series """

    def __init__(self, x, y):
        self.substrate = x
        self.activity = y

    def get_params(self):
        """ Obtain Vmax and kM, and their standard deviations, and residual sum of square """
        x = self.substrate
        y = self.activity

        def MM_model(s, Vmax, kM):
            """ Define Michaelis-Menten model """
            return Vmax*s/(kM + s)
        # Fit data using scipy.optimize.curve_fit,
        # popt array contains Vmax and kM:
        popt, pcov = optimize.curve_fit(MM_model, x, y)
        Vmax = popt[0]
```

```

kM = popt[1]

# Compute standard deviation from covariance array pcov:
perr = np.sqrt(np.diag(pcov))
Vmax_std = perr[0]
kM_std = perr[1]
return Vmax, Vmax_std, kM, kM_std

def get_Rsqr(self):
    """ Compute R-squared of regression curve """
    x = self.substrate
    y = self.activity
    # first extract parameters:
    Vmax, Vmax_std, kM, kM_std = self.get_params()
    # compute residual sum of square (ss_res):
    residuals = y - Vmax*x/(kM + x)
    ss_res = np.sum(residuals**2)
    # compute total sum of square (ss_tot):
    ss_tot = np.sum((y - np.mean(y))**2)
    # Obtain R-squared value:
    Rsqr = 1 - ss_res/ss_tot
    return Rsqr

def get_fitting_curve(self):
    """ Smooth data to plot """
    x = self.substrate
    y = self.activity
    # first extract parameters:
    Vmax, Vmax_std, kM, kM_std = self.get_params()
    x_smoothed = np.linspace(0, x.max()+x.min(), 200)
    y_smoothed = Vmax*x_smoothed / (kM + x_smoothed)
    return x_smoothed, y_smoothed

def get_efficient(self, molar_conc):
    """ Compute turnover number kcat, and kcat/kM ratio
    molar_conc -- molar concentration of enzyme in uM,
    only when velocity == specific activity"""
    Vmax, Vmax_std, kM, kM_std = self.get_params()
    m = molar_conc
    kcat = Vmax*1000 / m # 1/s, Vmax = umol/s/mg --> uM/s/mg
    kcat_per_kM = kcat / kM
    return kcat, kcat_per_kM
    
```

## 4. Circular dichroism spectra assay

Circular dichroism (CD) spectra in far-UV region (190 – 250 nm) were monitored using Jasco J-1500 spectropolarimeter. Measurements were run at 25°C using Peltier temperature control cuvette holder. Because the chloride ion absorbs the UV around the wavelength 195 nm thus interferes the expected CD signals, the proteins were firstly exchanged to buffer containing 20 mM Tris-H<sub>2</sub>SO<sub>4</sub> and 50 mM NaF, pH 7.5. Afterward, 10  $\mu$ M of protein was transferred to 100 mm path-length cuvette. The first baseline was determined using the same buffer. The baseline for CBA was firstly corrected with the first baseline, then was in turn used for protein-ligand experiment subtraction. Triplicate scanning was applied for each data set with 0.1 nm intervals and 1 mm bandwidth then averaged. For protein-ligand experiments, 25  $\mu$ M of CBA was added to protein sample and incubated for 1 hour at room temperature.

## 5. Molecular dynamics simulation

PenL-WT, PenL-Cys69Tyr, and PenL-Asn136Asp were subjected to all-atom molecular dynamics (MD) simulations in explicit solvent using Gromacs 5.0.7 suite [75] and Gromos96-43a1 force field [76]. Coordinate of PenL-WT can be obtained from RCSB Protein Data Bank by fetching the ID 5GL9 [41]. Molecules were immersed in a cubic TIP3P water box [77]. Systems were neutralized by adding suitable amount of counterions Na<sup>+</sup> and Cl<sup>-</sup> and maintained an ionic strength of 0.10. Particle Mesh Ewald method [78] was used to determine the electrostatic interaction of systems, with real space and van der Waals distance cut-off of 10 Å. LINCS Linear Constraint solver was used to constrain all bond lengths [79]. Time step was set at 2 fs. After energy minimization by 500-step steepest descent calculation, systems were heated to 300 K, then equilibrated in NPT ensemble with periodic boundary condition. Temperature and pressure were maintained constant using Velocity-rescale and Parrinello-Rahman algorithms [80, 81], respectively. Finally, data

collections were carried out in the same equilibration condition over 50 *ns*, with 100 frame intervals. MD trajectory analysis was performed packages.

## 6. Electrostatic potential calculation

Electrostatic distribution on surface of proteins was calculated employing Adaptive Poisson-Boltzmann Solver, or APBS [82]. The APBS plugin is available with PyMOL incentive version 2.0. The protein models in \*.pdb format were prepared using PDB2PQR [83] which adds hydrogens and missing side chain atoms, assigns partial charges and radii, as the first required step. The electrostatics were calculated in the default ionic strength condition (0.15) at 300 K with AMBER force field. The pH condition for all calculation was firmly fixed at 7.0 in which the  $pK_a$  values of particles were computed using Propka [84]. The specific command for the APBS calculation performed in PyMOL APBS plugin is as follow:

```
--with-ph=7 --ph-calc-method=propka --ff=AMBER --chain
```

Electrostatic potential is expressed in the unit of  $k_bT/e_c$ , or  $kT/e$  in short, where  $k_b$  (or  $k$ ) is Boltzmann constant ( $1.3806504 \times 10^{-23} \text{ J K}^{-1}$ ),  $T$  is temperature in calculation (300 K), and  $e_c$  (or  $e$ ) is the charge of an electron ( $1.60217646 \times 10^{-19} \text{ C}$ ). Electrostatic potential for all the computed proteins in this thesis is color coded from -3000  $kT/e$  (red) to zero (white) to 3000  $kT/e$  (blue), and visualized in PyMOL.

*Thinh-Phat Cao Ph.D. Dissertation*

*Chosun University, Department of Biomedical Science*

---

## **III. RESULTS AND DISCUSSION**

### III. RESULTS AND DISCUSSION

#### 1. Purification and X-ray crystallography

##### 1.1. Purification

The DNA constructs encoding for PenL-WT and four ESBL variants Cys69Tyr, Asn136Asp, Thr171del, and Ile173del do not contain the N-terminal signal peptide which may target the enzyme to the outer membrane association [85]. Instead, the N-terminus of the enzyme was fused with 6×His-tag that assists the purification by Ni-affinity method. After eluting from the Ni-agarose column, the purity of the fusion proteins attained approximately  $\geq 95\%$  (Figure 8A). The 6×His-tag was then successfully eliminated by thrombin treatment, leaving the intact proteins with a decent sustainability for further experiments (Figure 8B). The purity of the intact proteins were then polished employing size-exclusion chromatography (SEC) (Figure 9).

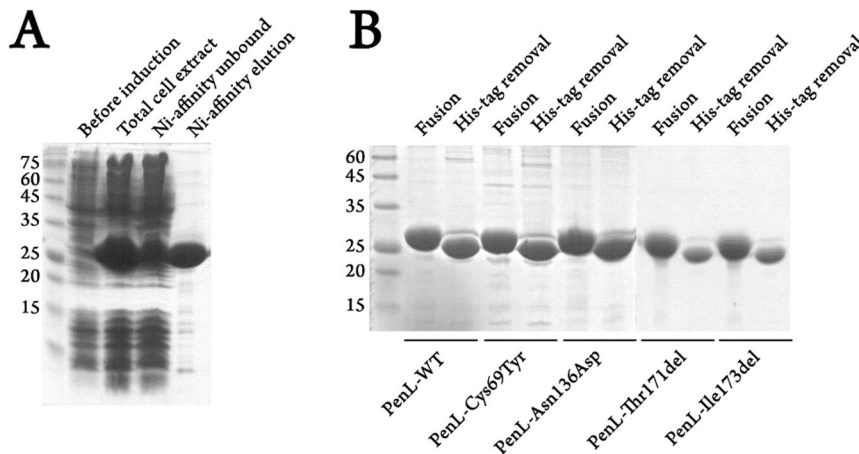


**Figure 8. Purification of four PenL ESBL variants**

(A) Representative Ni-affinity purification of PenL-Cys69Tyr (the other variants and wild-type are the same). (B) His-tag removal of target proteins by thrombin.

The retention volume in SEC result demonstrates a slightly lower molecular weight of PenL-Thr171del and PenL-Ile173del (Figure 9). This discrimination ought to the deletion of the single amino acid rather than the difference in the oligomeric state, because deviations displayed in the UV spectra do not indicate the sufficient change in molecular weight as a factor of two or greater.

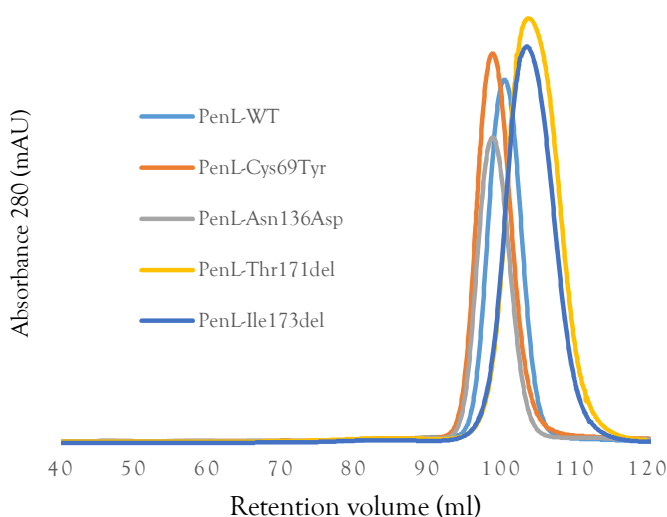


**Figure 9. Size-exclusion chromatography of four PenL ESBL variants.**

## 1.2. X-ray crystallography

After four days to two weeks, the initial crystals of four PenL ESBL variants grew in conditions listed in Table 2. All crystals appeared to be in sufficient quality (Figure 10) so that the X-ray diffraction experiment was proceeded straightforwardly, with a minor additional customization (using glycerol) in their growing condition for further quality maintenance (Table 2). The diffraction patterns exhibited an excellent resolution range reaching roughly 1.2 Å (Figure 10),



the atomic-resolution according to Sheldrick criterion[86]. However, after processing with several reasonable cut-off criteria, the maximal resolution marginally reduced to  $\sim 1.3 \text{ \AA}$ . Because the PenL-WT structure was solved before (PDB ID: 5GL9 [41]), it was subjected as reference model to determine the structures of four PenL ESBL variants employing molecular replacement routine. The successful solutions were then immediately refined by maximum likelihood method [67] so that appropriate R-factor values achieving the acceptable criteria ( $<30\%$ ) were produced. The excellently smooth 2Fo-Fc map was shown while unambiguous Fo-Fc map strongly indicated the presence of ligand (Figure 11). Further model fitting and refinements resulted in good final criteria including R-factors, Ramachandran plots, and allowed range of outliers, as shown in Table 3, 4.

**Table 2. Crystallization condition for PenL ESBL variants**

<i>Variant</i>	<i>Buffer</i>	<i>Precipitant 1</i>	<i>Precipitant 2</i>	<i>Additive</i>	<i>Temperature</i>
<i>Cys69Tyr</i>		0.2 M sodium acetate trihydrate	20% (w/v) polyethylene glycol 3350		4°C
<i>Asn136Asp</i>	0.1 M sodium acetate pH 5.0	0.2 M sodium chloride	25% (w/v) polyethylene glycol 3350		20°C
<i>Thr171del</i>		0.1 M potassium thiocyanate	30% (w/v) polyethylene glycol monomethyl ether 2000	7.5% glycerol	20°C
<i>Ileu173del</i>		0.1 M potassium thiocyanate	30% (w/v) polyethylene glycol monomethyl ether 2000	2.5% glycerol	20°C

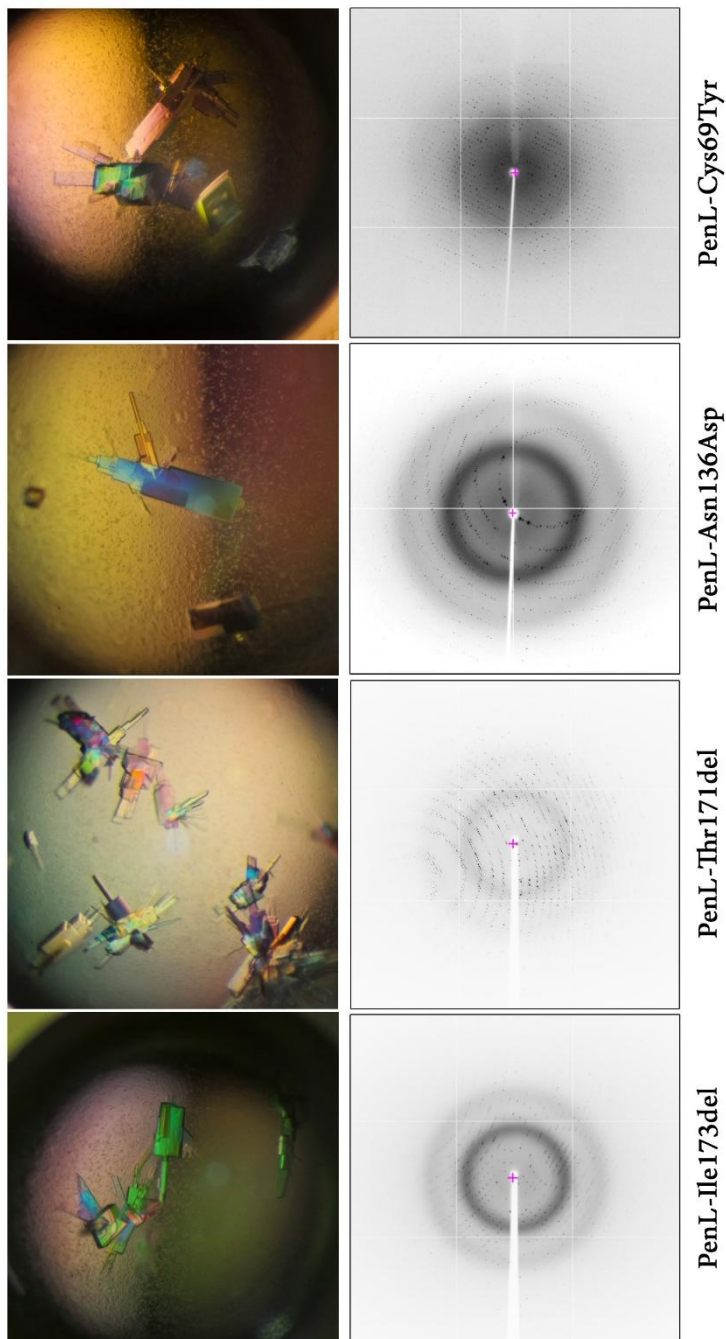


**Figure 10. Crystallographic study of four PenL ESBL variants.**

The images of crystal and their corresponding diffraction pattern are shown. Single crystals were picked up for X-ray diffraction. The edge of the diffraction images corresponds to 1.2 Å resolution.

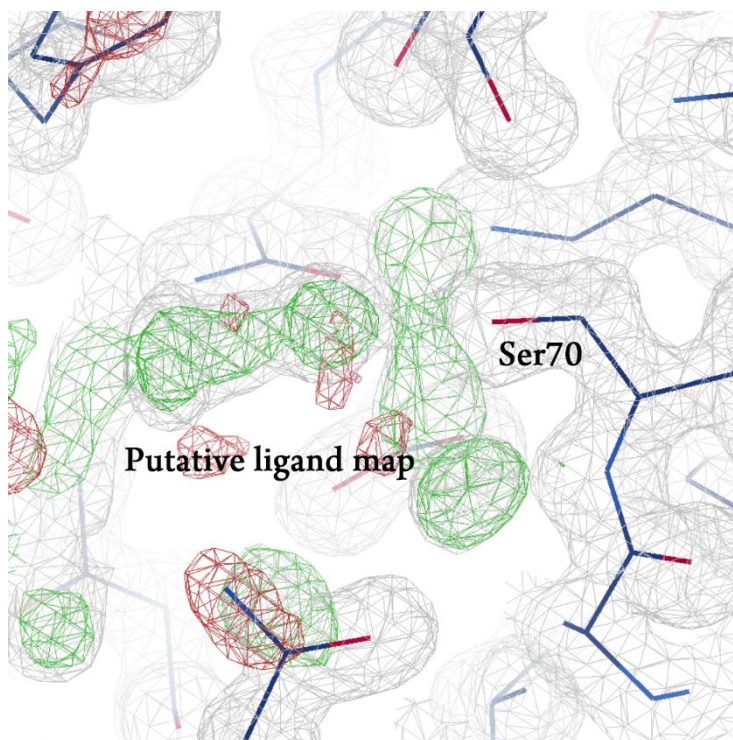


**Figure 11. Phasing snapshot for structure determination.**

The representative snapshot was obtained right after the molecular replacement and maximum likelihood refinement had been brought about for PenL-Cys69Tyr soaked with ligand. 2Fo-Fc map is depicted with grey meshes. The Fo-Fc map (green for positive and red for negative) indicates the presence of ligand that covalently bound to the reactive Ser70.

**Table 3. Data statistics summary for X-ray crystallography of PenL-Cys69Tyr and PenL-Asn136Asp**

	PenL-Cys69Tyr	PenL-Cys69Tyr CBA-bound	PenL-Asn136Asp	PenL-Asn136Asp CBA-bound
PDB ID	6AFM	6AFN	6AFO	6AFP
<b>Data collection</b>				
Beam line	PAL-5C	PAL-5C	PAL-5C	PAL-5C
Wavelength (Å)	0.97951	0.97954	0.97954	0.97857
Resolution (Å)	50 – 1.3 (1.32 – 1.3)	50 – 1.4 (1.42 – 1.40)	50 – 1.4 (1.42 – 1.40)	50 – 1.4 (1.42 – 1.40)
Space group	P2 <sub>1</sub> 2 <sub>1</sub> 2 <sub>1</sub>	P2 <sub>1</sub> 2 <sub>1</sub> 2 <sub>1</sub>	P2 <sub>1</sub>	P2 <sub>1</sub>
Unit cell dimension				
a, b, c (Å)	38.48, 52.98, 122.73	38.66, 53.24, 122.98	34.99, 92.72, 68.88	34.88, 92.39, 68.84
α, β, γ (°)	90.0, 90.0, 90.0	90.0, 90.0, 90.0	90.0, 92.7, 90.0	90.0, 94.3, 90.0
Total reflections	413760	618880	618880	516034
Unique reflections	62299 (3048)	50752 (2479)	86131 (4254)	84356 (4189)
R <sub>merge</sub> <sup>†</sup> (%)	5.3 (9.8)	7.8 (25.6)	8.0 (27.1)	8.9 (28.7)
Completeness (%)	99.3 (98.4)	99.6 (99.4)	99.0 (100.0)	98.6 (99.2)
Redundancy	6.6 (6.5)	12.2 (12.1)	7.5 (7.4)	6.1 (6.0)
Average I/σ (I)	49.47 (25.74)	43.78 (18.49)	40.23 (10.44)	36.43 (7.33)
Matthews coefficient (Å <sup>3</sup> Da <sup>-1</sup> )	2.18	2.21	1.95	1.93
Solvent (%)	43.68	44.33	37.0	36.45
<b>Refinement</b>				
R <sub>work</sub> / R <sub>free</sub> (%)	15.00/16.77	14.74/16.88	14.86/17.35	14.87/17.53
Protein residues	268	268	535	536
Waters	484	371	755	629
*CBA	-	1	-	2
RMSD				
Bond angles (°)	0.83	1.30	1.64	1.90
Bond lengths (Å)	0.005	0.012	0.015	0.020
Average B factors (Å <sup>2</sup> )	11.92	17.18	13.18	16.17
Ramachandran plot				
Favored (%)	97.37	97.74	97.18	98.31
Outliers (%)	0.00	0.00	0.19	0.00

Values in parentheses correspond to highest resolution shell.

<sup>†</sup>R-merge =  $\frac{\sum_{hkl} \sum_i |I_i(hkl) - \langle I(hkl) \rangle|}{\sum_{hkl} \sum_i I_i(hkl)}$ , where  $I_i(hkl)$  is the observed intensity and  $\langle I(hkl) \rangle$  is the average intensity of symmetry-related observations.

\*CBA: ceftazidime-like glycyloboronic acid

**Table 4. Data statistics summary for X-ray crystallography of PenL-Thr171del and PenL-Ile73del**

	PenL-Thr171del	PenL-Thr171del CBA-bound	PenL-Ile73del
<b>PDB ID</b>			
<b>Data collection</b>			
Beam line	PAL-5C	PAL-5C	PAL-5C
Wavelength (Å)	0.97934	0.97933	0.97934
Resolution (Å)	50 – 1.5 (1.53 – 1.50)	50 – 1.6 (1.58 – 1.55)	50 – 1.4 (1.39 – 1.37)
Space group	P2 <sub>1</sub> 2 <sub>1</sub> 2 <sub>1</sub>	P2 <sub>1</sub>	P2 <sub>1</sub>
Unit cell dimension			
a, b, c (Å)	69.25, 97.06, 34.14	34.89, 92.19, 68.76	34.72, 92.16, 69.07
α, β, γ (°)	90.0, 90.0, 90.0	90.0, 93.2, 90.0	90.0, 92.7, 90.0
Total reflections	371295	466642	664083
Unique reflections	37677 (1843)	62902 (3158)	90940 (4502)
R <sub>merge</sub> <sup>†</sup> (%)	6.8 (51.2)	7.1 (66.5)	6.7 (48.6)
Completeness (%)	99.7 (99.6)	99.9 (100)	99.7 (100.0)
Redundancy	9.9 (9.8)	7.4 (7.2)	7.4 (7.3)
Average I/σ (I)	39.32 (5.59)	27.94 (2.71)	30.56 (4.36)
Matthews coefficient (Å <sup>3</sup> Da <sup>-1</sup> )	1.75	1.75	1.75
Solvent (%)	29.86	29.86	29.86
<b>Refinement</b>			
R <sub>work</sub> / R <sub>free</sub> (%)	16.57/19.27	16.01/19.17	15.24/16.88
Protein residues	267	534	534
Waters	261	562	594
*CBA	-	2	-
RMSD			
Bond angles (°)	1.20	1.42	1.30
Bond lengths (Å)	0.012	0.013	0.012
Average B factors (Å <sup>2</sup> )	17.50	18.92	18.40
Ramachandran plot			
Favored (%)	96.98	97.73	97.55
Outliers (%)	0.00	0.00	0.00

Values in parentheses correspond to highest resolution shell.

<sup>†</sup>R-merge =  $\frac{\sum_{hkl} \sum_i |I_i(hkl) - \langle I(hkl) \rangle|}{\sum_{hkl} \sum_i I_i(hkl)}$ , where  $I_i(hkl)$  is the observed intensity and  $\langle I(hkl) \rangle$  is the average intensity of symmetry-related observations.

\*CBA: ceftazidime-like glycyloboronic acid

## 2. Kinetics study

### 2.1. Kinetics property of PenL-WT

Due to the poor spectroscopic property of CAZ, the reaction rate of PenL-WT (and of four variants) with CAZ concentration greater than 100  $\mu\text{M}$  cannot be monitored. The enzyme was thus adjusted with a suitable amount, and the reaction rate was examined with CAZ concentration ranging from 10 to 100  $\mu\text{M}$ . The CAZ hydrolysis reaction catalyzed by PenL-WT took place in a typical exponential decay pattern (Figure 12A) and thus far had remained in first-order state (Figure 12D), which restricted the calculation of  $K_M$  and  $k_{\text{cat}}$  individually.

**Table 5. Kinetic parameters for CAZ hydrolysis by PenL-WT and four ESB� variants**

<b>VARIANT</b>	<b><math>K_M</math> (<math>\mu\text{M}</math>)</b>	<b><math>k_{\text{cat}}</math> (<math>\text{s}^{-1}</math>)</b>	<b><math>k_{\text{cat}} / K_M</math> (<math>\mu\text{M}^{-1} \cdot \text{s}^{-1}</math>)</b>
PenL-WT	nm	nm	0.0027 (*)
PenL-Cys69Tyr (Initial phase)	14.140 $\pm$ 0.975	0.169 $\pm$ 0.003	0.0120
PenL-Cys69Tyr (Final phase)	4.528 $\pm$ 0.182	0.036 $\pm$ 0.000	0.0080
PenL-Asn136Asp (Initial phase)	10.457 $\pm$ 0.537	0.181 $\pm$ 0.002	0.0173
PenL-Asn136Asp (Final phase)	2.165 $\pm$ 0.011	0.041 $\pm$ 0.000	0.0189
PenL-Thr171del	16.118 $\pm$ 0.514	0.800 $\pm$ 0.007	0.0496
PenL-Ile173del	52.074 $\pm$ 4.390	1.987 $\pm$ 0.077	0.0382

nm: not measurable

(\*) estimated from linear regression

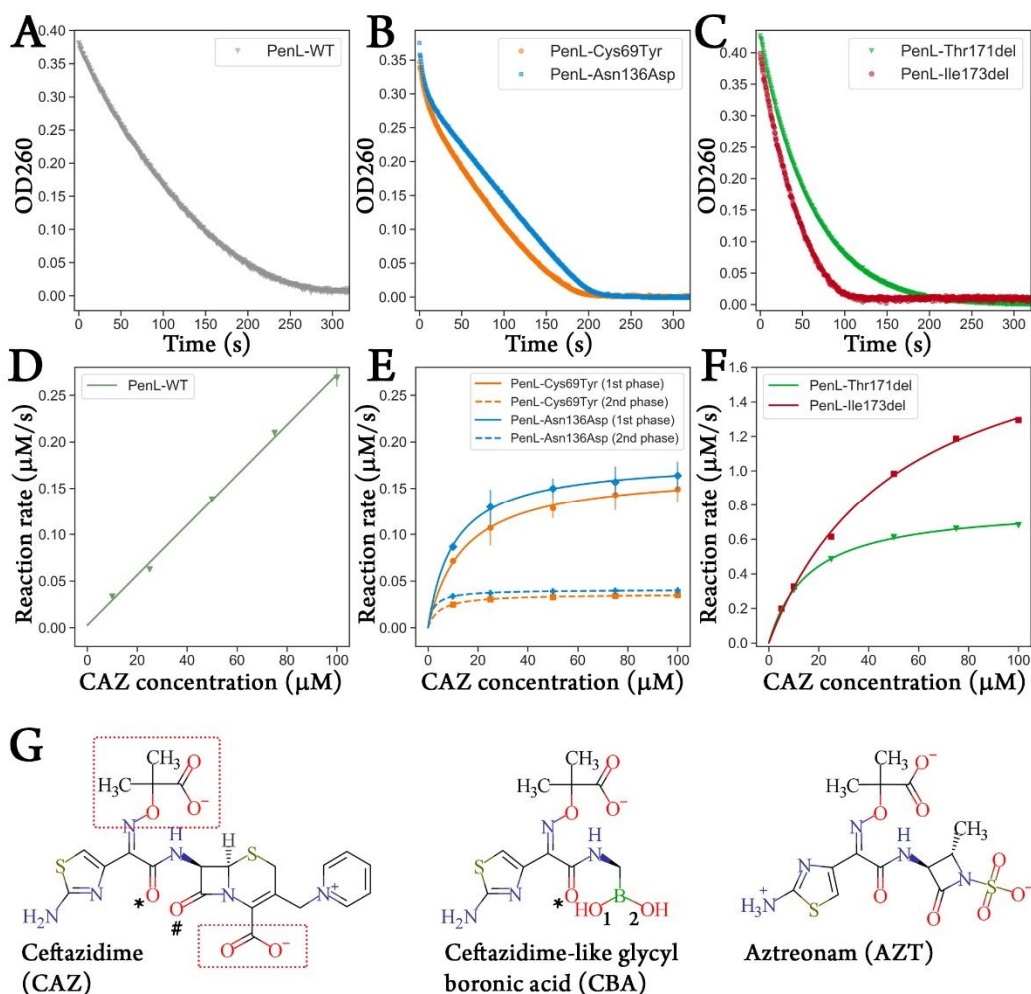


**Figure 12. Kinetic study on CAZ hydrolysis of PenL-WT and four ESBL variants.**

(A), (B) and (C) CAZ hydrolysis reaction of PenL-WT and four ESBL variant as a function of time (s). (B) PenL-Cys69Tyr and PenL-Asn136Asp catalyzed the reaction in a biphasic manner. (D) The CAZ hydrolysis reaction by PenL-WT maintained in the first-order state in the measurable range of CAZ concentration. (E) and (F) Fitting the initial velocity of four PenL ESBL variants into Michaelis-Menten equation. (C) Chemical structures of ceftazidime (CAZ), ceftazidime-like glycylic boronic acid (CBA), and aztreonam (AZT). Two negative charged groups of CAZ are marked with red dotted rectangles. The hydroxyl group  $-OH$  in CBA corresponds to the  $\beta$ -lactam carbonyl group of CAZ (marked with # sign). The acetamido hydroxyl groups of CAZ and CBA are marked with \* sign).

This result indicates that the  $K_M$  and  $k_{cat}$  for PenL-WT should be high, with the catalytic efficiency  $k_{cat}/K_M$  estimated from the slope of the regression curve is of  $\sim 0.0027 \mu\text{M}^{-1}\cdot\text{s}^{-1}$  (Table 5). Therefore the CAZ affinity of PenL-WT is very low, and the CAZ hydrolysis reaction rate strongly relies on substrate concentration, which is not an advantage for the bacteria in reality.

## 2.2. Biphasic kinetics of PenL-Cys69Tyr and PenL-Asn136Asp

The CAZ hydrolysis catalyzed by PenL-Cys69Tyr and PenL-Asn136Asp interestingly took place in a biphasic separating rapid (first phase) and slower (second phase) (Figure 12B). However, reaction rate at both initial and final phases of CAZ hydrolysis reaction by two PenL variants reached maximal regardless of substrate concentration (Figure 12E). As a result, the  $K_M$  for two PenL variants reduced in both phases, in comparison with PenL-WT (Table 5), indicating the augmentation of CAZ affinity in the active site of the substitution variants Cys69Tyr and Asn136Asp. Furthermore, the catalytic efficiency  $k_{cat}/K_M$  of two PenL substitution variants also increased in comparison with PenL-WT, ranging from  $\sim 2.9$  to  $\sim 7.0$  folds, respectively (Table 5). Remarkably, the slight decrease in  $K_M$  in the final phase in respect to initial phase was compensated by the decrease in  $k_{cat}$  (Table 5), resulting in the relatively comparable catalytic efficiency between two phases.

## 2.3. Kinetics of PenL-Thr171del and PenL-Ile173del

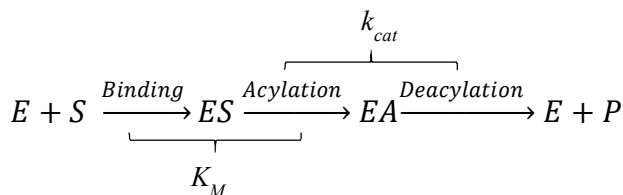
Unlike the two substitution mutations, the two deletion mutations PenL-Thr171del and PenL-Ile173del catalyzed the CAZ hydrolysis with the usual monophasic manner (Figure 12C), which allowed the estimation of  $k_{cat}$  and  $K_M$  (Figure 12F). However, the  $k_{cat}$  and  $K_M$  of PenL-Thr171del and PenL-Ile173del were substantially decreased in comparison with the wild-type enzyme, resulting in higher  $k_{cat}/K_M$  values than that in PenL-WT, approximately  $\sim 18.4$  and  $\sim 14.1$ , respectively (Table 5). The data indicate that the two PenL deletion mutations are more beneficial than the wild-type enzyme in term of CAZ resistance of *B. thailandensis*, which consistent to the high MIC values shown in



Figure 5. On the other hand, PenL-Thr171del has lower  $k_{cat}$  and  $K_M$  than those of PenL-Ile173del, yet their  $k_{cat}/K_M$  values are comparable (Table 5).

## 2.4. Implication from the distinctions of kinetic property of four PenL ESBL variants

In common, the  $\beta$ -lactam hydrolysis by  $\beta$ -lactamase is accepted to take place in three steps as in Scheme 1 below:



**Scheme 1: Principle for  $\beta$ -lactam hydrolysis by  $\beta$ -lactamase**

As previously stated and demonstrated in Figure 2 (*Introduction*), the hydrolysis of  $\beta$ -lactam backbone is conserved in all  $\beta$ -lactamases. The increase in hydrolysis activity toward different types of substrate (penicillin-, cephalosporin-, or carbapenem-type) is thus accomplished by the variations that influence the first step, binding of the substrate. Meanwhile, modifications in substrate recognition ensemble of the enzyme would lead the alteration in the substrate specificity. In this regard, the changes in kinetic property, primarily the decrease in  $K_M$ , in the four PenL ESBL variants indicate that the four single mutations prompted the alternative substrate recognition mode for the enzyme. This aspect is attractive because those single mutations occurred at non-catalytic and non-substrate-binding residues. To unveil the mechanism for such alterations, the structural study has been carried out and discussed in subsequent sections.

### **3. Structural study**

#### **3.1. Circular dichroism (CD) spectra analysis**

Because the catalytic activity of an enzyme is firmly correlated with its conformational integrity [87], the distinction in kinetic property of four PenL variants suggests that the mutations may trigger specific changes in conformation of the enzyme that leads to alter the substrate recognition. Even further, the prior study on the homologous PenI-Cys69Phe also proposed that the variant might exist in two different conformations, one of which exhibited the rapid CAZ hydrolysis reaction rate[88]. It is tempting to expect that the PenL-Cys69Tyr, and PenL-Asn136Asp as well, may resemble such characteristic because these two substitution variants also exhibit biphasic kinetics as seen in PenI-Cys69Phe [88]. Therefore, to examine the conformational changing of the four PenL variants comparing to PenL-WT in solution (at 25°C), the circular dichroism (CD) spectra analysis was carried out. To our surprise, the spectra of apo-form of the all four PenL variants were similar to that of PenL-WT (Figure 13), suggesting that the apo-form of the four PenL ESBL variants likely exists in a same conformation with the wild-type enzyme. However, in the presence of CBA, the spectra of the fours PenL ESBL variants appeared to deviate in both  $\alpha$  (~208 and 220 nm) and  $\beta$  (~198 nm) contents, while the spectrum of PenL-WT was likely to be due to the experimental error (Figure 13A). Noted that the concentration of CBA mixed in reaction (25  $\mu$ M) reaches  $K_M$  value of the four PenL ESBL variants toward CAZ (Table 5), indicating that the deviation between the spectrum of four PenL variants with and without CBA was reliable. Nonetheless, such CBA concentration may be considerably less than  $K_M$  value of PenL-WT, for which the deviation could not be detected. This experimental limitation is unable to overcome under the permissive condition, but it indicates the dependency of substrate amount on the catalytic activity of PenL-WT, as analyzed in previous section.

In overall, the CD spectra results implicate that the alternative conformation of the four PenL ESBL variants would be induced upon substrate binding, which supports to the hypothesis that those variants may recognize the CAZ with a different mode other than that of the wild-type enzyme.

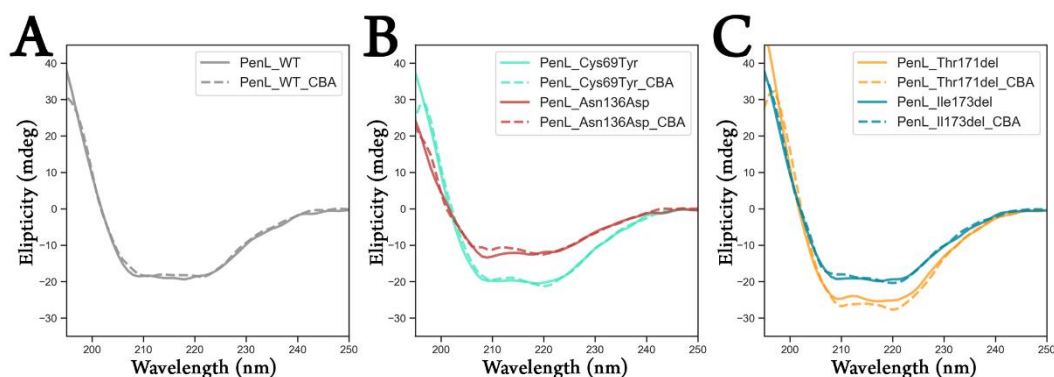


**Figure 13.** CD spectra analysis of PenL-WT and four PenL ESBL variants.

### 3.2. The overall structure of four PenL ESBL variants, Cys69Tyr, Asn136Asp, Thr171del, and Ile173del

The global structures of four PenL ESBL variants, Cys69Tyr, Asn136Asp, Thr171del, and Ile173del, are almost identical with that of the wild-type enzyme, with root mean squared deviation (RMSD) at  $C\alpha$  atom is of 0.221 Å, 0.186 Å, 0.227 Å, and 0.252 Å, respectively, comparing to PenL-WT (PDB ID: 5GL9 [41]). In particular, the configuration of the catalytic ensemble that involved in  $\beta$ -lactam backbone hydrolysis in four PenL ESBL variants is well conserved (Figure 14), except for the Asn170 in case of two PenL deletion mutants that flips away from the coordination with Glu166 and catalytic water (W4) (Figure 14C, 14E, 14F). The role of Asn170 in PenL-171del and PenL-Ile173del will be discussed further in the sequel. The strict identity in the configuration of the

catalytic ensemble in two PenL ESBL variants, in respect to PenL-WT, once again asserts that the single mutations do not likely affect the ground state of the active site that involved in basic  $\beta$ -lactam hydrolysis. In other words, four PenL ESBL variants catalyze the same processes of acylation and deacylation (Scheme 1, the last two steps) as in PenL-WT and common class A  $\beta$ -lactamases. Therefore, the increased CAZ hydrolysis capacity of the four PenL variants in comparison with PenL-WT must be rooted by the alteration in CAZ recognition and binding (Scheme 1, the first step). This deduction is consistent with the increase in CAZ affinity of two PenL ESBL variants which was described in the previous section.

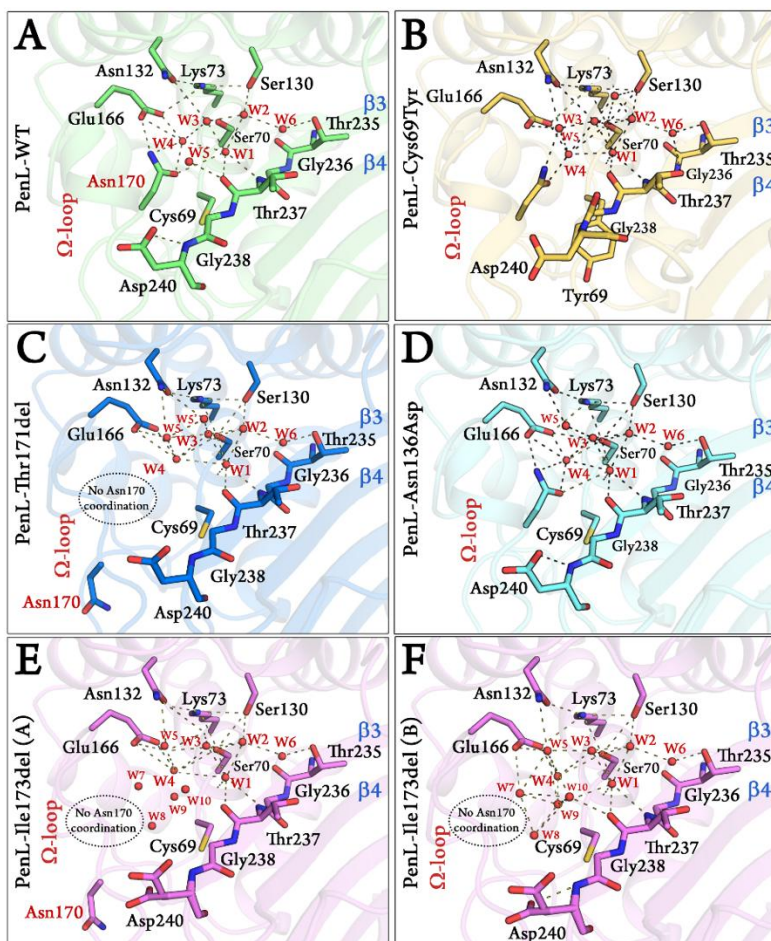


**Figure 14. Essential catalytic ensemble of PenL-WT and four ESBL variants**

The configuration of the catalytic ensemble is strictly conserved among class A  $\beta$ -lactamases. The catalytic water, W4, coordinates to Glu166 and Asn170 and participates to both acylation and deacylation steps.

### 3.3. Structural analysis of PenL-Thr171del and PenLIle173del

Despite sharing the most structural identity, the  $\Omega$ -loop of the PenL-Thr171del and PenL-Ile173del is shorter than that in wild-type enzyme due to the depletion of one amino acid. Consequently, the C-terminal part of  $\Omega$ -loop in the two variants is shifted 3.5 Å when superimposing to PenL-WT (Figure 15A). Although the conformation of  $\Omega$ -loop backbone in the two variants appears to be similar, the configuration of their side chains shows some distinctions as follow. In PenL-Thr171del, the residue Ala172 moved up 0.9 Å yet was still in the same position (Figure 15B), whereas in PenL-Ile173del, Ala172 moved down to occupy the inherent location of the deleted Ile173 (Figure 15C). As a consequence, the residue Thr173 in PenL-Ile171del rotated 180° to occupy the vacated location of Ala172 (Figure 15C). In both cases, the movement of Ala172 (in PenL-Thr171del) and the occupation of Thr171 (in PenL-Ile173del) created a steric hindrance to push the strand  $\beta$ 3 0.6 Å far away from its original position. As a result, the active site cleft at this region of the two variants was expanded ~3.5-4.1 Å. The expansion in this region may leave more space for large-size of antibiotics like CAZ.

The movement of  $\Omega$ -loop in two deletion mutations also led to changes in its internal stabilization network. In particular, once changing its conformation, Asn170 faced to the interior of  $\Omega$ -loop and formed a new interaction network, replacing the role of Arg164 of which the side chain swung (Figure 16B, 16C) out of the original position seen in PenL-WT (Figure 16A). The new interaction network probably helps maintains the rigidity of  $\Omega$ -loop. Hence, up until this point, the  $\Omega$ -loop of two PenL deletion variants is likely to not be as flexible as the other ESBL cases in class A  $\beta$ -lactamase of which the enhancement in flexibility of  $\Omega$ -loop was evidently correlated to the increase in third-generation cephalosporins affinity [89, 90]. The arguments for this aspect is discussed further in sequel.

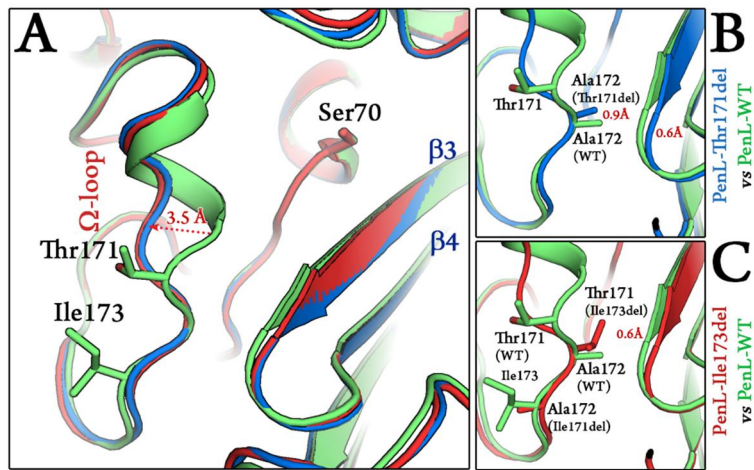


**Figure 15. Distinction in  $\Omega$ -loop of PenL-Thr171del and PenL-Ile173del**

(A) Superposition of PenL-Thr171del (sky-blue) and PenL-Ile173del (red) with PenL-WT (green). (B) and (C) Effect of deletion mutations on coordination of residues on  $\Omega$ -loop of PenL-Thr171del (B) and PenL-Ile173del (C).

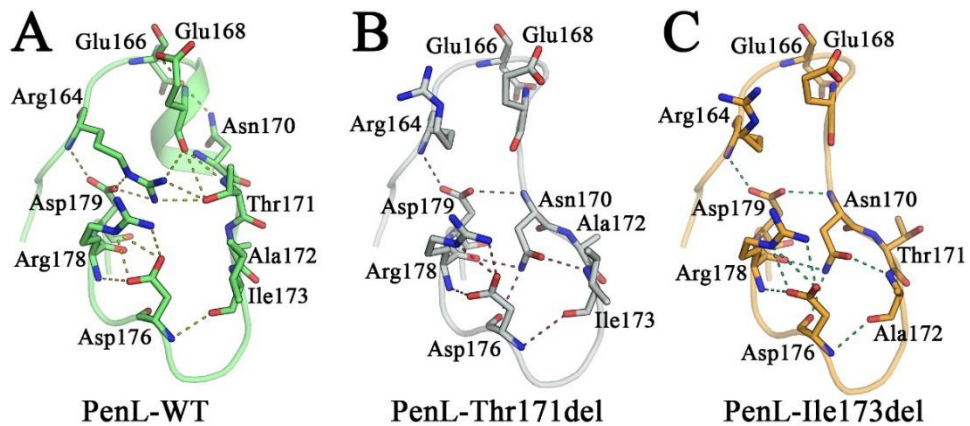


**Figure 16. Stabilization network in  $\Omega$ -loop of PenL-Thr171del and PenL-Ile173del**

It should be recalled that the  $\Omega$ -loop contains two important catalytic residues, Glu166 and Asn170, which both coordinate to the catalytic water (W4). In PenL-Thr171del and PenL-Ile173del, the Glu166 is still stabilized by Asn136 so that the N-terminal part of  $\Omega$ -loop still maintains the inherent conformation (Figure 14, 16A). However, because the conformation of the C-terminal part of  $\Omega$ -loop was changed as described previously, the residue Asn170 no longer coordinates to Glu166 and water W4 (Figure 14, 17A). The observation raises a question on the role of Asn170 in PenL. Obviously, Asn170 also interacts with Glu166, suggesting that Asn170 might be involved in the perturbation of Glu166  $pK_a$ . The absence of Asn170 coordination slightly affect the  $pK_a$  of Glu166 in PenL-Thr171del (5.33) and in PenL-Ile173del (4.74), while  $pK_a$  of PenL-WT Glu166 is of 5.08, as was calculated by Propka [84]. Notice that  $pK_a$  of Glu166 may also be affected by coordination with waters around (Figure 14). Because both PenL-Thr171del and PenL-Ile173del have the higher catalytic efficiency to CAZ hydrolysis than PenL-WT, these observations suggest that Asn170 is probably not important for the catalysis in the two deletion variants. Another possibility is that the absence of Asn170 coordination might assist to increase the CAZ hydrolysis activity by changing the reaction into an alternative manner. These deductions might be reasonable because previous studies also discussed that the depletion of Asn170 side chain could lead to alteration of product form (Asn170Gly) [91] or the activity would rely on substrate assistance (Asn170Leu) [92]. Nonetheless, in our permissive condition, we were unable to determine the product formation in the CAZ hydrolysis reaction by the two PenL deletion variants.

To further understand the mechanism for CAZ hydrolysis of the two variants, their ligand-bound complex structures are required. Unfortunately, we could not obtain the CBA bound-form of PenL-Ile173del, yet that of PenL-Thr171del was solved at 1.5 Å resolution (Table 4). Surprisingly, in one of two CBA-bound conformations, the  $\Omega$ -loop of PenL-Thr171del dramatically moved back to the inherent position, recovered the original conformation so that Asn170 coordinates to the



catalytic water W4 and Glu166 yet broke down the peptide backbone of Asn170-Ala172 (Figure 17D). Since the CBA molecule was in acylation-form, the frozen state portrayed in Figure 17D was likely to be in the stage just before the deacylation process took place. The same phenomenon was observed previously in case of tandem repeat mutations on  $\Omega$ -loop [41]. Of the interesting distinct, in tandem repeat mutations which duplicated or triplicated the length of  $\Omega$ -loop, the flexible  $\Omega$ -loop was relaxed so that Asn170 moved far away or even disordered from the crystal structure, then recovered its proper coordination upon CBA binding. However, the flexibility of  $\Omega$ -loop in PenL-Thr171del and PenL-Ile173del stemmed from the deletion of single amino acid, which also rooted the disruption of the peptide backbone in this region. To this observation, the  $\Omega$ -loop of PenL-Thr171del likely to be more flexible than in PenL-WT, in contrast to the prior deduction from apo-form which supposed its rigidity. In another aspect, the movement of  $\Omega$ -loop also slightly altered the electrostatic potential around the typical oxyanion hole of PenL-Thr171del and PenL-Ile173del into positive (Figure 17A, 17C, 18C), in comparison to PenL-WT (Figure 18A). This effect explains for the higher CAZ affinity of these two variants in respect to the wild-type enzyme (Table 5).

In the meantime, the deletion Ile173del generated a different outcome in term of electrostatics in comparison with Thr171del. The widen space created by the movement of  $\Omega$ -loop in PenL-Ile173del became extremely positive (Figure 18C, LEFT). This effect resulted in an obvious bi-regional active site cleft of PenL-Ile173del, wherein, two opposite charge areas situated adjacently (Figure 18C). Notwithstanding the complex structure for PenL-Ile173del was unable to obtain, we overlap the CBA-bound complex structure of PenL-Thr171del with apo-form of PenL-Ile173del in order to predict the binding mode of ligand in PenL-Ile173del. As our expectation, the positively charged area around the typical oxyanion hole of PenL-Ile173del might certainly appeal the oxyimino group, while the negatively charged area might attract the amino-thiazol group of CBA, as illustrated in Figure 18E.

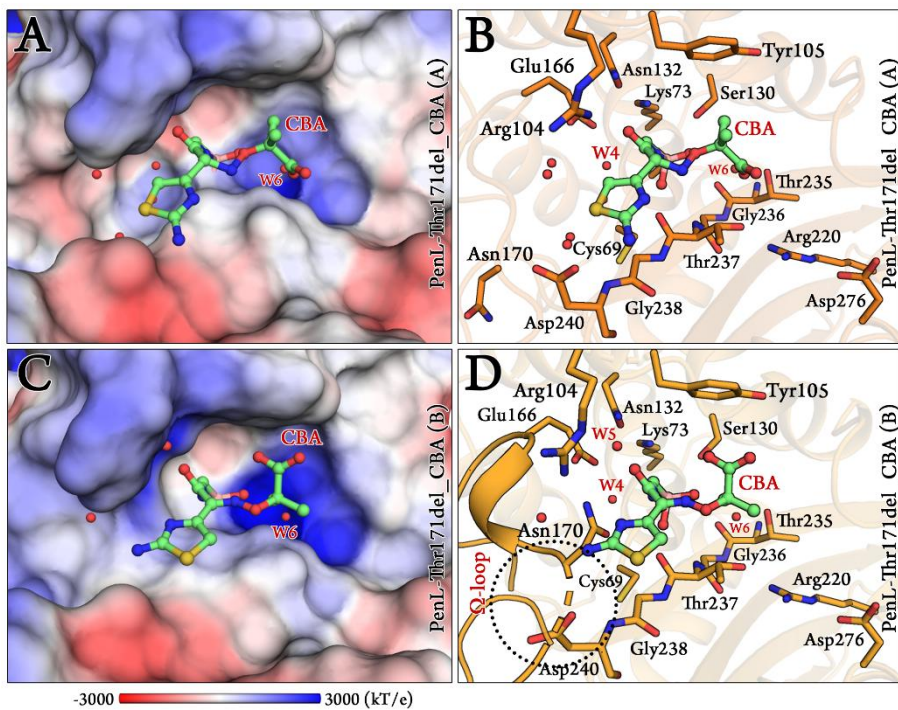


**Figure 17. Different conformations of  $\Omega$ -loop in PenL-Thr171del upon ligand binding**

(A) Configuration of  $\Omega$ -loop and Asn170 in PenL-Thr171del apo-form. (B) Configuration of  $\Omega$ -loop and Asn170 in PenL-Thr171del upon CBA binding.

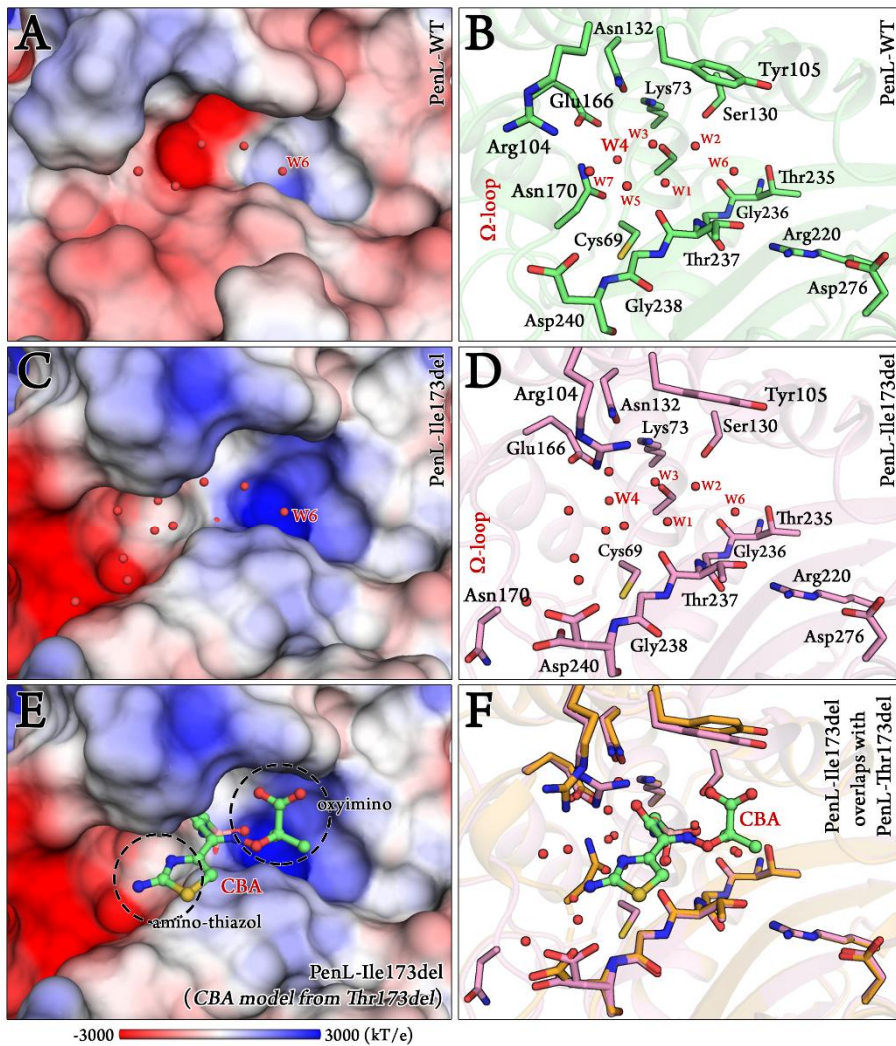


**Figure 18. Electrostatic property in active site cleft of PenL-WT and PenL-Ile173del**

(A) and (B) Electrostatic distribution and configuration in active site cleft of PenL-WT. (C) and (D) Electrostatic distribution and configuration in active site cleft of PenL-Ile173del. (E) and (F) Overlapping the CBA-bound complex structure of PenL-Thr171del with apo-form of PenL-Ile173del.

As described so far, the increase in CAZ hydrolysis ability of two PenL deletion variants is majorly rooted by the flexibility of  $\Omega$ -loop. To further verify how these deletion mutations, which shortened the length yet increased the flexibility of  $\Omega$ -loop, the dynamic motions of the two variants, PenL-Thr171del and PenL-Ile173del, were modeled employing Ensemble Refinement tool [93]. As expected, the  $\Omega$ -loop of the two PenL variants was strongly flexible, in contrast to the sustainable  $\Omega$ -loop in PenL-WT (Figure 19).

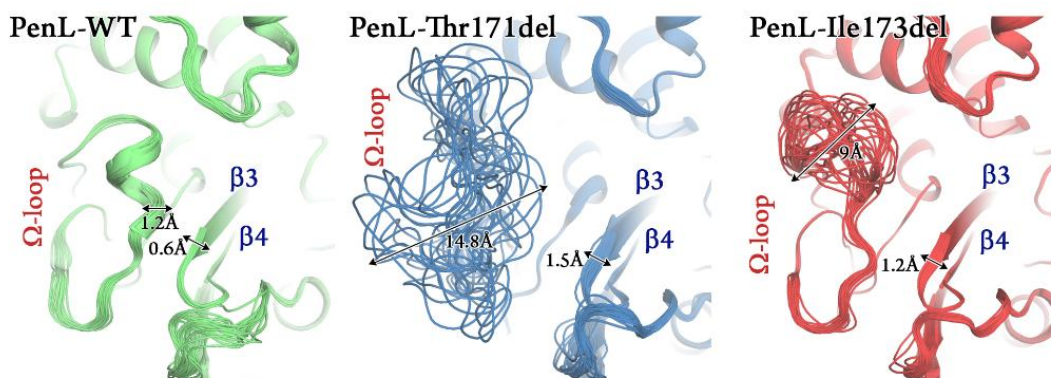


**Figure 19. Modelling dynamic motion of the deletion variants by Ensemble Refinement**

Notice that the entire  $\Omega$ -loop in PenL-Thr171del was more drastically fluctuated, whereas the C-terminal of  $\Omega$ -loop in PenL-Ile173del was steady. This result may explain for the higher CAZ affinity of PenL-Thr171del than PenL-Ile173del (Table 5) because substrate binding space in PenL-Thr171del is more widened upon the motion of  $\Omega$ -loop.

In another notable aspect, the strand  $\beta$ 3 in the two PenL deletion variants appeared to spread with a larger amplitude than that in PenL-WT (Figure 19). This outcome may be accounted by the steric hindrance caused by the drastic movement of  $\Omega$ -loop, likewise the effects that were described

in case of PenL-Asn136Asp. As discussed in the case of two substitution variants PenL-Cys69Tyr and PenL-Asn136Asp, the flexibility of the strand  $\beta_3$  strongly contributes to the substrate spectrum extension of the enzyme. In case of the two deletion mutations, the fluctuation of  $\Omega$ -loop also affects the fluctuation of strand  $\beta_3$  in a slightly similar manner, indicating that the increase in CAZ hydrolysis of them is either attributed by the fluctuation of strand  $\beta_3$ .

In overall, the contributions of the single deletion mutations, Thr171del and Ile173del, to the enhancement of CAZ affinity of the enzyme can be summarized with three following effects: (i) to increase the degree of freedom of  $\Omega$ -loop; (ii) to enlarge the active site cleft; and (iii) to alter the electrostatic potential at active site cleft.

### **3.3. Structural analysis of PenL-Cys69Tyr**

Situated next to the reactive Ser70, the Cys69 should not be involved in neither catalysis nor substrate recognition/binding due to its original orientation in the peptide sequence. Instead, Cys69 side chain directly confronts the strands  $\beta_3\beta_4$  (Figure 20, 21A); hence, the substitution at this position into bulky tyrosine creates the steric hindrance that leading to distortion of the loop  $\beta_3\text{-}\beta_4$  far away from  $\Omega$ -loop (Figure 20, 21B). Notice that half of the residues involved in substrate binding (Thr235, Gly236, Thr237, Gly238, Asp240) and oxyanion hole formation (Thr237) are located on strand  $\beta_3$  (Figure 6, 14). Physical modification on strand  $\beta_3$  and loop  $\beta_3\text{-}\beta_4$  were reported to be responsible for the binding of third-generation cephalosporins. For instance, the direct mutation at Gly238 to Val, Ser, or Cys in an SHV-type  $\beta$ -lactamase produced the steric confliction with Met69 that pushed strand  $\beta_3$  away by 1~2 Å to facilitate the CAZ accommodation, resulting in the decrease in  $K_M$  [94].

Reversely in case of PenL-Cys69Tyr, the mutated site Tyr69 is located outside yet pushes the loop  $\beta$ 3- $\beta$ 4 and  $\Omega$ -loop (Figure 20, 21).

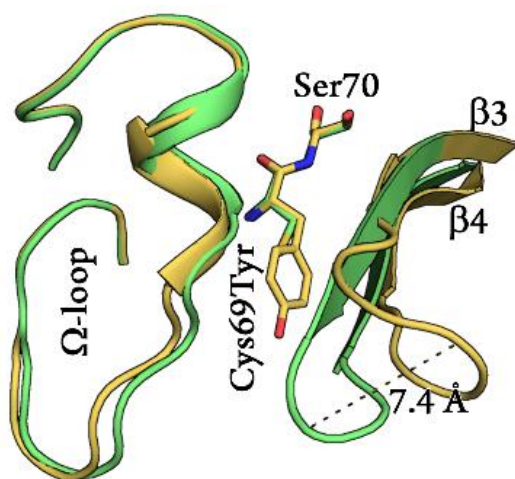


**Figure 20. Effect of mutation Cys69Tyr on  $\Omega$ -loop and strands  $\beta$ 3 $\beta$ 4.**

PenL-WT and PenL-Cys69Tyr are colored in green and yellow, respectively.

As a result, the regions from Gly236-Asp240 (on strand  $\beta$ 3) and Thr243-Gly244 are discharged from strand structure and becomes a loop, prolonging the loop  $\beta$ 3- $\beta$ 4 (Figure 21B). This physical distortion expands the binding cleft. Furthermore, the movement of loop  $\beta$ 3- $\beta$ 4 subsequently pushes the loop  $\beta$ 5- $\alpha$ 8 along the same direction, resulting in the extension of helix  $\alpha$ 8 by four amino acids. Consequently, the Arg275 side chain, which formerly faces down in wild-type enzyme, is rotated  $\sim 180^\circ$  to face toward the cluster Gly236-Thr237-Arg220-Asp276 (Figure 21B, 21D, 21F). This cluster was proved mediate  $\beta$ -lactam binding and hydrolysis of KPC-2  $\beta$ -lactamase [95, 96]. As a consequence, the penetration of Arg276 toward this cluster dramatically switched the electrostatic distribution around the oxyanion hole from slightly negative (originally seen in PenL-WT, Figure 18A) into highly positive (Figure 21C, 21D). This effect facilitates the accommodation of CAZ which possesses two negatively charged group (Figure 12G).

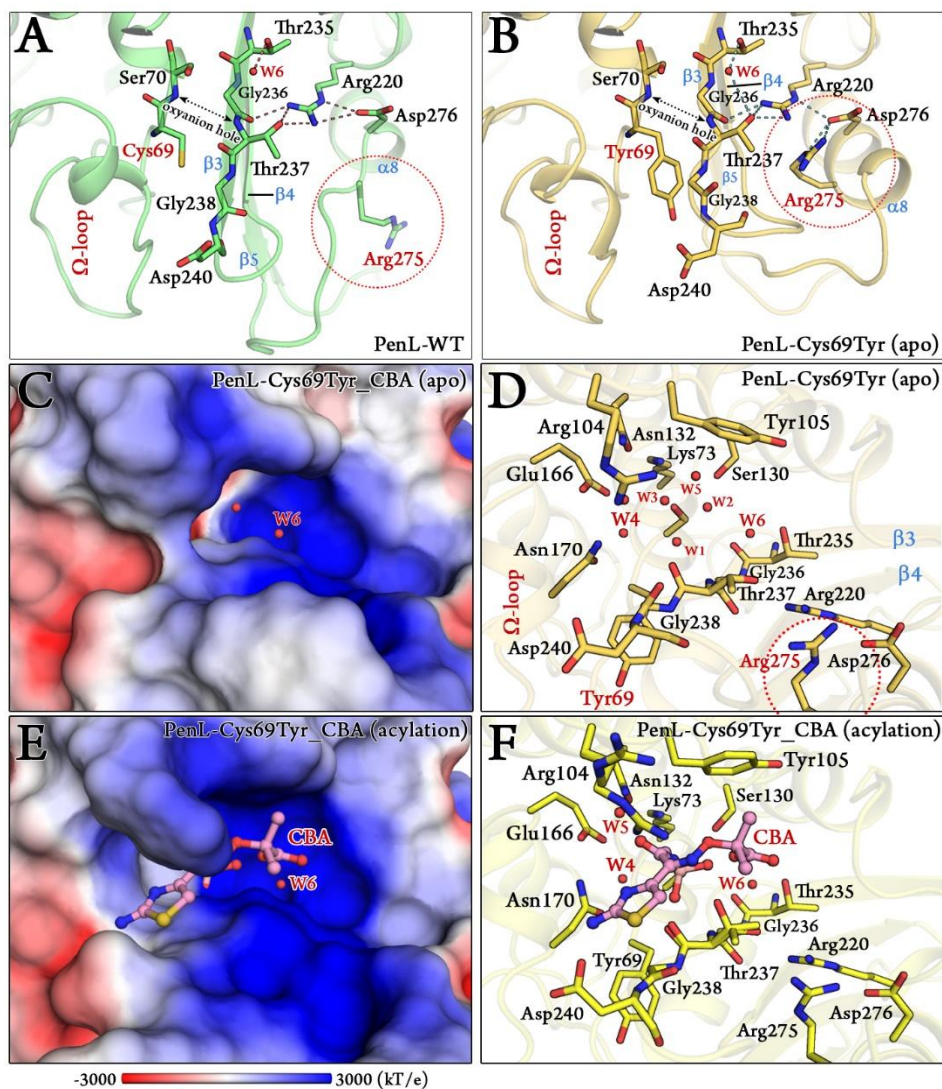


**Figure 21. Structural analysis of PenL-Cys69Tyr.**

(A) Position Cys69 in PenL-WT structure. (B) Serial effects of bulky Tyr69 in the structure of PenL-Cys69Tyr resulted in the rotation of Arg275. (C) and (E) Electrostatic distribution in active site cleft of PenL-Cys69Tyr apo-form and CBA-bound form (acylation), respectively. (D) and (F) Active site cleft of PenL-Cys69Tyr apo-form and CBA-bound form (acylation), respectively, in the same view with (C) and (E).

Upon CBA binding, the orientation of Arg276 is still maintained as in apo-form, but the loop  $\beta 3$ - $\beta 4$  in PenL-Cys69Tyr is slightly shifted backward, where Gly238 and Thr237 participate to the stabilization of CBA acetamido backbone (Figure 21F, 22). The Thr237 side chain shows two conformations from which the hydroxyl group may momentarily interact with both Arg220 side chain and the flexible oxyimino group of CBA (Figure 21F). The residue Asp240 which originally located at the C-terminal end of strand  $\beta 3$  (in wild-type enzyme) also shows movement to interact with the amino group of CBA thiazol ring (Figure 21F, 22). Noted that the CBA in this structure is in acylation form, in which the boron atom is covalently bonded to Ser70 hydroxyl group, and the catalytic water (W4) is ready to attack one of the hydroxyl groups of boron (-OH1), which corresponds to the  $\beta$ -lactam carbonyl group of CAZ (Figure 12G). As expected, the Tyr61 side chain does not interact to CBA (Figure 21F, 22A).

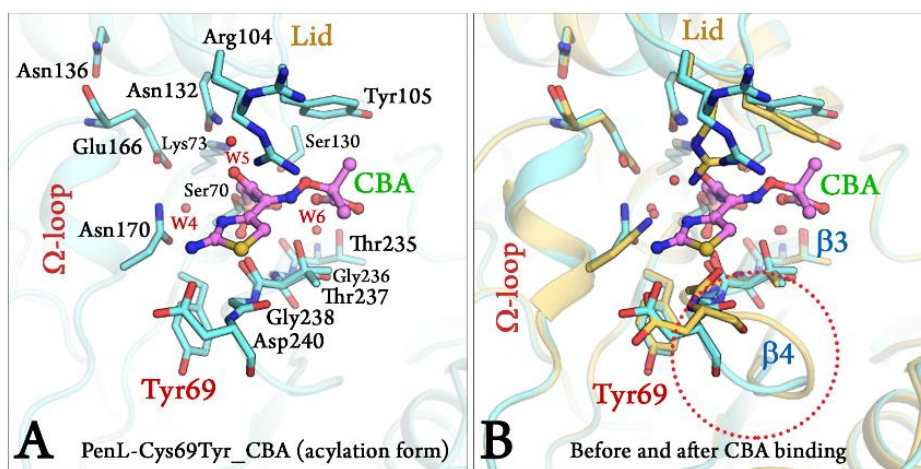


**Figure 22. Conformational changes in PenL-Cys69Tyr upon ligand binding.**

(A) Binding of CBA in active site cleft of PenL-Cys69Tyr, in a slightly different view angle with Figure 16B. (B) Overlapping of PenL-Cys69Tyr apo-form (yellow) with CBA-bound form (cyan) demonstrates fluctuations in structures, especially at loop  $\beta 3$ - $\beta 4$ .



### **3.4. Structural analysis of PenL-Asn136Asp**

Positioned away from active site cleft, Asn136 is also never involved in catalysis or substrate binding. The role of Asn136 is to stabilize the energetically unfavorable non-proline *cis*-peptide Glu166-Thr167 (Figure 23A). Since Glu166-Thr167 is located on  $\Omega$ -loop, Asn136 thus also anchor the  $\Omega$ -loop *via* two hydrogen bonds with Glu166 backbone (Figure 23A). The replacement Asn136 to aspartate abolishes on hydrogen bond (Figure 23B), which probably lead to an increase in flexibility of  $\Omega$ -loop. To our surprise, the structure of PenL-Asn136Asp demonstrates no significant difference in comparison with PenL-WT. Nonetheless, PenL-Asn136Asp can accommodate the CBA into its active site wherein the conformation does not change substantially. Residue Arg275 also adopts the same configuration as that of the wild-type enzyme, certainly does not lead to alteration of electrostatic distribution around active site cleft as seen in PenL-Cys69Tyr described in previous section (data not shown). In overall, no considerable distinction between PenL-Asn136Asp and PenL-WT, as well as between PenL-Asn136Asp apo-form, acylation- and deacylation-CBA-bound form, is observed. The interesting question is raised here, on the manner that the excessively negative CAZ can be strongly attracted into a negative active site cleft PenL-As136Asp (Figure 24) which is not different from that of PenL-WT (Figure 18A). Taking together with the CD spectra data (Figure 13), these observations indicating that the increase in binding of CAZ into its active site should be governed by latent factors other than the electrostatic attraction seen in PenL-Cys69Tyr, and could not be revealed in the static crystal structure.

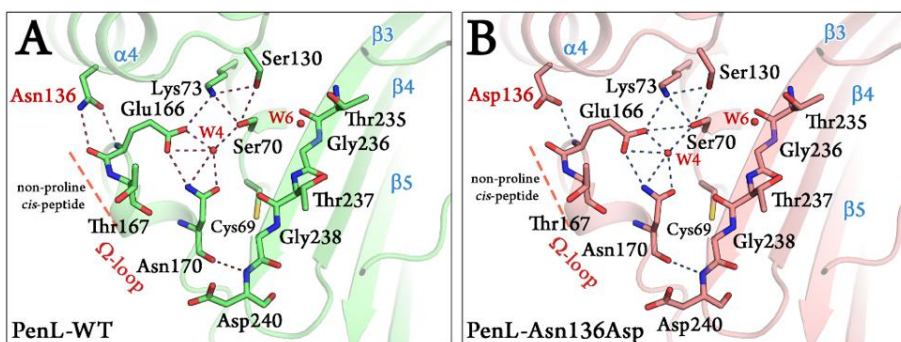


**Figure 23. Structural analysis of PenL-Asn136Asp.**

(A) Position of Asn136Asp in PenL-WT structure. (B) Substitution of Asn136 into Asp abolishes one hydrogen bond to stabilizes the non-proline *cis*-peptide Glu166-Thr167.

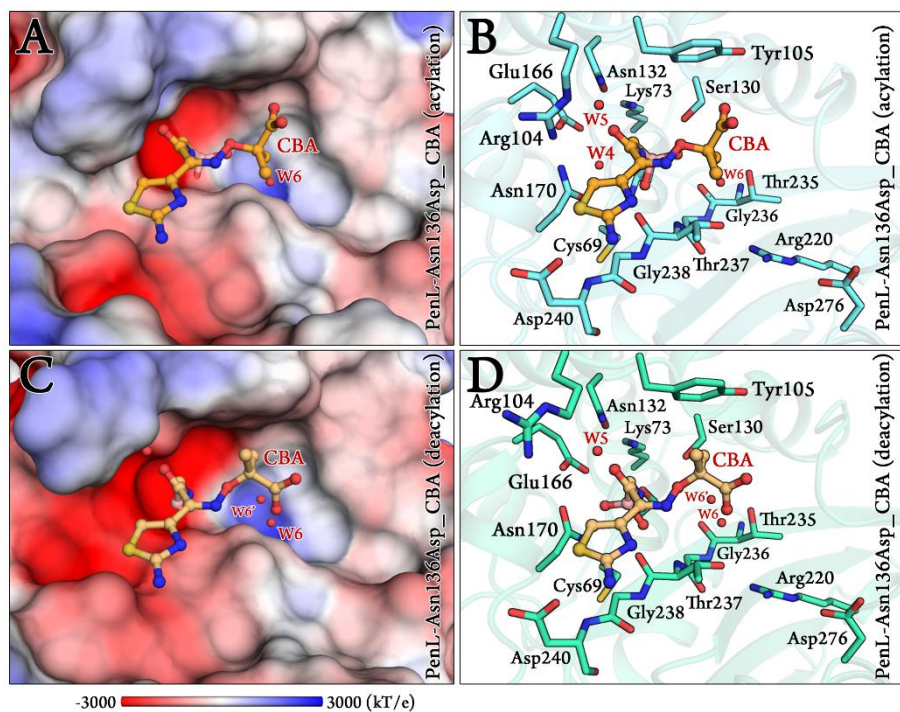


**Figure 24. Binding of ligand into active site of PenL-Asn136Asp.**

(A) and (B) show the CBA binding mode in acylation form, while (C) and (D) display the CBA in deacylation form. Movement of Arg104 may raise the apparent alteration in electrostatic distribution.

We thereby suggested two hypotheses. First, the higher degree of freedom would be induced to  $\Omega$ -loop of PenL-Asn136Asp owing to the loss of one hydrogen bond by the mutation Asn136Asp occurred outside the  $\Omega$ -loop. This effect, indeed, would resemble other ESBL cases in class A  $\beta$ -lactamase where the stabilization network on  $\Omega$ -loop *per se* was devastated, i.e. the displacement at Ambler position Arg164 or Asp179 [89, 90] (Table 6). In those cases, the enhanced flexible motion of  $\Omega$ -loop resulted in the transient enlargement of active site cleft, which was proposed to facilitate the accommodation of third-generation cephalosporins. The akin effect would be able to ascribe to PenL-Asn136Asp. Second, the mutation Asn136Asp may create an intrinsic dynamic conformer that would efficiently accommodate CAZ. The viewpoint of promiscuity in protein conformation has been suggested formerly, whereby the evolvability of proteins to adapt novel substrates would be promoted by the conformational diversity caused by accumulation of single mutations [97].

The molecular dynamics (MD) simulation is therefore conducted to compare the dynamic property of PenL-Asn136Asp with PenL-WT. The RMSD plot (Figure 25) indicates that the overall structure of PenL-Asn136Asp was stable through 50 ns trajectory, and roughly similar to PenL-WT. However, RMSD at three critical segments of PenL-Asn136Asp, as similar as PenL-Cys69Tyr, was higher than PenL-WT, and appeared to fluctuate robustly, especially at the lid region (Figure 25). Furthermore, the radius of gyration (Rgyr) plots also demonstrate potential unfolding of two PenL substitution variants, in contrast to the sustainable motion of PenL-WT (Figure 26). These observations strongly suggest that PenL-Asn136Asp (and PenL-Cys69Tyr) has higher tendency for disorder than PenL-WT, which is correlated with the higher adaptability toward CAZ in term of *protein dynamism* [97].

In the further analysis, the root mean squared fluctuation (RMSF) plot shows that, the three critical segments  $\Omega$ -loop, lid, and strands  $\beta 3\beta 4$  fluctuated in higher degree than those of PenL-WT (Figure 27). The RMSF analysis result is well consistent with RMSD and Rgyr analyses above.

Intuitively, in PenL-WT, the conformations of primary residues such as Asn136, Glu166, reactive Ser70, and the three essential catalytic segments were sustainable through MD trajectory (Figure 28, LEFT). In contrast, the mutated Asp136 side chain in PenL-Asn136Asp dramatically swung away ( $\sim 6.3 \text{ \AA}$ ) from the Glu166 backbone, leading to the robust fluctuation of Glu166 on  $\Omega$ -loop and Ser70 (Figure 28, RIGHT). Afterward, the high degree fluctuation of  $\Omega$ -loop and Ser70 likely pushes the loop  $\beta 3$ - $\beta 4$  via steric confliction, which simultaneously augmented by a breakdown of the hydrogen bond between Asn170 on  $\Omega$ -loop and Asp240 on  $\beta 3$  (Figure 28, RIGHT). The changes in the regions, which intensively involved in substrate recognition, may result in the momentary expansion of the active site space and the improvement of CAZ binding, likewise observed from PenL-Cys69Tyr.

Especially, residue Arg275 in PenL-Asn136Asp never rotated to adopt similar conformation of Arg275 in PenL-Cys69Tyr (data not shown), suggesting that the electrostatic potential in active site cleft of PenL-Asn136Asp should not be altered as was seen in PenL-Cys69Tyr but interestingly identical with that of PenL-WT. Therefore, the comparable  $K_M$  values (in both phases of biphasic kinetic course) of PenL-Asn136Asp in respect to PenL-Cys69Tyr indicates that an unknown factor may drive the increase in CAZ affinity of PenL-Asn136Asp. It is worth to propose that, the CAZ affinity enhancement in PenL-Asn136Asp would be synergistically attributed by the dynamic motions of all three critical segments  $\Omega$ -loop, lid, and strands  $\beta 3$  $\beta 4$ , under the effect of the mutation. In other words, the substitution effect eventually reached to both three critical segments surrounding active site, so that it favored the momentary conformation of the enzyme that elevated the facile CAZ accommodation [97, 98].

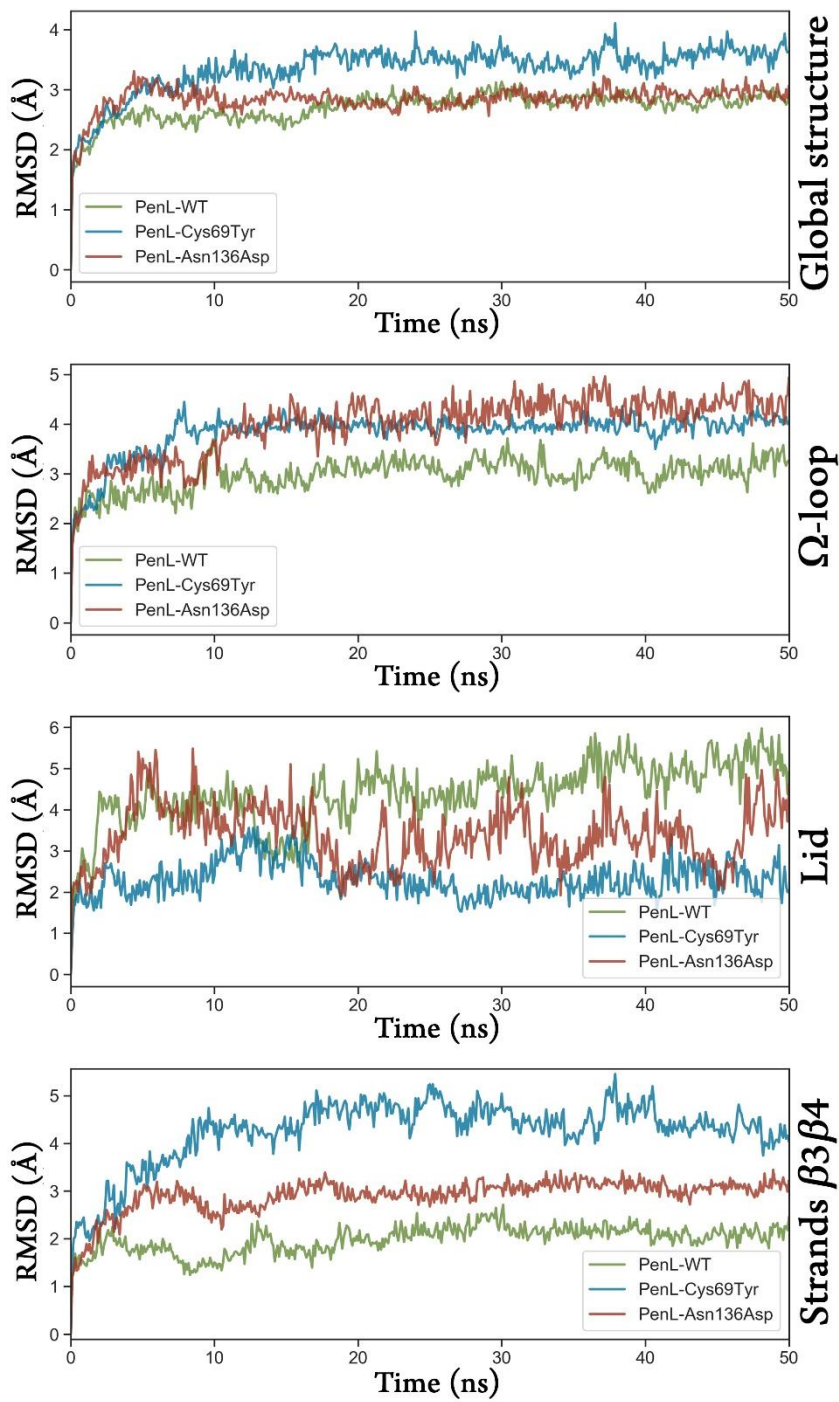


**Figure 25.** Root mean squared deviation (RMSD) of PenL-Asn136Asp during 50 ns simulation  
 The RMSD of PenL-WT and PenL-Cys69Tyr are shown as reference.

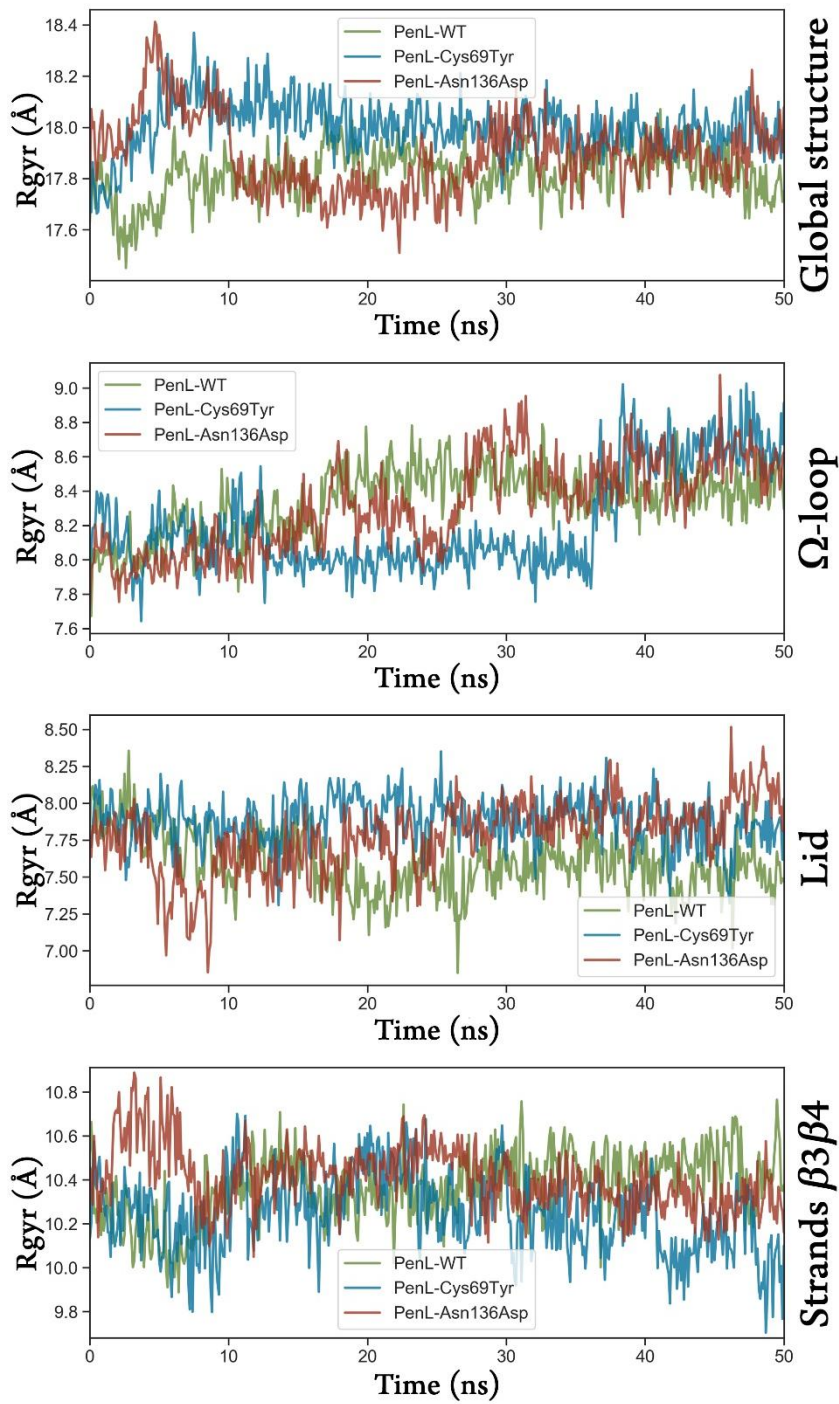


**Figure 26. Radius of gyration (Rgyr) of PenL-Asn136Asp during 50 ns simulation**

The Rgyr of PenL-WT and PenL-Cys69Tyr are shown as reference.

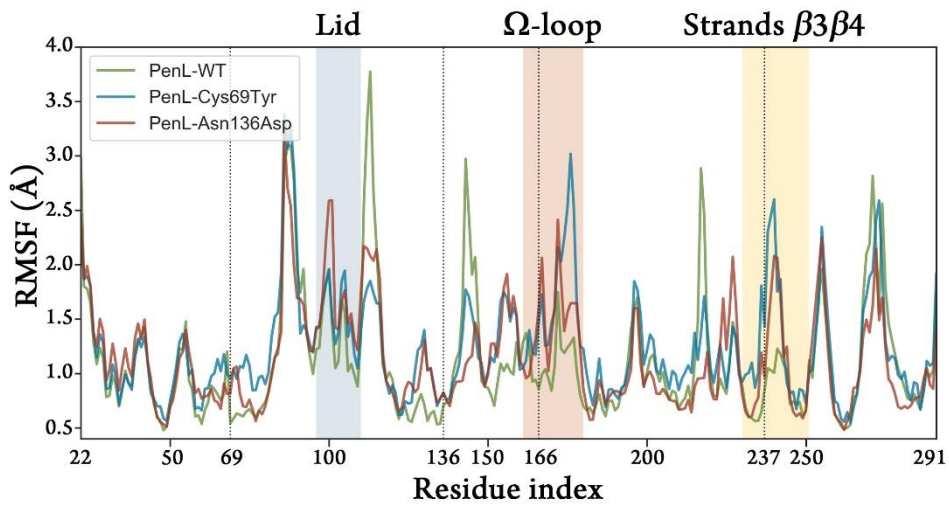


**Figure 27. Root mean squared fluctuation (RMSF) at C $\alpha$  of PenL-Asn136Asp during 50 ns simulation**

RMSF of PenL-WT and PenL-Cys69Tyr are shown as reference.

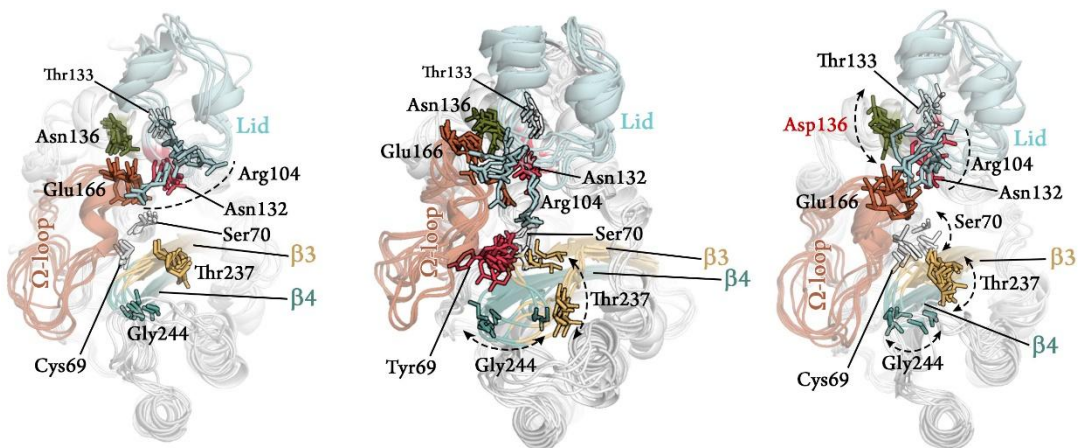


**Figure 28. Conformation of PenL-Asn136Asp during 50 ns simulation**

RMSF of PenL-WT and PenL-Cys69Tyr are shown as reference.

### **3.5. Role of Arg104, Tyr105 in substrate recognition**

In both CBA-bound complex structures of PenL ESBL variants that have been obtained so far, the tetrahedral intermediate of the substrate is certainly stabilized by the typical oxyanion hole, which is well studied in class A  $\beta$ -lactamases. The typical oxyanion hole, which comprised by N atoms of reactive Ser70 and Thr237, and water W6 (Figure 29), is responsible for sustaining the carbonyl group of  $\beta$ -lactam backbone once the  $\beta$ -lactam is attacked by nucleophilic Ser70. Interestingly, we discovered another potential oxyanion hole that further stabilizes the substrate intermediate. This oxyanion hole may be attributed by Asn132 N $\delta$ , Arg104 N $\epsilon$  and N $\eta$ 1 (or N $\eta$ 2 optionally), and water W5 (Figure 29). The presence of this potential oxyanion hole has been described sometimes previously in case of ESBLs that possess N-contained residues such as Asn or Gln [45, 99]. Nonetheless, to best of our knowledge, the term “the second oxyanion hole” has not been recommended so far, may be due to the accepted canonical definition that, oxyanion hole stabilizes the transition state negative charge on deprotonated oxygen or alkoxide that developed from a nucleophilic attack [100]. With this regard, the interaction network Asn132-Arg104-W6 may not be recognized as a full-feature oxyanion hole, because this network merely stabilizes the acetamido hydroxyl group of CBA (Figure 29), which is permanently present in the ligand (in both CBA and CAZ, Figure 12G). Although the definition may be controversial to some extent, the appearance of "the potential second oxyanion hole" in the structure of PenL ESBL variants further stabilizes the substrate intermediate.

It should be recalled that Arg104 is available in either PenL-WT. As was mentioned in *Introduction* part, the occupation of Arg at position 104 is one of the reasons for the intrinsic CAZ hydrolysis ability of PenL-WT, in comparison the other non-ESBL class A  $\beta$ -lactamases that possess an acidic residue at this position, e.g., TEM-1 [43] and SHV-1 [42]. It has been proposed so far that a basic or N-contained residue at position 104 may mediate the binding of the negative oxyimino



group of oxyimino-cephalosporins. However, as observed in our structural data, the oxyimino group directly interact with the aromatic Tyr105 *via*  $\pi$ -anion interaction, whereas Arg104 may attract it by electrostatic interaction rather than direct hydrogen bond or salt bridge (Figure 17B, 17D, 21F, 24B, 24D). Tyr105 is less agitated due to its rigidity so that its fluctuation is moderately restricted to adapt the substrate oxyimino group.

On the other hand, the flexible movement of Arg104 can modulate the electrostatic potential in the active site cleft (Figure 17, 21, 24). Even further, in CBA-deacylation-bound form of PenL-Asn136Asp in which the ligand is mimicking the stage just before product release, Arg104 discharged from the interaction network with Asn132 and water W5, disrupting “the potential second oxyanion hole” (Figure 29C). Taken together, it can be concluded that the fluctuation of Arg104 is one of the important factors that facilitate the accommodation of CAZ into active site cleft of PenL.

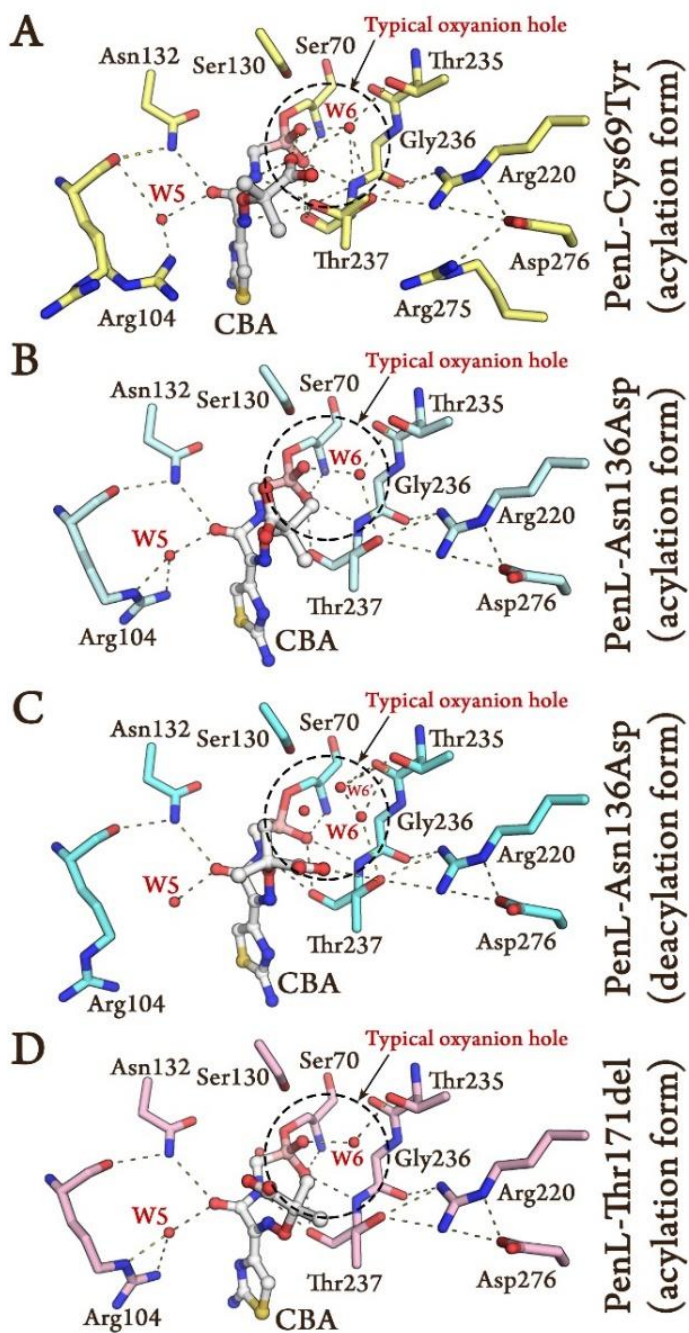


**Figure 29. Role of Arg104 in substrate binding.**

The typical oxyanion hole is comprised by N atoms of reactive Ser70 and Thr237, and water W6 (sometimes is called oxyanion water in literatures). The “potential second oxyanion” is formed by Asn132 N $\delta$  atom, Arg104 N $\epsilon$  and N $\eta$ 1 (or N $\eta$ 2 optionally) atoms, and water W5. Notice that the projection of Arg275 only occurs in PenL-Cys69Tyr (A).

## **IV. PERSPECTIVE**

## IV. PERSPECTIVE

### Effects of single mutations on the ceftazidime hydrolysis enhancement of PenL $\beta$ -lactamase

The emergence of ESBLs has been identified and studied roughly half of century, with remarkable cases reported in class A  $\beta$ -lactamase, not to mention the other three classes. In most cases, ESBLs are induced by mutations that directly occurred in three critical segments involved in catalysis and substrate recognition:  $\Omega$ -loop (160-180 by the Ambler system), lid (92-118), and strands  $\beta$ 3- $\beta$ 4 (230-251), as was categorized in two most common types of class A  $\beta$ -lactamase, SHV and TEM (<https://www.lahey.org/Studies/> and Appendix 1 Table 6). Wherein, the mutations unambiguously affect the properties of the segments, for instance, increase the flexibility of  $\Omega$ -loop [41, 90, 101], improve the binding space by mutations on strand  $\beta$ 3 [89, 94, 102], or alter charged property at position 104 on lid [32, 103]. It should be noted that several of mutations occurred outside of these three regions, yet those are proved to stabilize the structural integrity of the enzyme [58, 89, 102, 104] so that they always emerged in accompany with certain major mutation(s) arise in one of three critical segments. Therefore, the single mutations in PenL  $\beta$ -lactamase that are reported in this thesis are distinctively attracted because they occur at the residues outside those three critical segments (Cys69Tyr and Asn136Asp), or on  $\Omega$ -loop yet participate in neither catalysis nor substrate binding (Thr171del and Ile173del). The emergence of ESBLs caused by substitution at the Ambler position 69 is isolated in frequent among class A  $\beta$ -lactamases [58, 62, 104-111], especially in case Cys69Tyr of PenI that was isolated from a patient infected with *B. pseudomallei* [54, 55], yet the lack of high-resolution structure has restricted the insightful explanation for its effect. Whereas, the

substitution mutation Asn136Asp and two deletion mutations Thr171del, Ile173del are the novel reported ESBL [14].

In this study, we described the first ever structure of Cys69Tyr in Pen-type  $\beta$ -lactamases, PenL. We also determined the high-resolution structures of the other mutations, Asn136Asp, Thr171del, and Ile173del, in complex with the ligand. Together with CD and MD analysis, our data reveal that those single mutations finally converge to the influence on critical segments, particularly  $\Omega$ -loop and strands  $\beta 3\beta 4$ . As a consequence, these structural effects lead to change in the kinetic property of the enzyme, specifically the CAZ binding affinity ( $K_M$ ) and reaction rate ( $k_{cat}$ ).

### ***Single mutations on outside residues influence both $\Omega$ -loop and strands $\beta 3\beta 4$***

$\Omega$ -loop and strands  $\beta 3\beta 4$  are the two most critical segments in the structure of  $\beta$ -lactamase since these two segments are involved in both catalysis and substrate recognition. Because of their sensibility, a certain change in their property would result in alteration on the feature of the enzyme, i.e., the substrate specificity. Therefore in most ESBLs, the substitution mutations on these two regions are predominant. In some cases, the insertion mutations on  $\Omega$ -loop extend its length and the number of residues involved in substrate recognition, thus enhance the hydrolysis ability of enzyme toward third-generation cephalosporins [15, 41, 112].

In contrast, the two deletion mutations Thr171del and Ile173del, despite shortening the length of  $\Omega$ -loop but confer the increase in CAZ hydrolysis ability to PenL. Originally, Thr171 and Ile173 never participate in catalysis or substrate recognition. The single deletions of these two amino acids were shown to expand the substrate binding cavity and rearrangement of residues on  $\Omega$ -loop (Figure 15, 16), which resulting in the electrostatic alteration potential in the active site cleft (Figure 17, 18). The shortened  $\Omega$ -loop might be thought to be less flexible than the original one, however, our structural data demonstrate that the  $\Omega$ -loop of the two deletion mutations, Thr171del and Ile173del,

is more agitated than that of the wild-type enzyme (Figure 19), which may lead to the disruption in the peptide backbone of  $\Omega$ -loop (Figure 17). Notice that the more drastic flexibility of  $\Omega$ -loop in PenL-Thr171del (Figure 19) may correlate to its 3-fold higher CAZ affinity in respect to PenL-Ile173del, expressed by their  $K_M$  values are of  $16.118 \pm 0.514$  and  $52.074 \pm 4.390 \mu\text{M}$  (Table 5). Furthermore, the high degree fluctuation of  $\Omega$ -loop also caused the increase in fluctuation of strand  $\beta_3$  in these two deletion variants (Figure 19).

In another aspect, our data demonstrate that the single substitution mutations occur outside  $\Omega$ -loop, and even outside strands  $\beta_3\beta_4$  also create similar effects. Specifically, the steric hindrance created by mutation Cys69Tyr pushed both strands  $\beta_3\beta_4$  and  $\Omega$ -loop, making a wider active site cleft (Figure 20, 21). The rearrangements also prompted the projection of Arg275 toward the cluster Arg220-Asp276-Thr237 that is important for substrate binding (Figure 22), switching the electrostatic potential around the typical oxyanion hole into highly positive so that the excessively negative CAZ would be firmly attracted. The Asn136Asp, on the other hand, enhanced the flexibility of  $\Omega$ -loop by loosening the anchoring of non-proline *cis*-peptide Glu166-Thr167 (Figure 23). As a consequence, the movement of  $\Omega$ -loop also created steric confliction to dynamically push strands  $\beta_3\beta_4$ , resulting in the momentary enlargement of the active site cleft (Figure 28). Interestingly, although the electrostatic property at active site cleft of PenL-Asn136Asp is not switched into positive as was seen in static crystal structure (Figure 23), the dynamic rearrangement of  $\Omega$ -loop and strands  $\beta_3\beta_4$  has still resulted in comparable CAZ affinity of PenL-Asn136Asp as of PenL-Cys69Tyr, expressed by their  $K_M$  values are of  $14.140 \pm 0.975$  and  $10.475 \pm 0.537 \mu\text{M}$  for initial phase, and  $4.528 \pm 0.182$  and  $2.165 \pm 0.011 \mu\text{M}$  for final phase, respectively (Table 5). However, we could not rule out the nature of biphasic kinetics of PenL-Asn136Asp at the moment.

## ***Effect on strand $\beta_3\beta_4$ is more critical than on $\Omega$ -loop in term of CAZ affinity enhancement***

As has been described so far, the two substitution mutations, Cys169Tyr and Asn136Asp, which affect more drastic on strands  $\beta_3\beta_4$  has higher CAZ affinity than the two deletion mutations, Thr171del and Ile173del, which majorly influence the  $\Omega$ -loop. With this observation, it is tempting to suggest that the fluctuation on strands  $\beta_3\beta_4$  is more critical than the fluctuation of  $\Omega$ -loop for the binding of CAZ into active site cleft of PenL, and Pen-type  $\beta$ -lactamase in general. In consistency, previous studies also proposed that mutations on strand  $\beta_3$  and/or the loop  $\beta_3$ - $\beta_4$  increase the recognition of class A  $\beta$ -lactamases toward third-generation cephalosporins [48, 94]. In this regard, it is worth to collect and analyze all the kinetic property of the ESBLs that confer the resistance to third-generation cephalosporins for bacteria. However, because of the extremely poor spectroscopic property of CAZ, it is very difficult to directly obtain the kinetic parameters for this substrate among class A  $\beta$ -lactamases. In most cases, the  $K_M$  and  $k_{cat}$  values for CAZ of ESBLs was not measurable or represented by competition parameter  $K_I$  and  $k_{inact}$ , respectively. Therefore, the proposal that strands  $\beta_3\beta_4$  are more critical for the binding of CAZ requires further attempts to clarify.

In summary, our study provides the evidence underlying the critical role of strands  $\beta_3\beta_4$ , besides the  $\Omega$ -loop, in substrate spectrum alteration of Pen-type class A  $\beta$ -lactamase. In a good agreement, because the two substitution mutations Cys69Tyr and Asn136Asp influence the strands  $\beta_3\beta_4$  more robustly, the CAZ affinity of these two PenL variants is higher than that of the two deletion mutations Thr171del and Ile173del, may up to  $\sim 26$  folds (Table 5). Nonetheless, upon the expansion of active site cleft by movement of strands  $\beta_3\beta_4$ , the  $\beta$ -lactam substrate might be restrained slightly away from reactive Ser70, resulting in the decrease in  $k_{cat}$  value of the two substitutions mutations [94] up to  $\sim 12$  folds in comparison with that of two deletion mutations (Table

5). Furthermore, the augmented  $K_M$  may lead to the formation of the stable acyl-enzyme complex that slows down the reaction rate, explaining for the biphasic kinetics of the CAZ hydrolysis by the two PenL substitution variants (Figure 12A). On the other hand, the reasonable decrease in  $K_M$  and  $k_{cat}$  in the two PenL deletion variants results in greater catalytic efficiency  $k_{cat}/K_M$  value from  $\sim 2$  to  $\sim 6$  folds, in respect to the two substitution variants (Table 5). The  $k_{cat}/K_M$  values in our work are consistent with the previously published MIC values presented in Figure 5, which demonstrated the more resistance to CAZ in *B. thailandensis* that acquired deletion variant PenL-Thr171del or PenL-Ile173del than that bacterium possesses substitution variant PenL-Cys69Tyr or PenL-Asn136Asp.

## Implication to drug design and medical treatment against *Burkholderia* pathogens

The understandings described in this study about the molecular mechanism for the CAZ resistance of *Burkholderia* through the evolution of PenL  $\beta$ -lactamase may imply strategy for potential drug design. One of the examples is to preferably block the fluctuation of strands  $\beta 3$ - $\beta 4$ . Or, in case when the emergence of the mutant Cys69Tyr had been identified, the novel types of  $\beta$ -lactamase inhibitors can be developed with extra negative charged groups. This kind of inhibitor could be used in a combination which would help to improve the effectiveness of ceftazidime treatment.

On the other hand, the current study alerts the potential emergence of novel and unanticipated ESBLs in which the ability to hydrolyze the latest antibiotics of the enzyme can be enhanced by any single mutation regardless of the position they occur. For instance, likewise CAZ, the monobactam aztreonam (AZT) also possesses two negatively charged groups which may be strongly attracted to



the ESBLs like Cys69Tyr variants (Figure 12G), etc. The usage of  $\beta$ -lactam antibiotics should be therefore attentively prudent. In fact, over ninety years since the first  $\beta$ -lactam, penicillin was discovered (1928), and seventy-six years since penicillin was approved to be used in treatment, human being has invented and innovated many kinds of  $\beta$ -lactam drug which intentionally to prevent or avoid the action of  $\beta$ -lactamases. Nevertheless, the adaptability of  $\beta$ -lactamases are much faster and more sophisticated than the innovation of drugs, leaving the difficulty for the human being to defeat the pathogens. The development of novel drugs, therefore, should not be longer focused on the improvement of  $\beta$ -lactam drug, yet the better strategy should consider on other targets, e.g. the expression of  $\beta$ -lactamase. With this regard, the promoter of  $\beta$ -lactamase gene, and the corresponding transcription factors should be profoundly considered.

*Thinh-Phat Cao Ph.D. Dissertation*

*Chosun University, Department of Biomedical Science*

---

## **V. Appendix 1: Supplementary Data**

## V. Appendix 1: Supplementary Data

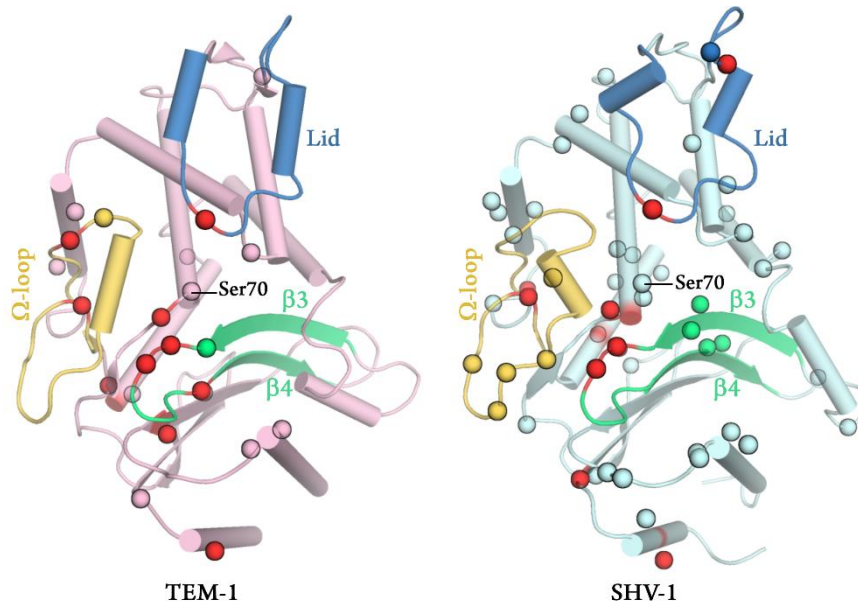


**Figure 30. Appendix: Variation positions in TEM and SHV  $\beta$ -lactamases that promote ESBL emergence.**

Three critical catalytic segments are colored in yellow ( $\Omega$ -loop), blue (Lid), and green (strands  $\beta_3\beta_4$ ). The hotspots where the mutations occur frequently are colored in red. The information in this figure is curated from Appendix 1 Table 6.

**Table 6. Appendix: Hotspots of mutation that induce the emergence of ESBLs on TEM and SHV  $\beta$ -lactamases**

This table is adopted from <https://www.lahey.org/Studies/>, in which, the listed ESBL cases have been described with references. The variants which have only genebank number or have not been recognized as ESBL are excluded. This table has been updated up to November 2018.

ESBL	Alternative name	Segment						PDB ID	Ligand	Structure-based explanation	Ref
		$\Omega$ -loop	Lid	Strands $\beta$ 3- $\beta$ 4	$\alpha$ 1- $\beta$ 1	$\beta$ 5	Other				
TEM-3	CTX-1, TEM-14		E104K	G238S	Q39K					[113]	
TEM-4			E104K	G238S	L21F	T265M				[114, 115]	
TEM-5	CAZ-1	R164S		A237T, E240K						[115, 116]	
TEM-6		R164H	E104K							[117, 118]	
TEM-7		R164S			Q39K					[119]	
TEM-8	CAZ-2	R164S	E104K	G238S	Q39K					[105, 120, 121]	
TEM-9	RHH-1	R164S	E104K		L21F	T265M				[117, 122]	
TEM-10	MGH-1, TEM-E3, TEM-23	R164S		E240K						[105, 123, 124]	
TEM-11	CAZ-1o	R164H			Q39K					[105, 118, 125]	
TEM-12	YOU-2, CAZ-3, TEM-E2	R164S								[105, 126, 127]	
TEM-13					Q39K	T265M				[105, 118]	
TEM-15			E104K	G238S						[105, 118]	

Think-Phat Cao Ph.D. Dissertation

Chosun University, Department of Biomedical Science

TEM-16	CAZ-7	R164H			Q39K						[119, 121]
TEM-17			E104K								[128]
TEM-18			E104K		Q39K						[118]
TEM-19				G238S							[118]
TEM-20		D179T		G238S							[129-131]
TEM-21			E104K	G238S	Q39K		H153R				[129-132]
TEM-22			E104K	A237G, G238S	Q39K						[131, 133]
TEM-24	CAZ-6	R164S	E104K	A237T, E240K	Q39K						[105, 120, 121]
TEM-25	CTX-2			G238S	L21F	T265M					[127, 134]
TEM-26	YOU-1	R164S	E104K								[135]
TEM-27		R164H		E240K		T265M					[136]
TEM-28		R164H		E240K							[137]
TEM-29		R164H									[130]
TEM-30	IRT-2, TRI-2, E-GUER			R244S				1LHY		R244S: removes a conserved water that coordinates to R244, V216 and $\beta$ -lactam C3 atom $\rightarrow$ reduce affinity and proper orientation of inhibitor	[58, 138, 139]
TEM-31	IRT-1, TRI-1, E-SAL			R244C							[138, 139]
TEM-32	IRT-3						M69I, M182T	1L10		<ul style="list-style-type: none"> <li>M69I causes distortion on S70 <math>\rightarrow</math> conformational change in S130 that reduces its nucleophilicity <math>\rightarrow</math> weakening cross-linking of inhibitor with S70 and S130</li> </ul>	[58, 104]

										• M182T: strengthens the dense hydrogen bond network that stabilizes the active site	
TEM-33	IRT-5						M69L				[62, 105-107]
TEM-34	IRT-6						M69V	1LI9		M69V: causes distortion on S70 → conformational change in S130 → attenuated S130 O <sup>γ</sup> by K73 and K234 → reduces nucleophilicity of S130 and cross-linking of inhibitor with S70 and S130	[58, 106]
TEM-35	IRT-4						M69L, N276D				[106]
TEM-36	IRT-7						M69V, N276D				[106]
TEM-37	IRT-8						M69I, N276D				[140]
TEM-38	IRT-9						M69V, R275L				[140]
TEM-39	IRT-10	W165R					M69L, N276D				[140]
TEM-40	IRT-167						M69I				[107, 108]
TEM-42				G238S, E240K	Q39K, A42V	T265M					[141]
TEM-43		R164H	E104K				M182T				[142]
TEM-44	IRT <sub>2</sub> -2, IT-13			R244S	Q39K						[143]
TEM-45	IRT-14						M69L, R275Q				[144]
TEM-46	CAZ-9	R164S	E104K	E240K	Q39K						[103]
TEM-47				G238S, E240K		T265M					[145]
TEM-48				G238S, E240K	L21F	T265M					[145]
TEM-49				G238S, E240K	L21F	T265M	S268G				[145]

TEM-50	CMT-1		E104K	G238S			M69L, N276D				[109]
TEM-51	IRT-15			R244H							[146]
TEM-52			E104K	G238S			M182T	1HTZ		<ul style="list-style-type: none"> <li>• G238S: expands active site</li> <li>• E104K: stabilizes the reorganized topology (of the active site?)</li> <li>• M182T: stabilizes the enzyme</li> </ul>	[89, 102]
TEM-53		R164S			L21F						[105]
TEM-54				R244L							[105]
TEM-56			E104K		Q39K		H153R				[147]
TEM-58				R244S		V262I					[148]
TEM-59	IRT-17				Q39K		S130G				[149]
TEM-60		R164S	E104K		Q39K, L51P						[150]
TEM-61	CAZ-hi	R164H		E240K	Q39K						[105]
TEM-63	TEM-64	R164S	E104K		L21F		M182T	1JWZ		R164S: breaks the inherent salt bridge between R164-E171 that stabilizes $\Omega$ -loop $\rightarrow$ increases flexibility of $\Omega$ -loop and expands active site cleft	[90, 101]
TEM-65				R244C	Q39K						[151]
TEM-66			G92D, E104K	G238S	Q39K						[151]
TEM-67				R244C	L21I, Q39K						[152]
TEM-68	CMT-2			G238S, E240K		T265M	R275L				[153]
TEM-71				G238S, E240K							[154]
TEM-72				G238S, E240K	Q39K		M182T	3P98	Citrate (in crystallization buffer)	Increase flexibility, especially at loop $\beta$ 4- $\beta$ 5	[155, 156]
TEM-73	IRT-18			R244C	L21F	T265M					[151]

Think-Phat Cao Ph.D. Dissertation

Chosun University, Department of Biomedical Science

TEM-74	IRT-19			R244S	L21F	T265M					[151]
TEM-75		R164H			L21F	T265M					[157]
TEM-76	IRT-20						S130G	1YT4		S130G: no side chain → prevents the cross-linking of inhibitor to S70 and S130 (two waters are displaced in S130 side chain position instead)	[110, 158]
TEM-77	IRT-21			R244S			M69L				[110]
TEM-78	IRT-22	W165R					M69V, N276D				[110]
TEM-79				R244G							[110]
TEM-80	IRT-24						M69L, I127V, N276D				[111]
TEM-81							M69L, I127V				[111]
TEM-82							M69V, R275W				[111]
TEM-83		W165C					M69L, R275W				[111]
TEM-84							N276D	1CK3		<ul style="list-style-type: none"> <li>• Significant movement of D276</li> <li>• Salt bridge formation between D276 and R244, the counterion of inhibitor carboxylate</li> <li>• Lacking of critical water for the inactivation by clavulanate</li> </ul>	[111, 159]
TEM-85		R164S		E240K	L21F	T265M					[160]
TEM-86		R164S		R237T, E240K	L21F	T265M					[160]
TEM-87		D163H, R164C	E104K		Q6K		M182T				[161]
TEM-88			E104K	G238S			M182T, G196D				[162]
TEM-89	CMT-3		E104K	G238S	Q39K		S130G				[163]
TEM-90	TLE-1		D115G								[164]



*Think-Phat Cao Ph.D. Dissertation*

*Chosun University, Department of Biomedical Science*

TEM-91		R164C		E240K			M182T			[165]
TEM-92			E104K	G238S	Q6K		M182T			[166]
TEM-93				G238S, E240K			M182T			[160]
TEM-94			E104K	G238S	L21F	T265M	M182T			[160]
TEM-95							P145A			[167]
TEM-102		R164S			L21F	T265M				[168]
TEM-103	IRT-28						R275L			[169]
TEM-109	CMT-5	R164H	E104K				M69L			[170]
TEM-110					L21F	T265M				[171]
TEM-112				G238S			H153R			[172]
TEM-113			E104K	G238S	Q39K		M182T			[172]
TEM-114		R164S		A237T, E240K	Q39K					[172]
TEM-115		R164H			L21F					[173]
TEM-118	TEM-HM	R164H				T265M				[174]
TEM-120				G238S	L21F					[172]
TEM-121	CMT-4	R164S	E104K	A237T, E240K, R244S	Q39K					[175]
TEM-122							R275Q			[176]
TEM-125	CMT-type	R164S, W165R			F16L		M69L, N276D			[177]
TEM-126		D179E					M182T			[172]
TEM-129		R164S	E104K		Q39K					[178]
TEM-131		R164S	E104K	A237T	L21F		M182T			[179]

*Think-Phat Cao Ph.D. Dissertation*

*Chosun University, Department of Biomedical Science*

TEM-132		R164H, I173V		E240K						[180]
TEM-133		R164S	E104K		L21F					[181]
TEM-134		R164H	E104K	G238S	Q39K					[182]
TEM-135							M182T	IJWP		[90, 183]
TEM-136		R164S		A237T, E240K			S268G			[184]
TEM-137		R164S		E240R						[185]
TEM-138		N175I	E104K	G238S						[186]
TEM-139			E104K	G238S	Q39K, L49M					[187]
TEM-144		R164C		E240K						[188]
TEM-149		R164S	E104K	E240V			M182T			[189]
TEM-151	CMT-type	R164H					M69V, N276D, A284G			[190]
TEM-152	CMT-type	R164H		E240K			M69V, N276D			[190]
TEM-153			E104K	G267V			M182T			[191]
TEM-154	CMT-type	R164S					M69L			[191]
TEM-155		R164S		E240K	Q39K					[192]
TEM-158	CMT-9	R164S					M69L, N276D			[193]
TEM-159					L21F		M69I, M182T			[171]
TEM-160					Q39K		M69V			[171]
TEM-164					L40V		I279T			[194]
TEM-167			E104K	G238S	L21F	T265M	A224V			
TEM-168						T265M				[195]

Think-Phat Cao Ph.D. Dissertation

Chosun University, Department of Biomedical Science

TEM-177		R164S	E104K	A237T, E240K	Q6K, Q39K		M182T				[196]
TEM-178		R178A		G238R	G42S, R43T, V44S		P145S, K146Q, E212del				[197]
TEM-181							A184V				[198]
TEM-186		D176N									[199]
TEM-187		R164H			L21F	T265M	A184V				[200]
SHV-2				G238S				1N9B		Conformational displacement of loop $\beta$ 3- $\beta$ 4 away from $\Omega$ -loop was supposed to expand the binding site	[201, 202]
SHV-2A				G238S	L35Q						[203]
SHV-3				G238S			R205L				[204]
SHV-4				G238S, E240K			R205L				[205]
SHV-5				G238S, E240K							[206]
SHV-6		D179A									[207]
SHV-7				G238S, E240K	I8F, R43S						[208]
SHV-8		D179N									[209]
SHV-9	SHV-5a			G238S, E240K			G54del, A140R, K192N, L193V				[210]
SHV-10				G238S, E240K			G54del, S130G, A140R, K192N, L193V				[211]
SHV-11	SHV-1-2a				L35Q						[212]
SHV-12	SHV-5-2a			G238S, E240K	L35Q						[212]

*Think-Phat Cao Ph.D. Dissertation*

*Chosun University, Department of Biomedical Science*

SHV-13				G238A	L35Q						[213]
SHV-14					I8F, R43S						[214]
SHV-16		163DRW ET167 insertion									[112]
SHV-18				G238A, E240K	I8F, R43S						[215]
SHV-19		L173F									[101]
SHV-20		L173F		G238S							[101]
SHV-21		L173F		G238S			L122F				[101]
SHV-22		N158K		G238S, E240K							[101]
SHV-23				G238S, E240K			L122F, A188G				[216]
SHV-24		D175G									[217]
SHV-25					T18A, L35Q		M129V				[218]
SHV-26							A187T				[218]
SHV-29				G238A	L35Q, R43S						[219]
SHV-30				G238S	I8F, R43S						[220]
SHV-31				E240K	L35Q						[221]
SHV-32		G156D					A124V				[222]
SHV-33							P226S				[222]
SHV-34				G238S	I8F, R43S		E64G				[223]
SHV-38							A146V				[224]
SHV-40				A234G	L35Q						[173]
SHV-41							V142F				[173]

*Think-Phat Cao Ph.D. Dissertation*

*Chosun University, Department of Biomedical Science*

SHV-42					A25S		M129V			[173]
SHV-43			L113F				T149S			[225]
SHV-44							R205L			[226]
SHV-46				G238S, E240K			T195N			[227]
SHV-49							M69I			[228]
SHV-50				G238S, E240K	Y7F					[229]
SHV-56				K234R	L35Q					[230]
SHV-57		L169R								[231]
SHV-60					L35Q		A187T			[232]
SHV-61					L10R, L35Q					[232]
SHV-62			H112Y		L35Q					[232]
SHV-70					L35Q		L148V			[233]
SHV-71			H112Y				A146V			[232]
SHV-73				K234R	Y7del		A146V			[232]
SHV-74					A22T, L35Q					[232]
SHV-75							N254H			[232]
SHV-76					T18A, L35Q		D213S			[232]
SHV-77					L35Q		V75A			[232]
SHV-78							G54S			[232]
SHV-79		A172V			L35Q					[232]
SHV-80					L35Q		A146T			[232]
SHV-81					L35Q		G144S			[232]

*Think-Phat Cao Ph.D. Dissertation*

*Chosun University, Department of Biomedical Science*

SHV-82					I8V, L35Q, A25T						[232]
SHV-83					M5K						[232]
SHV-85					L19M, L35Q						[234]
SHV-89					L35Q		M129V				[235]
SHV-90				G238S, E240K			A187T				[191]
SHV-91				E240K	P20S						[191]
SHV-92					L35Q		M69I, T141I				[236]
SHV-98							S271I				[237]
SHV-99			D104G								[237]
SHV-100					35SESQLSG RVGMIE36 insertion						[237]
SHV-101							D214G				[238]
SHV-102				G238A							[239]
SHV-103				L250R							[240]
SHV-105		G156D		G238S, E240K	I8F, R43S						[192]
SHV-106				G238S	I8F						[232]
SHV-107				T235A	L35Q						[232]
SHV-108					L35Q		T141I				[232]
SHV-109					L10R, L35Q		T268M				[241]
SHV-110		G156D			L35Q						[242]
SHV-111		P174S									[242]
SHV-129				G238S, E240K	L35Q		R275L, N276D				[243]

*Think-Phat Cao Ph.D. Dissertation*

*Chosun University, Department of Biomedical Science*

SHV-142					T18A, L35Q						[244]
SHV-147					T71A		P269S				[245]
SHV-148							R292Q				[245]
SHV-149					Q30R, R43S		F151S				[245]
SHV-150				A248V							[245]
SHV-151					L40P, R43S						[245]
SHV-152				G238S			W60R				[245]
SHV-153				G238S			A273V				[245]
SHV-154				G238S, E240K	R43S						[245]
SHV-155					L35Q		R292Q				[245]
SHV-156					L35Q		L91P, A150T				[245]
SHV-157					L35Q		V75M				[245]
SHV-158					L35Q, S53A						[245]
SHV-159					L35Q		D213G				[245]
SHV-160				G238S, E240K	L35Q, S38G						[245]
SHV-161					R43S						[245]
SHV-162				G238S	R43S, I47V						[245]
SHV-163				G238S	R43S		R292Q				[245]
SHV-165				G238S, E240K	T18P						[245]
SHV-167			H112Y				G87D, A146V				[246]

*Think-Phat Cao Ph.D. Dissertation*

*Chosun University, Department of Biomedical Science*

---



**VI. Appendix 2: Crystal structure implies an  
alternative opinion on the CAZ resistance of  
*Burkholderia thailandensis* acquired the PenL variant  
165\_167delinsPro**

## **VI. Appendix 2: Structural study implies an alternative strategy for the CAZ resistance of *Burkholderia thailandensis* acquired the PenL variant 165\_167delinsPro**

### **Opinion**

In their previous study published on the journal Antimicrobial Agents and Chemotherapy, volume 58(10), 2014, Hwang *et al.* described the four deletion mutations of PenL  $\beta$ -lactamase isolated from large-scale mutant selection on *B. thailandensis* [56]. Two of them, PenL-Thr171del and PenL-Ile173del, have been already characterized at atomic level in previous part of this thesis. Noticeably, a special deletion mutation, namely 165\_167delinsPro, also exhibited significantly high MIC value for CAZ, as shown in Figure 31 below, and even higher when being transferred to the *B. thailandensis* penL-null mutation [56]. This PenL variant was selectively deleted three amino acid  $\Omega$ -loop region, from Arg165-Glu166-Thr167, and thereby a Pro was inserted displacing. The MIC result may suggest that the PenL-165\_167delinsPro would probably confer the resistance to CAZ for *B. thailandensis*, and thus should be considered as a potential threat from the diverse evolution of pathogens to survive under pressure of novel strong antibiotics.

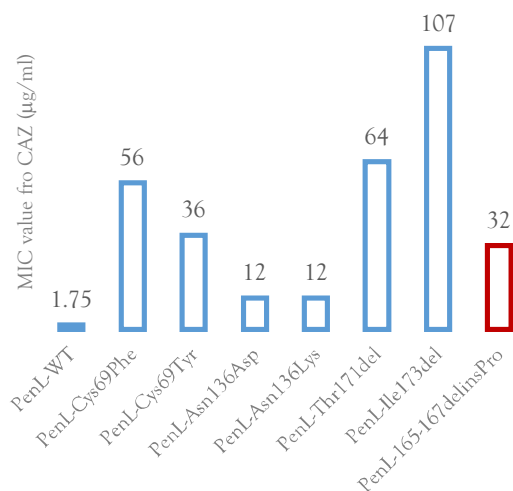


**Figure 31. Appendix: Minimal inhibitory concentration (MIC) of CAZ for *B. thailandensis* acquired PenL-165\_166delinsPro**

Data adapted from Yi et al., 2012[14] and Hwang et al., 2014[56]

However, it should be cautious when claiming that the PenL-165\_166delinsPro was the cause of the CAZ resistance seen. In fact, the finding about the PenL variant 165-167delinsPro has been a surprise. To best of our knowledge, the residue Glu166 has been well documented to be strictly conserved among class A  $\beta$ -lactamases, in which it plays the indispensable role in the deacylation step of  $\beta$ -lactam hydrolysis, as described early in this thesis (Figure 2 and Scheme 1). Deletion of Glu166 thus should lead to the functional deficiency of the enzyme. In agreement, the lack of Glu166 was reported to diminish the microscopic rate constant for deacylation though that for acylation was not abolished [247, 248]. Moreover, X-ray crystallography studies also proved that the acylation was able to take place in the absence of Glu166 but deacylation was impaired [249, 250]. Nonetheless, except for the MIC data, the authors did not provide the kinetic or enzymatic data that would support

the role of PenL-165\_167delinsPro in case of PenL. The suggestion about PenL-165\_167delinsPro thus has been still ambiguous.

Upon this point, we over-expressed and purified PenL-165\_167delinsPro to homogeneity to investigate the kinetic parameters. As was expected, the catalytic activity of PenL-165\_167delinsPro is extremely low in comparison with PenL-WT (Figure 32). Notably, the reaction catalyzed by PenL-165\_167delinsPro appeared to be in the biphasic manner, somewhat similar to the two substitution variants PenL-Cys69Tyr and PenL-Asn136Asp (Figure 12). This result may indicate the formation stable acyl-enzyme complex, when the next step, deacylation, was attenuated due to lacking of Glu166. Because of such low activity, we could not further determine the kinetic parameters for PenL-165\_167delinsPro.

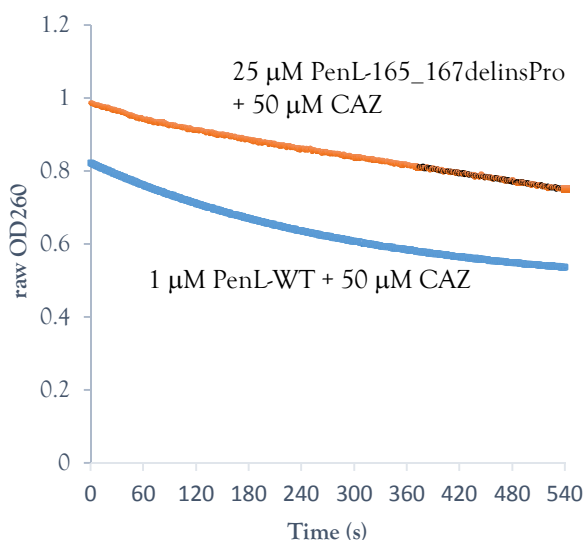


**Figure 32. Appendix: CAZ hydrolysis activity of PenL-165\_167delinsPro**

Decrease in CAZ amount was measured at 25°C in buffer consisted of 10 mM potassium phosphate supplemented with 20 μg/ml of bovine serum albumin, pH 7.0. The raw data without subtracting the experimental error were shown.

To further asserting, we crystalized and determined the structure of PenL-165\_167delinsPro at 1.34 Å resolution (Table 7). The overall structure of PenL-165\_167delinsPro is superimposed well with PenL-WT and PenL-Thr171del, with RMSD at C $\alpha$  of 0.268 and 0.295 Å, respectively. Exceptionally, the  $\Omega$ -loop of PenL-165\_167delinsPro is disordered in a different fashion rather than that of PenL-WT and PenL-Thr171del (Figure 33A). Inside the active site cleft, most of residues in the catalytic ensemble are same as seen in PenL-WT and the others (Figure 14). Distinctively, the inserted Pro O atom is likely to displaced the carboxylate of original Glu166, while the position of catalytic water W4 tends to be occupied by three waters W4-1, W4-2, W4-3 (Figure 33B). The electrostatic potential in active site cleft of PenL-165\_167delinsPro portrayed in Figure 33C appears to resemble that in the two single deletion mutations PenL-Thr171del and PenL-Ile173del (Figure 17, 18), suggesting that PenL-165\_167delinsPro might also have a considerable CAZ affinity, as described in previous parts.

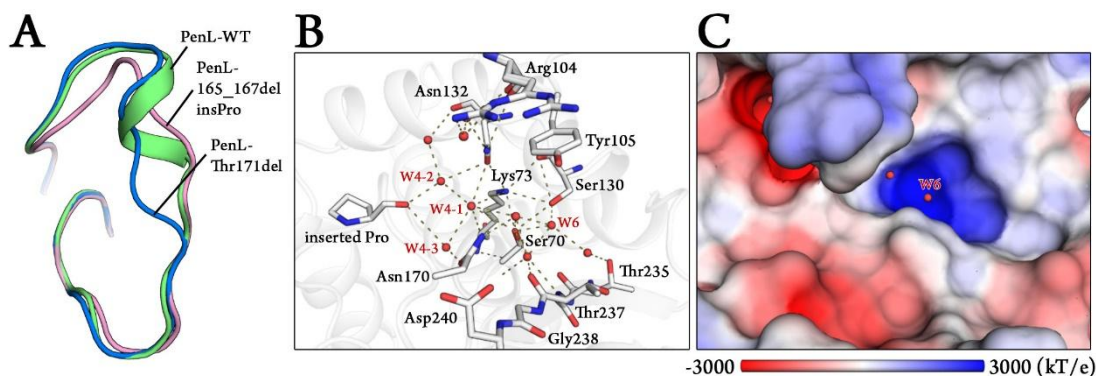


**Figure 33. Appendix: Structural analysis of PenL-165\_167delinsPro**

(A) Distinctions in  $\Omega$ -loop of PenL-165\_167delinsPro (pink) with that of PenL-WT (green) and PenL-Thr171del (blue). (B) Active site of PenL-165\_167delinsPro shows the inserted Pro (on  $\Omega$ -loop) and the interaction network with three putative waters that displayed the catalytic water W4. (C) Electrostatic potential at active site cleft of PenL-165\_167delinsPro with the same view angle with Figure 17, 20, 23, 24.

The presence of three waters displaced for the original catalytic water W4 might be thought to assist the catalysis, because the following observations. First, water W4-1 coordinates to both Asn170 and Lys73, likewise the original W4. Second, waters W4-2 and W4-3 might also be involved in the proton transfer network due to their coordination with Lys73 and Asn170, respectively, and with the inserted Pro O atom (Figure 33B). And third, the pKa of residue Lys73 in PenL-165\_167delinsPro is calculated as 5.92 by Propka [84], in comparison with 9.16 in Lys73 of PenL-WT. Noted that pKa of Glu166 in PenL-WT and the other ESBL variants is of ~5. With those reasons, a question might be raised that whether the Lys73, the inserted Pro and the three additional waters might act replacing the role of Glu166. Nonetheless, this assumption is not supported, firstly by the enzyme assay data shown in Figure 32. Secondly, prior studies on other class A  $\beta$ -lactamases either described the reduction in pKa of Lys73 to ~6 when the carboxylate residue at position 166 was depleted (from ~8-8.5 in the presence of Glu166 originally), however, in both cases, the deacylation rate was greatly reduced [247-251]. The study by Meroueh *et al.*, 2005 further emphasized the pivotal role of Glu166 to protonate Lys73 and activate the nucleophilicity of Ser70, both *via* the catalytic water [251]. Such role evidently could not be taken when the carboxylate at position 166 was depleted, even when replacing the Glu166 with its closest brothers Asn or Gln<sup>239-242</sup>. We are therefore unable to believe that the backbone O atom of the inserted Pro (Figure 33B) is strong enough to interchange the role of Glu166 carboxylate. Taken together, we conclude that the variant PenL-165\_167delinsPro should not be a full functional enzyme. It should be notice that the PenL-165\_167delinsPro is still able to accommodate  $\beta$ -lactam substrate and the acylation is able to take place, yet the lack of Glu166 prevents the release of product out of the active site cleft, leaving the strong acyl-enzyme complex.

In summary, although in the work of Hwang *et al.*, the authors did not state clearly, any suggestion that the PenL-165\_167delinsPro is the major factor for the CAZ resistance of *B. thailandensis* might be incorrect. However, the work of Hwang *et al.* may indicate another interesting

fact. As was stated in *Introduction* part, bacteria in *Burkholderia* group possess the high-level intrinsic resistance to antibiotics. Several of resistance machineries of these bacteria have been being studied elsewhere [5, 8, 9]. Among those, Pen-type  $\beta$ -lactamase is commonly approved to be the prominent factor. With this regards, we suppose that the deficiency of the most important enzyme, PenL, by the mutation 165\_167delinsPro, would invoke other machineries that help the *B. thailandensis* to survive with high pressure of CAZ. This deduction would explain for the high MIC value of *B. thailandensis* that acquired the PenL-165\_167delinsPro (Figure 31) [56], and further suggest that other powerful resistance factor of the bacteria must be existed. This topic will be a future goal of study.

## Materials and Methods

Gene encoded for PenL-165\_167delinsPro (without N-terminal signal peptide) was sub-cloned into pET28a(+) expression vector then was transformed into *E. coli* BL21 (DE3). Protocols of over-expression, purification, crystallization, enzyme assay, and electrostatic potential calculation are same as for the four PenL ESBL variants described in part IV. Crystals of PenL-165\_167delinsPro were grown in the condition consisted of 100 mM Tris pH 8.5, 100 mM magnesium chloride, 20% polyethylene glycol 400, 20% polyethylene glycol 8000. Suitable crystals were transferred into the same growing condition added 20% glycerol for 30 s, then flash-frozen in liquid nitrogen for X-ray diffraction experiments. No CBA-soaked crystal was successfully resolved.

**Table 7. Appendix: Data statistics summary for X-ray crystallography of PenL-165\_167delinsPro**

<b>Data collection</b>	
Beam line	PAL-5C
Wavelength (Å)	0.97934
Resolution (Å)	50 – 1.5 (1.53 – 1.50)
Space group	C222 <sub>1</sub>
Unit cell dimension	
a, b, c (Å)	52.63, 93.96, 102.71
α, β, γ (°)	90.0, 90.0, 90.0
Total reflections	570098
Unique reflections	57272 (2825)
R <sub>merge</sub> † (%)	6.8 (31.2)
Completeness (%)	99.7 (99.6)
Redundancy	10.0 (8.4)
Average I/σ (I)	32.14 (8.02)
Matthews coefficient (Å <sup>3</sup> Da <sup>-1</sup> )	2.24
Solvent (%)	45.18
<b>Refinement</b>	
R <sub>work</sub> / R <sub>free</sub> (%)	15.85/17.24
Protein residues	266
Waters	329
RMSD	
Bond angles (°)	1.48
Bond lengths (Å)	0.037
Average B factors (Å <sup>2</sup> )	18.83
Ramachandran plot	
Favored (%)	95.83
Outliers (%)	0.00

Values in parentheses correspond to highest resolution shell.

†R-merge =  $\frac{\sum_{hkl} \sum_i |I_i(hkl) - \langle I(hkl) \rangle|}{\sum_{hkl} \sum_i I_i(hkl)}$ , where  $I_i(hkl)$  is the observed intensity and  $\langle I(hkl) \rangle$  is the average intensity of symmetry-related observations.

\*CBA: ceftazidime-like glycyloboronic acid



## **VI. REFERENCES**

## VI. REFERENCES

1. *Textbook of Military Medicine: Medical Aspects of Chemical and Biological Warfare*. 2007, Office of the Surgeon General at TMM Publications: Washington, DC.
2. Currie, B.J., *Burkholderia pseudomallei and Burkholderia mallei: Melioidosis and glanders.*, in *Principles and Practice of Infectious Diseases*. 2004, Churchill Livingstone.
3. Gan, Y.-H., *Interaction between Burkholderia pseudomallei and the Host Immune Response: Sleeping with the Enemy?* The Journal of Infectious Diseases, 2005. **192**: p. 1845-1850.
4. Wuthiekanun V and P. SJ, *Management of melioidosis*. Expert Rev Anti Infect Ther. , 2006. **4**(3): p. 445-455.
5. Schweizer, H.P., *Mechanisms of antibiotic resistance in Burkholderia pseudomallei: implications for treatment of melioidosis*. Future Microbiol, 2012. **7**(12): p. 1389-1399.
6. Dance, D., *Treatment and prophylaxis of melioidosis*. Int J Antimicrob Agents, 2014. **43**(4): p. 310-318.
7. White NJ, Dance DA, Chaowagul W, Wattanagoon Y, Wuthiekanun V, and P. N, *Halving of mortality of severe melioidosis by ceftazidime*. Lancet., 1989. **2**(8665): p. 697-701.
8. Rhodes, K.A. and H.P. Schweizer, *Antibiotic Resistance in Burkholderia Species*. Drug Resistance Updates, 2016.
9. Sunisa Chirakul, Michael H. Norris, Sirawit Pagdepanichkit, Nawarat Somprasong, Linnell B. Randall, James F. Shirley, Bradley R. Borlee, Olga Lomovskaya, A. Tuanyok, and H.P. Schweizer, *Transcriptional and posttranscriptional regulation of PenA  $\beta$ -lactamase in acquired Burkholderia pseudomallei  $\beta$ -lactam resistance*. Scientific Reports, 2018. **8**.
10. Brett PJ, DeShazer D, and W. DE., *Burkholderia thailandensis sp. nov., a Burkholderia pseudomallei-like species*. Int J Syst Bacteriol., 1998. **48**: p. 317-320.
11. Wuthiekanun V, Smith MD, Dance DA, Walsh AL, Pitt TL, and W. NJ., *Biochemical characteristics of clinical and environmental isolates of Burkholderia pseudomallei*. J Med Microbiol., 1996. **45**(6): p. 408-412.
12. Yu Y, Kim HS, Chua HH, Lin CH, Sim SH, Lin D, Derr A, Engels R, DeShazer D, Birren B, Nierman WC, and T. P., *Genomic patterns of pathogen evolution revealed by comparison of*

- Burkholderia pseudomallei*, the causative agent of melioidosis, to avirulent *Burkholderia thailandensis*. BMC Microbiol., 2006. **26**: p. 6-46.
13. Haraga A, West TE, Brittnacher MJ, Skerrett SJ, and M. SI., *Burkholderia thailandensis* as a model system for the study of the virulence-associated type III secretion system of *Burkholderia pseudomallei*. Infect Immun, 2008. **76**(11): p. 5402-5411.
  14. Dobson, R., H. Yi, K.-H. Cho, Y.S. Cho, K. Kim, W.C. Nierman, and H.S. Kim, *Twelve Positions in a  $\beta$ -Lactamase That Can Expand Its Substrate Spectrum with a Single Amino Acid Substitution*. PLoS ONE, 2012. **7**(5): p. e37585.
  15. Yi, H., H. Song, J. Hwang, K. Kim, W.C. Nierman, and H.S. Kim, *The Tandem Repeats Enabling Reversible Switching between the Two Phases of  $\beta$ -Lactamase Substrate Spectrum*. PLoS Genetics, 2014. **10**(9): p. e1004640.
  16. Jed F. Fisher, Samy O. Meroueh, and S. Mobashery, *Bacterial Resistance to  $\beta$ -lactam Antibiotics: Compelling Opportunism, Compelling Opportunity*. Chem. Rev., 2005. **105**: p. 395-424.
  17. Abraham, E.P. and E. Chain, *An Enzyme from Bacteria Able to Destroy Penicillin*. Nature, 1940. **146**(3713): p. 837-837.
  18. Torok, E., E. Moran, and F. Cooke, *Oxford Handbook of Infectious Diseases and Microbiology*. 2009: OUP Oxford.
  19. Drawz, S.M. and R.A. Bonomo, *Three Decades of  $\beta$ -Lactamase Inhibitors*. Clin. Microbiol. Rev., 2010. **23**(1): p. 160-201.
  20. Bush, K., G.A. Jacoby, and A.A. Medeiros, *A functional classification scheme for beta-lactamases and its correlation with molecular structure*. Antimicrob. Agents. Chemother, 1995. **39**(6): p. 1211-1233.
  21. Bush, K. and G.A. Jacoby, *Updated Functional Classification of  $\beta$ -Lactamases*. Antimicrob. Agents. Chemother, 2010. **54**(3): p. 969-976.
  22. Ambler, R.P., *The structure of  $\beta$ -lactamases*. Philos. Trans. R. Soc. Lond. B Biol. Sci., 1980. **289**: p. 321-331.
  23. R. P. Ambler, A. F. W. Coulson, J.-M. Frère, J.-M. Ghuysen, B. Joris, M. Forsman, R. C. Levesque, G. Tiraby, and S.G. Waley, *A standard numbering scheme for the Class A  $\beta$ -lactamase*. Biochem. J., 1991. **276**: p. 269-272.

24. Jaurin, B. and T. Grundström, *ampC* cephalosporinase of *Escherichia coli* K-12 has a different evolutionary origin from that of beta-lactamases of the penicillinase type. *Proc. Nat. Acad. Sci. USA*, 1981. **78**(8): p. 4897-4901.
25. Ouellette, M., L. Bissonnette, and P.H. Roy, *Precise insertion of antibiotic resistance determinants into Tn21-like transposons: nucleotide sequence of the OXA-1 beta-lactamase gene*. *Proc. Nat. Acad. Sci. USA*, 1987. **84**(21).
26. Page, M.G.P., *Extended-spectrum  $\beta$ -lactamases: structure and kinetic mechanism*. *Clinical Microbiology and Infection*, 2008. **14**: p. 63-74.
27. Papp-Wallace, K.M., M.A. Taracila, J.A. Gatta, N. Ohuchi, R.A. Bonomo, and M. Nukaga, *Insights into  $\beta$ -Lactamases from Burkholderia Species, Two Phylogenetically Related yet Distinct Resistance Determinants*. *J. Biol. Chem.*, 2013. **288**(26): p. 19090-19102.
28. D. Sirot, C. Recule, E. B. Chaibi, L. Bret, J. Croize, C. Chanal-Claris, R. Labia, and J. Sirot, *A Complex Mutant of TEM-1  $\beta$ -Lactamase with Mutations Encountered in Both IRT-4 and Extended-Spectrum TEM-15 Produced by an Escherichia coli Clinical Isolate*. *Antimicrob. Agents Chemother.*, 1997. **41**(6): p. 1322–1325.
29. Celenza, G., C. Luzi, M. Aschi, B. Segatore, D. Setacci, C. Pellegrini, C. Forcella, G. Amicosante, and M. Perilli, *Natural D240G Toho-1 mutant conferring resistance to ceftazidime: biochemical characterization of CTX-M-43*. *Journal of Antimicrobial Chemotherapy*, 2008. **62**(5): p. 991-997.
30. Levitt, P.S., K.M. Papp-Wallace, M.A. Taracila, A.M. Hujer, M.L. Winkler, K.M. Smith, Y. Xu, M.E. Harris, and R.A. Bonomo, *Exploring the Role of a Conserved Class A Residue in the  $\Omega$ -Loop of KPC-2  $\beta$ -Lactamase*. *Journal of Biological Chemistry*, 2012. **287**(38): p. 31783-31793.
31. Doucet, N., P.-Y. De Wals, and J.N. Pelletier, *Site-saturation Mutagenesis of Tyr-105 Reveals Its Importance in Substrate Stabilization and Discrimination in TEM-1  $\beta$ -Lactamase*. *Journal of Biological Chemistry*, 2004. **279**(44): p. 46295-46303.
32. Bethel, C.R., A.M. Hujer, K.M. Hujer, J.M. Thomson, M.W. Ruszczycky, V.E. Anderson, M. Pusztai-Carey, M. Taracila, M.S. Helfand, and R.A. Bonomo, *Role of Asp104 in the SHV  $\beta$ -Lactamase*. *Antimicrobial Agents and Chemotherapy*, 2006. **50**(12): p. 4124-4131.
33. Sanders, C.C. and J. W. Eugene Sanders, *Emergence of Resistance to Cefamandole: Possible Role of Cefoxitin-Inducible Beta-Lactamases*. *Antimicrob. Agents. Chemother.*, 1979. **15**(6): p. 792-797.

34. Philippe Lagacé-Wiens, Andrew Walkty, and J.A. Karlowsky, *Ceftazidime–avibactam: an evidence-based review of its pharmacology and potential use in the treatment of Gram-negative bacterial infections*. *Core Evid.*, 2014. **9**: p. 13-25.
35. Zhanell GG, Lawson CD, Adam H, Schweizer F, Zelenitsky S, Lagacé-Wiens PR, Denisuk A, Rubinstein E, Gin AS, Hoban DJ, Lynch JP 3rd, and K. JA., *Ceftazidime-avibactam: a novel cephalosporin/β-lactamase inhibitor combination*. *Drugs*, 2013. **2**(159-177).
36. Zasowski, E.J., J.M. Rybak, and M.J. Rybak, *The β-Lactams Strike Back: Ceftazidime-Avibactam*. *Pharmacotherapy*, 2015. **35**(8): p. 755-770.
37. Elizabeth Temkin, Julian Torre-Cisneros, Bojana Beovic, Natividad Benito, Maddalena Giannella, Raúl Gilarranz, Cameron Jeremiah, Belén Loeches, Isabel Machuca, María José Jiménez-Martín, José Antonio Martínez, Marta Mora-Rillo, Enrique Navas, Michael Osthoff, Juan Carlos Pozo, Juan Carlos Ramos Ramos, Marina Rodriguez, Miguel Sánchez-García, Pierluigi Viale, Michel Wolff, and Y. Carmeli, *Ceftazidime-Avibactam as Salvage Therapy for Infections Caused by Carbapenem-Resistant Organisms*. *Antimicrob Agents Chemother*, 2017. **61**(2): p. e01964-16.
38. Ryan K. Shields, Liang Chen, Shaoji Cheng, Kalyan D. Chavda, Ellen G. Press, Avin Snyder, Ruchi Pandey, Yohei Doi, Barry N. Kreiswirth, M. Hong Nguyen, and C.J. Clancy, *Emergence of Ceftazidime-Avibactam Resistance Due to Plasmid-Borne blaKPC-3 Mutations during Treatment of Carbapenem-Resistant Klebsiella pneumoniae Infections*. *Antimicrob Agents Chemother*, 2017. **61**(3): p. e02097-16.
39. Humphries RM, Yang S, Hemarajata P, Ward KW, Hindler JA, Miller SA, and G. A., *First Report of Ceftazidime-Avibactam Resistance in a KPC-3-Expressing Klebsiella pneumoniae Isolate*. *Antimicrob Agents Chemother*, 2015. **59**(10): p. 6605-6607.
40. Marla J. Giddins, Nenad Macesic, Medini K. Annabhajjala, Stephania Stump, Sabrina Khan, Thomas H. McConville, Monica Mehta, Angela Gomez-Simmonds, and A.-C. Uhlemann, *Successive Emergence of Ceftazidime-Avibactam Resistance through Distinct Genomic Adaptations in blaKPC-2-Harboring Klebsiella pneumoniae Sequence Type 307 Isolates*. *Antimicrob Agents Chemother*, 2018. **62**(3): p. e02101-17.
41. Yi, H., J.M. Choi, J. Hwang, F. Prati, T.-P. Cao, S.H. Lee, and H.S. Kim, *High adaptability of the omega loop underlies the substrate-spectrum-extension evolution of a class A β-lactamase, PenL*. *Scientific Reports*, 2016. **6**(1).

42. Kuzin AP, Nukaga M, Nukaga Y, Hujer AM, Bonomo RA, and K. JR., *Structure of the SHV-1 beta-lactamase*. *Biochemistry*, 1999. **38**(18): p. 5720-5727.
43. Minasov G, Wang X, and S. BK, *An ultrahigh resolution structure of TEM-1 beta-lactamase suggests a role for Glu166 as the general base in acylation*. *J Am Chem Soc*, 2002. **124**(19): p. 5330-5340.
44. DT, K., K. AM, L. SM, W. GD, and S. NC, *Molecular Mechanism of Avibactam-Mediated  $\beta$ -Lactamase Inhibition*. *ACS Infect Dis.*, 2015. **1**(4): p. 175-184.
45. Shimamura T, Ibuka A, Fushinobu S, Wakagi T, Ishiguro M, Ishii Y, and M. H, *Acyl-intermediate structures of the extended-spectrum class A beta-lactamase, Toho-1, in complex with cefotaxime, cephalothin, and benzylpenicillin*. *J Biol Chem*, 2002. **277**(48): p. 46601-46608.
46. OA, P., Z. X, and C. Y, *Molecular Basis of Substrate Recognition and Product Release by the Klebsiella pneumoniae Carbapenemase (KPC-2)*. *J. Med. Chem.*, 2017. **60**(8): p. 3525-3530.
47. Samuel Tranier, Anne-Typhaine Bouthors, Laurent Maveyraud, Valérie Guillet, W. Sougakoff, and J.-P. Samama, *The High Resolution Crystal Structure for Class A  $\beta$ -Lactamase PER-1 Reveals the Bases for Its Increase in Breadth of Activity*. *J Biol Chem*, 2000. **275**: p. 28075-28082.
48. Palzkill, T., *Structural and Mechanistic Basis for Extended-Spectrum Drug-Resistance Mutations in Altering the Specificity of TEM, CTX-M, and KPC  $\beta$ -lactamases*. *Front Mol Biosci*, 2018. **5**(16).
49. Bush, K. and J.F. Fisher, *Epidemiological expansion, structural studies, and clinical challenges of new  $\beta$ -lactamases from gram-negative bacteria*. *Annu Rev Microbiol*, 2011. **65**: p. 455-478.
50. Shimizu-Ibuka, A., M. Oishi, S. Yamada, Y. Ishii, K. Mura, H. Sakai, and H. Matsuzawa, *Roles of Residues Cys69, Asn104, Phe160, Gly232, Ser237, and Asp240 in Extended-Spectrum  $\beta$ -Lactamase Toho-1*. *Antimicrobial Agents and Chemotherapy*, 2011. **55**(1): p. 284-290.
51. Ruggiero, M., F. Kerff, R. Herman, F. Sapunaric, M. Galleni, G. Gutkind, P. Charlier, E. Sauvage, and P. Power, *Crystal Structure of the Extended-Spectrum  $\beta$ -Lactamase PER-2 and Insights into the Role of Specific Residues in the Interaction with  $\beta$ -Lactams and  $\beta$ -Lactamase Inhibitors*. *Antimicrob. Agents. Chemother*, 2014. **58**(10): p. 5994-6002.
52. Tzouveleakis LS, Tzelepi E, Tassios PT, and L. NJ, *CTX-M-type beta-lactamases: an emerging group of extended-spectrum enzymes*. *Int J Antimicrob Agents*, 2000. **14**(2): p. 137-142.

53. Abbott, I.J. and A.Y. Peleg, *Stenotrophomonas, Achromobacter, and Nonmeliod Burkholderia Species: Antimicrobial Resistance and Therapeutic Strategies*. Semin Respir Crit Care Med, 2015. **36**: p. 99-110.
54. Sam, I.C., K.H. See, and S.D. Puthuchery, *Variations in Cefazidime and Amoxicillin-Clavulanate Susceptibilities within a Clonal Infection of Burkholderia pseudomallei*. Journal of Clinical Microbiology, 2009. **47**(5): p. 1556-1558.
55. Sarovich, D.S., E.P. Price, A.T.V. Schulze, J.M. Cook, M. Mayo, L.M. Watson, L. Richardson, M.L. Seymour, A. Tuanyok, D.M. Engelthaler, T. Pearson, S.J. Peacock, B.J. Currie, P. Keim, and D.M. Wagner, *Characterization of Cefazidime Resistance Mechanisms in Clinical Isolates of Burkholderia pseudomallei from Australia*. PLoS ONE, 2012. **7**(2).
56. Hwang, J., K.-H. Cho, H. Song, H. Yi, and H.S. Kim, *Deletion Mutations Conferring Substrate Spectrum Extension in the Class A  $\beta$ -Lactamase*. Antimicrob. Agents. Chemother, 2014. **58**(10): p. 6265-6269.
57. Helfand, M.S., A.M. Hujer, F.D. Sönnichsen, and R.A. Bonomo, *Unexpected Advanced Generation Cephalosporinase Activity of the M69F Variant of SHV  $\beta$ -Lactamase*. Journal of Biological Chemistry, 2002. **277**(49): p. 47719-47723.
58. Wang, X., G. Minasov, and B.K. Shoichet, *The Structural Bases of Antibiotic Resistance in the Clinically Derived Mutant  $\beta$ -Lactamases TEM-30, TEM-32, and TEM-34*. Journal of Biological Chemistry, 2002. **277**(35): p. 32149-32156.
59. S Lin, M.T., D.M. Shlaes, S.D. Rudin, J.R. Knox, V. Anderson, and R.A. Bonomo, *Kinetic analysis of an inhibitor-resistant variant of the OHIO-1 beta-lactamase, an SHV-family class A enzyme*. Biochem J., 1998. **333**(2): p. 395-400.
60. Giakkoupi, P., V. Miriagou, M. Gazouli, E. Tzelepi, N.J. Legakis, and L.S. Tzouveleki, *Properties of Mutant SHV-5  $\beta$ -Lactamases Constructed by Substitution of Isoleucine or Valine for Methionine at Position 69*. Antimicrob. Agents. Chemother, 1998. **42**(5): p. 1281-1283.
61. Monica A. Totir, Pius S. Padayatti, Marion S. Helfand, Marianne P. Carey, Robert A. Bonomo, Paul R. Carey, and F.v.d. Akker, *Effect of the Inhibitor-Resistant M69V Substitution on the Structures and Populations of trans-Enamine  $\hat{\alpha}$ -Lactamase Intermediates*. Biochemistry, 2006. **45**: p. 11895-11904.

62. Samy O. Meroueh, Pierre Roblin, Dasantila Golemi, Laurent Maveyraud, Sergei B. Vakulenko, Yun Zhang, Jean-Pierre Samama, and S. Mobashery, *Molecular Dynamics at the Root of Expansion of Function in the M69L Inhibitor-Resistant TEM b-Lactamase from Escherichia coli*. J. Am. Chem. Soc., 2002. **124**: p. 9422-9430.
63. Banerjee, S., U. Pieper, G. Kapadia, L.K. Pannell, and O. Herzberg, *Role of the  $\Omega$ -Loop in the Activity, Substrate Specificity, and Structure of Class A  $\beta$ -Lactamase*. Biochemistry, 1998. **37**: p. 3286-3296.
64. MP, P., Hu L, Stojanoski V, Sankaran B1, Prasad BVV, and P. T, *The Drug-Resistant Variant P167S Expands the Substrate Profile of CTX-M  $\beta$ -Lactamases for Oxyimino-Cephalosporin Antibiotics by Enlarging the Active Site upon Acylation*. Biochemistry, 2017. **56**(27): p. 3443-3453.
65. Chanwit Tribuddharat, Richard A. Moore, Patricia Baker, and D.E. Woods, *Burkholderia pseudomallei Class A  $\beta$ -Lactamase Mutations That Confer Selective Resistance against Ceftazidime or Clavulanic Acid Inhibition*. Antimicrob Agents Chemother, 2003. **47**(7): p. 2082-2087.
66. Abergel, C., *Molecular replacement: tricks and treats*. Acta Cryst. D, 2013. **69**(11): p. 2167-2173.
67. Murshudov, G.N., A.A.Vagin, and E.J.Dodson, *Refinement of Macromolecular Structures by the Maximum-Likelihood method*. Acta Cryst. D, 1997. **53**: p. 240-255.
68. Afonine PV, Grosse-Kunstleve RW, H.J. Echols N, M.M. Moriarty NW, Terwilliger TC, Urzhumtsev A, Zwart PH, and A. PD., *Towards automated crystallographic structure refinement with phenix.refine*. Acta Crystallogr D Biol Crystallogr, 2012. **68**: p. 352-67.
69. Echols, N., N.W. Moriarty, H.E. Klei, P.V. Afonine, G. Bunkóczi, J.J. Headd, A.J. McCoy, R.D. Oeffner, R.J. Read, T.C. Terwilliger, and P.D. Adams, *Automating crystallographic structure solution and refinement of protein-ligand complexes*. Acta Crystallographica Section D Biological Crystallography, 2013. **70**(1): p. 144-154.
70. N.W. Moriarty, R.W. Grosse-Kunstleve, and P.D. Adams, *electronic Ligand Builder and Optimization Workbench (eLBOW): a tool for ligand coordinate and restraint generation*. Acta Crystallogr D Biol Crystallogr, 2009. **65**: p. 1074-1080.



71. Emsley P, Lohkamp B, Scott W, and C. K, *Features and Development of Coot*. Acta Crystallogr D Biol Crystallogr, 2010. **66**: p. 486-501.
72. Chen, V.B., W.B. Arendall, J.J. Headd, D.A. Keedy, R.M. Immormino, G.J. Kapral, L.W. Murray, J.S. Richardson, and D.C. Richardson, *MolProbity: all-atom structure validation for macromolecular crystallography*. Acta Cryst. D, 2009. **66**(1): p. 12-21.
73. Oliphant, T.E., *Python for Scientific Computing*. Computing in Science & Engineering, 2007. **9**: p. 10-20.
74. Hunter, J.D., *Matplotlib: A 2D graphics environment*. Computing In Science & Engineering, 2007. **9**(3): p. 90--95.
75. Spoel, D.V.D., E. Lindahl, B. Hess, G. Groenhof, A.E. Mark, and H.J.C. Berendsen, *GROMACS: Fast, flexible, and free*. J. Comput. Chem. , 2005. **26**: p. 1701-1718.
76. Scott, W.R.P., P.H. Hunenberger, I.G. Tironi, A.E. Mark, S.R. Billeter, J. Fennen, A.E. Torda, T. Huber, P. Kruger, and W.F.v. Gunsteren, *The GROMOS Biomolecular Simulation Program Package*. J. Phys. Chem. A 1999. **103**: p. 3596-3607.
77. William L. Jorgensen, Jayaraman Chandrasekhar, J.D. Madura, R.W. Impey, and M.L. Klein, *Comparison of simple potential functions for simulating liquid water*. J. Chem. Phys., 1983. **79**(926).
78. Tom Darden, Darrin York, and L. Pedersen, *Particle mesh Ewald: An N·log(N) method for Ewald sums in large systems* J. Chem. Phys., 1993. **98**(10089).
79. Hess, B., *P-LINCS: A Parallel Linear Constraint Solver for Molecular Simulation*. J. Chem. Theory Comput., 2008. **4**(1): p. 116-122.
80. M. Parrinello and A. Rahman, *Polymorphic transitions in single crystals: A new molecular dynamics method* J. Appl. Phys., 1981. **52**: p. 7182.
81. Andersen, H.C., *Molecular dynamics simulations at constant pressure and/or temperature*. J. Chem. Phys., 1980. **72**: p. 2384.
82. Jurrus E, Engel D, Star K, Monson K, Brandi J, Felberg LE, Brookes DH, Wilson L, Chen J, Liles K, Chun M, Li P, Gohara DW, Dolinsky T, Konecny R, Koes DR, Nielsen JE, Head-Gordon T, Geng W, Krasny R, Wei GW, Holst MJ, McCammon JA, and B. NA., *Improvements to the APBS biomolecular solvation software suite*. Protein Science, 2018. **27**: p. 112-128.

83. Dolinsky TJ, Nielsen JE, McCammon JA, and B. NA., *PDB2PQR: an automated pipeline for the setup, execution, and analysis of Poisson-Boltzmann electrostatics calculations*. Nucleic Acids Res, 2004. **32**: p. W665-W667.
84. Olsson, M.H., Chresten R. Søndergaard, Michal Rostkowski, and J.H. Jensen, *PROPKA3: Consistent Treatment of Internal and Surface Residues in Empirical pKa Predictions*. J. Chem. Theory Comput., 2011. **7**(2): p. 525-537.
85. Linnell B. Randall, Karen Dobos, Krisztina M. Papp-Wallace, Robert A. Bonomo, and H.P. Schweizer, *Membrane-Bound PenA  $\beta$ -Lactamase of Burkholderia pseudomallei*. Antimicrob Agents Chemother, 2015. **60**(3): p. 1509-1514.
86. Sheldrick, G.M., *Phase annealing in SHELX-90: direct methods for larger structures*. Acta Cryst A, 1990. **46**: p. 467-473.
87. Rigos, C.F., H.d.L. Santos, G.T. Jr, R.J. Ward, and P. Ciancaglini, *Influence of enzyme conformational changes on catalytic activity investigated by circular dichroism spectroscopy*. Biochem Mol Biol Educ., 2006. **31**(5): p. 329-332.
88. Papp-Wallace, K.M., S.A. Becka, M.A. Taracila, M.L. Winkler, J.A. Gatta, D.A. Rholl, H.P. Schweizer, and R.A. Bonomo, *Exposing a  $\beta$ -Lactamase "Twist": the Mechanistic Basis for the High Level of Ceftazidime Resistance in the C69F Variant of the Burkholderia pseudomallei PenI  $\beta$ -Lactamase*. Antimicrobial Agents and Chemotherapy, 2016. **60**(2): p. 777-788.
89. M. Cecilia Orenca, Jun S. Yoon, Jon E. Ness, W.P.C. Stemmer, and R.C. Stevens, *Predicting the emergence of antibiotic resistance by directed evolution and structural analysis*. Nat. Struct. Mol. Biol, 2001. **8**: p. 238-242.
90. Wang X, Minasov G, and S. BK, *Evolution of an antibiotic resistance enzyme constrained by stability and activity trade-offs*. J Mol Biol, 2002. **320**(1): p. 85-95.
91. Lewis, E.R., K.M. Winterberg, and A.L. Fink, *A point mutation leads to altered product specificity in  $\beta$ -lactamase catalysis*. Proc. Natl. Acad. Sci. U.S.A., 1997. **94**(2): p. 443-447.
92. Brown, N.G., S. Shanker, B.V.V. Prasad, and T. Palzkill, *Structural and Biochemical Evidence That a TEM-1  $\beta$ -Lactamase N170G Active Site Mutant Acts via Substrate-assisted Catalysis*. J. Biol. Chem., 2009. **284**(48): p. 33703-33712.
93. Burnley, B.T., P.V. Afonine, P.D. Adams, and P. Gros, *Modelling dynamics in protein crystal structures by ensemble refinement*. eLife, 2012.

94. Huletsky, A., J.R. Knox, and R.C. Levesque, *Role of Ser-238 and Lys-240 in the hydrolysis of third-generation cephalosporins by SHV-type  $\beta$ -lactamases probed by site-directed mutagenesis and three-dimensional modeling*. J. Biol. Chem., 1992. **268**: p. 3690-3697.
95. Papp-Wallace, K.M., M.A. Taracila, K.M. Smith, Y. Xu, and R.A. Bonomo, *Understanding the molecular determinants of substrate and inhibitor specificities in the carbapenemase KPC-2: exploring the roles of Arg220 and Glu276*. Antimicrob Agents Chemother, 2012. **56**: p. 4428-4438.
96. Papp-Wallace, K.M., M. Taracila, J.M. Hornick, A.M. Hujer, K.M. Hujer, A.M. Distler, A. Endimiani, and R.A. Bonomo, *Substrate selectivity and a novel role in inhibitor discrimination by residue 237 in the KPC-2  $\beta$ -lactamase*. Antimicrob Agents Chemother, 2010. **54**(2867-2877).
97. Tokuriki, N. and D.S. Tawfik, *Protein Dynamism and Evolvability*. Science, 2009. **324**: p. 203-207.
98. Hart, K.M., C.M.W. Ho, S. Dutta, M.L. Gross, and G.R. Bowman, *Modelling proteins' hidden conformations to predict antibiotic resistance*. Nat. Commun., 2016.
99. Yu Chen, Brian Shoichet, and R. Bonnet, *Structure, Function, and Inhibition along the Reaction Coordinate of CTX-M  $\beta$ -Lactamases*. J. Am. Chem. Soc., 2005. **127**: p. 5423-5434.
100. Berg, J.M., J.L. Tymoczko, and L. Stryer, *Biochemistry*. 7th ed. 2012, W. H. Freeman and Company: Kate Ahr Parker.
101. Essack SY, Hall LM, Pillay DG, McFadyen ML, and L. DM, *Complexity and diversity of Klebsiella pneumoniae strains with extended-spectrum beta-lactamases isolated in 1994 and 1996 at a teaching hospital in Durban, South Africa*. Antimicrob Agents Chemother, 2001. **45**(1): p. 88-95.
102. Poyart C, Mugnier P, Quesne G, Berche P, and T.-C. P, *A novel extended-spectrum TEM-type beta-lactamase (TEM-52) associated with decreased susceptibility to moxalactam in Klebsiella pneumoniae*. Antimicrob Agents Chemother, 1998. **42**(1): p. 108-113.
103. Chanal-Clariss C, Sirot D, Bret L, Chatron P, Labia R, and S. J, *Novel extended-spectrum TEM-type beta-lactamase from an Escherichia coli isolate resistant to ceftazidime and susceptible to cephalothin*. Antimicrob Agents Chemother, 1997. **41**(3): p. 715-716.

104. Blazquez, J., M.R. Baquero, R. Canton, I. Alos, and F. Baquero, *Characterization of a new TEM-type beta-lactamase resistant to clavulanate, sulbactam, and tazobactam in a clinical isolate of Escherichia coli*. *Antimicrob. Agents. Chemother*, 1993. **37**(10): p. 2069-2063.
105. Goussard, S. and P. Courvalin, *Updated sequence information for TEM beta-lactamase genes*. *Antimicrob Agents Chemother*, 1999. **43**(2): p. 367-370.
106. X Y Zhou, F Bordon, D Sirot, M D Kitzis, and L. Gutmann, *Emergence of clinical isolates of Escherichia coli producing TEM-1 derivatives or an OXA-1 beta-lactamase conferring resistance to beta-lactamase inhibitors*. *Antimicrob Agents Chemother*, 1994. **38**(5): p. 1085-1089.
107. Chaibi, E.B., J. Péduzzi, S. Farzaneh, M. Barthélémy, D. Sirot, Roger Labia, J. Peduzzi, S. Farzaneh, and M. Barthelemy, *Clinical inhibitor-resistant mutants of the b-lactamase TEM-1 at amino-acid position 69. Kinetic analysis and molecular modelling*. *BBA - Protein Structure and Molecular Enzymology*, 1998. **1382**(1): p. 38-46.
108. Stapleton, P., P.J. Wu, A. King, K. Shannon, G. French, and I. Phillips, *Incidence and mechanisms of resistance to the combination of amoxicillin and clavulanic acid in Escherichia coli*. *Antimicrob. Agents. Chemother*, 1995. **39**(11): p. 2478-2483.
109. Sirot D, Recule C, Chaibi EB, Bret L, Croize J, Chanal-Claris C, Labia R, and S. J, *A complex mutant of TEM-1 beta-lactamase with mutations encountered in both IRT-4 and extended-spectrum TEM-15, produced by an Escherichia coli clinical isolate*. *Antimicrob Agents Chemother*, 1997. **41**(6): p. 1322-1325.
110. Leflon-Guibout, V., V. Speldooren, B. Heym, and M.-H. Nicolas-Chanoine, *Epidemiological Survey of Amoxicillin-Clavulanate Resistance and Corresponding Molecular Mechanisms in Escherichia coli Isolates in France: New Genetic Features of blaTEM Genes*. *Antimicrob Agents Chemother*, 2000. **44**(10): p. 2709-2714.
111. Arpin C, Labia R, Dubois V, Noury P, Souquet M, and Q. C, *TEM-80, a novel inhibitor-resistant beta-lactamase in a clinical isolate of Enterobacter cloacae*. *Antimicrob Agents Chemother*, 2002. **46**(5): p. 1183-1189.
112. Arpin C, Labia R, Andre C, Frigo C, El Harrif Z, and Q. C, *SHV-16, a beta-lactamase with a pentapeptide duplication in the omega loop*. *Antimicrob Agents Chemother*, 2001. **45**(9): p. 2480-2485.

113. Sougakoff, W., S. Goussard, and P. Courvalin, *The TEM-3  $\beta$ -lactamase, which hydrolyzes broad-spectrum cephalosporins, is derived from the TEM-2 penicillinase by two amino acid substitutions*. FEMS Microbiology Letters, 1988. **56**(3): p. 343-348.
114. G C Paul, G Gerbaud, A Bure, A M Philippon, B Pangon, and P. Courvalin, *TEM-4, a new plasmid-mediated beta-lactamase that hydrolyzes broad-spectrum cephalosporins in a clinical isolate of Escherichia coli*. Antimicrob Agents Chemother, 1989. **33**(11): p. 1958-1963.
115. Sougakoff, W., A.Petit, S.Goussard, D.Sirot, A.Burec, and P.Courvalin, *Characterization of the plasmid genes blaT-4 and blaT-5 which encode the broad-spectrum  $\beta$ -lactamases TEM-4 and TEM-5 in Enterobacteriaceae*. Gene, 1989. **78**(2): p. 339-348.
116. A Petit, D L Sirot, C M Chanal, J L Sirot, R Labia, G Gerbaud, and R.A. Cluzel, *Novel plasmid-mediated beta-lactamase in clinical isolates of Klebsiella pneumoniae more resistant to ceftazidime than to other broad-spectrum cephalosporins*. Antimicrob Agents Chemother, 1988. **32**(5): p. 626-630.
117. Bauernfeind, A. and G. Hörl, *Novel R-factor borne  $\beta$ -lactamase of Escherichia coli conferring resistance to cephalosporins*. Infection, 1987. **15**(4): p. 257-259.
118. C, M. and C. P., *Development of "oligotyping" for characterization and molecular epidemiology of TEM beta-lactamases in members of the family Enterobacteriaceae*. Antimicrob Agents Chemother, 1990. **34**(11): p. 2210-2216.
119. Gutmann, L., M.D. Kitzis, D. Billot-Klein, F. Goldstein, G.T.V. Nhieu, T. Lu, J. Carlet, E. Collatz, and R. Williamson, *Plasmid-Mediated  $\beta$ -Lactamase (TEM-7) Involved in Resistance to Cefazidime and Aztreonam* Reviews of Infectious Diseases, 1988. **10**(4): p. 860-866.
120. C M Chanal, D L Sirot, A Petit, R Labia, A Morand, J L Sirot, and R.A. Cluzel, *Multiplicity of TEM-derived beta-lactamases from Klebsiella pneumoniae strains isolated at the same hospital and relationships between the responsible plasmids*. Antimicrob Agents Chemother, 1989. **33**(11): p. 1915-1920.
121. Chanal C, Poupart MC, Sirot D, Labia R, Sirot J, and C. R., *Nucleotide sequences of CAZ-2, CAZ-6, and CAZ-7 beta-lactamase genes*. Antimicrob Agents Chemother, 1992. **36**(9): p. 1817-1820.

122. Spencer RC, Wheat PF, Winstanley TG, Cox DM, and P. SJ, *Novel beta-lactamase in a clinical isolate of Klebsiella pneumoniae conferring unusual resistance to beta-lactam antibiotics*. J Antimicrob Chemother, 1987. **20**(6): p. 919-921.
123. J P Quinn, D Miyashiro, D Sahm, R Flamm, and K. Bush, *Novel plasmid-mediated beta-lactamase (TEM-10) conferring selective resistance to ceftazidime and aztreonam in clinical isolates of Klebsiella pneumoniae*. Antimicrob Agents Chemother, 1989. **33**(9): p. 1451-1456.
124. Rice LB1, Marshall SH, Carias LL, Sutton L, and J. GA, *Sequences of MGH-1, YOU-1, and YOU-2 extended-spectrum beta-lactamase genes*. Antimicrob Agents Chemother, 1993. **37**(12): p. 2760-2761.
125. Vuye A, Verschraegen G, and C. G, *Plasmid-mediated beta-lactamases in clinical isolates of Klebsiella pneumoniae and Escherichia coli resistant to ceftazidime*. Antimicrob Agents Chemother, 1989. **33**(5): p. 757-761.
126. Weber DA1, Sanders CC, Bakken JS, and Q. JP, *A novel chromosomal TEM derivative and alterations in outer membrane proteins together mediate selective ceftazidime resistance in Escherichia coli*. J Infect Dis., 1990. **162**(2): p. 460-465.
127. C Chanal, D.S., H. Malaure, M.C. Poupart, and J. Sirot, *Sequences of CAZ-3 and CTX-2 extended-spectrum beta-lactamase genes*. Antimicrob Agents Chemother, 1994. **38**(10): p. 2452-2453.
128. Agnes Rosenau, Blandine Cattier, N. Gousset, Patrick Harriau, Alain Philippon, and R. Quentin, *Capnocytophaga ochracea: Characterization of a Plasmid-Encoded Extended-Spectrum TEM-17  $\beta$ -Lactamase in the Phylum Flavobacter-Bacteroides*. Antimicrob Agents Chemother, 2000. **44**(3): p. 760-762.
129. Ben Redjeb S, Fournier G, Mabilat C, Ben Hassen A, and P. A, *Two novel transferable extended-spectrum beta-lactamases from Klebsiella pneumoniae in Tunisia*. FEMS Microbiol Lett, 1990. **55**: p. 33-38.
130. Arlet G, Brami G, Décrè D, Flippo A, Gaillot O, Lagrange PH, and P. A, *Molecular characterisation by PCR-restriction fragment length polymorphism of TEM beta-lactamases*. FEMS Microbiol Lett, 1995. **134**: p. 203-208.

131. Arlet G, Goussard S, Courvalin P, and P. A, *Sequences of the genes for the TEM-20, TEM-21, TEM-22, and TEM-29 extended-spectrum beta-lactamases*. Antimicrob Agents Chemother, 1999. **43**(4): p. 969-971.
132. Tessier F, Arpin C, Allery A, and Q. C, *Molecular characterization of a TEM-21 beta-lactamase in a clinical isolate of Morganella morganii*. Antimicrob Agents Chemother, 1998. **42**(8): p. 2125-2127.
133. Arlet G, Rouveau M, Fournier G, Lagrange PH, and P. A, *Novel, plasmid-encoded, TEM-derived extended-spectrum beta-lactamase in Klebsiella pneumoniae conferring higher resistance to aztreonam than to extended-spectrum cephalosporins*. Antimicrob Agents Chemother, 1993. **37**(9): p. 2020-2023.
134. Poupart MC, Chanal C, Sirot D, Labia R, and S. J, *Identification of CTX-2, a novel cefotaximase from a Salmonella mbandaka isolate*. Antimicrob Agents Chemother, 1991. **35**(7): p. 1498-1500.
135. Naumovski L, Quinn JP, Miyashiro D, Patel M, Bush K, Singer SB, Graves D, Palzkill T, and A. AM, *Outbreak of ceftazidime resistance due to a novel extended-spectrum beta-lactamase in isolates from cancer patients*. Antimicrob Agents Chemother, 1992. **36**(9): p. 1991-1996.
136. M I Morosini, R Canton, J Martinez-Beltran, M C Negri, J C Perez-Diaz, F Baquero, and J. Blazquez, *New extended-spectrum TEM-type beta-lactamase from Salmonella enterica subsp. enterica isolated in a nosocomial outbreak*. Antimicrob Agents Chemother, 1995. **39**(2): p. 458-461.
137. P A Bradford, N V Jacobus, N Bhachech, and K. Bush, *TEM-28 from an Escherichia coli clinical isolate is a member of the His-164 family of TEM-1 extended-spectrum beta-lactamases*. Antimicrob Agents Chemother, 1996. **40**(1): p. 260-262.
138. Vedel G, Belaouaj A, Gilly L, Labia R, Philippon A, Nénot P, and P. G, *Clinical isolates of Escherichia coli producing TRI beta-lactamases: novel TEM-enzymes conferring resistance to beta-lactamase inhibitors*. Antimicrob Agents Chemother, 1992. **30**(4): p. 449-462.
139. Belaouaj A, Lapoumeroulie C, Caniça MM, Vedel G, Nénot P, Krishnamoorthy R, and P. G, *Nucleotide sequences of the genes coding for the TEM-like beta-lactamases IRT-1 and IRT-2 (formerly called TRI-1 and TRI-2)*. FEMS Microbiol Lett, 1994. **120**: p. 75-80.

140. Henquell C, Chanal C, Sirot D, Labia R, and S. J, *Molecular characterization of nine different types of mutants among 107 inhibitor-resistant TEM beta-lactamases from clinical isolates of Escherichia coli*. Antimicrob Agents Chemother, 1995. **39**(2): p. 427-430.
141. P Mugnier, P Dubrous, I Casin, G Arlet, and E. Collatz, *A TEM-derived extended-spectrum beta-lactamase in Pseudomonas aeruginosa*. Antimicrob Agents Chemother, 1996. **40**(11): p. 2488-2493.
142. Yang Y, Bhachech N, Bradford PA, Jett BD, Sahm DF, and B. K, *Ceftazidime-resistant Klebsiella pneumoniae and Escherichia coli isolates producing TEM-10 and TEM-43 beta-lactamases from St. Louis, Missouri*. Antimicrob Agents Chemother, 1998. **42**(7): p. 1671-1676.
143. Bret L, Chanal C, Sirot D, Labia R, and S. J, *Characterization of an inhibitor-resistant enzyme IRT-2 derived from TEM-2 beta-lactamase produced by Proteus mirabilis strains*. J Antimicrob Chemother, 1996. **38**(2): p. 183-191.
144. Caniça MM, Barthélémy M, Gilly L, Labia R, Krishnamoorthy R, and P. G, *Properties of IRT-14 (TEM-45), a newly characterized mutant of TEM-type beta-lactamases*. Antimicrob Agents Chemother, 1997. **41**(2): p. 274-278.
145. Gniadkowski M, Schneider I, Jungwirth R, Hryniewicz W, and B. A, *Ceftazidime-resistant Enterobacteriaceae isolates from three Polish hospitals: identification of three novel TEM- and SHV-5-type extended-spectrum beta-lactamases*. Antimicrob Agents Chemother, 1998. **42**(3): p. 514-520.
146. Bret L, Chaibi EB, Chanal-Claris C, Sirot D, Labia R, and S. J, *Inhibitor-resistant TEM (IRT) beta-lactamases with different substitutions at position 244*. Antimicrob Agents Chemother, 1997. **41**(11): p. 2547-2549.
147. Neuwirth C, Labia R, Siebor E, Pechinot A, Madec S, Chaibi EB, and K. A, *Characterization of TEM-56, a novel beta-lactamase produced by a Klebsiella pneumoniae clinical isolate*. Antimicrob Agents Chemother, 2000. **44**(2): p. 453-455.
148. Valérie Speldooren, Beate Heym, Roger Labia, and M.-H. Nicolas-Chanoine, *Discriminatory Detection of Inhibitor-Resistant  $\beta$ -Lactamases in Escherichia coli by Single-Strand Conformation Polymorphism-PCR*. Antimicrob Agents Chemother, 1998. **42**(2): p. 879-884.
149. H. Bermudes, F. Jude, E. B. Chaibi, C. Arpin, C. Bebear, R. Labia, and C. Quentin, *Molecular Characterization of TEM-59 (IRT-17), a Novel Inhibitor-Resistant TEM-Derived  $\beta$ -Lactamase*



- in a Clinical Isolate of *Klebsiella oxytoca*. *Antimicrob Agents Chemother*, 1999. **43**(7): p. 1657–1661.
150. Franceschini N, Perilli M, Segatore B, Setacci D, Amicosante G, Mazzariol A, and C. G, *Ceftazidime and aztreonam resistance in Providencia stuartii: characterization of a natural TEM-derived extended-spectrum beta-lactamase, TEM-60*. *Antimicrob Agents Chemother*, 1998. **42**(6): p. 1459-1462.
  151. Bonnet R, De Champs C, Sirot D, Chanal C, Labia R, and S. J, *Diversity of TEM mutants in Proteus mirabilis*. *Antimicrob Agents Chemother*, 1999. **43**(11): p. 2671-2677.
  152. Thierry Naas, Marie Zerbib, Delphine Girlich, and P. Nordmann, *Integration of a Transposon Tn1-Encoded Inhibitor-Resistant  $\beta$ -Lactamase Gene, blaTEM-67 from Proteus mirabilis, into the Escherichia coli Chromosome*. *Antimicrob Agents Chemother*, 2003. **47**(1): p. 19-26.
  153. Fiett J, Pałucha A, Miaczyńska B, Stankiewicz M, Przondo-Mordarska H, Hryniewicz W, and G. M, *A novel complex mutant beta-lactamase, TEM-68, identified in a Klebsiella pneumoniae isolate from an outbreak of extended-spectrum beta-lactamase-producing Klebsiellae*. *Antimicrob Agents Chemother*, 2000. **44**(6): p. 1499-1505.
  154. Rasheed JK, Anderson GJ, Queenan AM, Biddle JW, Oliver A, Jacoby GA, Bush K, and T. FC, *TEM-71, a novel plasmid-encoded, extended-spectrum beta-lactamase produced by a clinical isolate of Klebsiella pneumoniae*. *Antimicrob Agents Chemother*, 2002. **46**(6): p. 2000-2003.
  155. Perilli M, Segatore B, de Massis MR, Riccio ML, Bianchi C, Zollo A, Rossolini GM, and A. G, *TEM-72, a new extended-spectrum beta-lactamase detected in Proteus mirabilis and Morganella morganii in Italy*. *Antimicrob Agents Chemother*, 2000. **44**(9): p. 2537-2539.
  156. Jean-Denis Docquier, Manuela Benvenuti, Vito Calderone, Gian-Maria Rossolini, and S. Mangani, *Structure of the extended-spectrum  $\beta$ -lactamase TEM-72 inhibited by citrate*. *Acta Crystallogr Sect F Struct Biol Cryst Commun*, 2011. **67**(3): p. 303-306.
  157. Stobberingh EE, Arends J, Hoogkamp-Korstanje JA, Goessens WH, Visser MR, Buiting AG, Debets-Ossenkopp YJ, van Ketel RJ, van Ogtrop ML, Sabbe LJ, Voorn GP, Winter HL, and v.Z. JH, *Occurrence of extended-spectrum betalactamases (ESBL) in Dutch hospitals*. *Infection*, 1999. **27**(6): p. 348-354.

158. Thomas VL, Golemi-Kotra D, Kim C, Vakulenko SB, Mobashery S, and S. BK, *Structural consequences of the inhibitor-resistant Ser130Gly substitution in TEM beta-lactamase*. *Biochemistry*, 2005. **44**(26): p. 9330-9338.
159. Swarén P, Golemi D, Cabantous S, Bulychev A, Maveyraud L, Mobashery S, and S. JP, *X-ray structure of the Asn276Asp variant of the Escherichia coli TEM-1 beta-lactamase: direct observation of electrostatic modulation in resistance to inactivation by clavulanic acid*. *Biochemistry*, 1999. **38**(30): p. 9570-9576.
160. Baraniak A, Fiett J, Mrówka A, Walory J, Hryniewicz W, and G. M, *Evolution of TEM-type extended-spectrum beta-lactamases in clinical Enterobacteriaceae strains in Poland*. *Antimicrob Agents Chemother*, 2005. **49**(5): p. 1872-1880.
161. Perilli M, Segatore B, De Massis MR, Franceschini N, Bianchi C, Rossolini GM, and A. G, *Characterization of a new extended-spectrum beta-lactamase (TEM-87) isolated in Proteus mirabilis during an Italian survey*. *Antimicrob Agents Chemother*, 2002. **46**(3): p. 925-928.
162. Hyunjoo Pai, Hoan-Jong Lee, Eun-Hwa Choi, Jungmin Kim, and G.A. Jacoby, *Evolution of TEM-Related Extended-Spectrum  $\beta$ -Lactamases in Korea*. *Antimicrob Agents Chemother*, 2001. **45**(12): p. 3651-3653.
163. Neuwirth C, Madec S, Siebor E, Pechinot A, Duez JM, Pruneaux M, Fouchereau-Peron M, Kazmierczak A, and L. R, *TEM-89 beta-lactamase produced by a Proteus mirabilis clinical isolate: new complex mutant (CMT 3) with mutations in both TEM-59 (IRT-17) and TEM-3*. *Antimicrob Agents Chemother*, 2001. **45**(12): p. 3591-3594.
164. Pai H and J. GA, *Sequences of the NPS-1 and TLE-1 beta-lactamase genes*. *Antimicrob Agents Chemother*, 2001. **45**(10): p. 2947-2948.
165. Kurokawa H, Shibata N, Doi Y, Shibayama K, Kamachi K, Yagi T, and A. Y, *A new TEM-derived extended-spectrum beta-lactamase (TEM-91) with an R164C substitution at the omega-loop confers ceftazidime resistance*. *Antimicrob Agents Chemother*, 2003. **47**(9): p. 2981-2983.
166. de Champs C, Monne C, Bonnet R, Sougakoff W, Sirot D, Chanal C, and S. J, *New TEM variant (TEM-92) produced by Proteus mirabilis and Providencia stuartii isolates*. *Antimicrob Agents Chemother*, 2001. **45**(4): p. 1278-1280.

167. Briñas L, Zarazaga M, Sáenz Y, Ruiz-Larrea F, and T. C, *Beta-lactamases in ampicillin-resistant Escherichia coli isolates from foods, humans, and healthy animals*. Antimicrob Agents Chemother, 2002. **46**(10): p. 3156-3163.
168. Morris D, O'Hare C, Glennon M, Maher M, Corbett-Feeney G, and C. M, *Extended-spectrum beta-lactamases in Ireland, including a novel enzyme, TEM-102*. Antimicrob Agents Chemother, 2003. **47**(8): p. 2572-2578.
169. Alonso R, Gerbaud G, Galimand M, and C. P, *TEM-103/IRT-28 beta-lactamase, a new TEM variant produced by Escherichia coli BM4511*. Antimicrob Agents Chemother, 2002. **46**(11): p. 3627-3629.
170. Robin F, Delmas J, Chanal C, Sirot D, Sirot J, and B. R, *TEM-109 (CMT-5), a natural complex mutant of TEM-1 beta-lactamase combining the amino acid substitutions of TEM-6 and TEM-33 (IRT-5)*. Antimicrob Agents Chemother, 2005. **49**(11): p. 4443-4447.
171. Aragón LM, Mirelis B, Miró E, Mata C, Gómez L, Rivera A, Coll P, and N. F, *Increase in beta-lactam-resistant Proteus mirabilis strains due to CTX-M- and CMY-type as well as new VEB- and inhibitor-resistant TEM-type beta-lactamases*. J Antimicrob Chemother, 2008. **61**(5): p. 1029-1032.
172. De Champs C, Chanal C, Sirot D, Baraduc R, Romaszko JP, Bonnet R, Plaidy A, Boyer M, Carroy E, Gbadamassi MC, Laluque S, Oules O, Poupart MC, Villemain M, and S. J, *Frequency and diversity of Class A extended-spectrum beta-lactamases in hospitals of the Auvergne, France: a 2 year prospective study*. J Antimicrob Chemother, 2004. **54**(3): p. 634-639.
173. Mulvey MR, Bryce E, Boyd D, Ofner-Agostini M, Christianson S, Simor AE, P. S., Canadian Hospital Epidemiology Committee, and H.C. Canadian Nosocomial Infection Surveillance Program, *Ambler class A extended-spectrum beta-lactamase-producing Escherichia coli and Klebsiella spp. in Canadian hospitals*. Antimicrob Agents Chemother, 2004. **48**(4): p. 1204-1214.
174. Leverstein-van Hall MA, Fluit AC, Paauw A, Box AT, Brisse S, and V. J, *Evaluation of the Etest ESBL and the BD Phoenix, VITEK 1, and VITEK 2 automated instruments for detection of extended-spectrum beta-lactamases in multiresistant Escherichia coli and Klebsiella spp.* J Clin Microbiol, 2002. **40**(10): p. 3703-3711.
175. Poirel L, Mammeri H, and N. P, *TEM-121, a novel complex mutant of TEM-type beta-lactamase from Enterobacter aerogenes*. Antimicrob Agents Chemother, 2004. **48**(12): p. 4528-4531.

176. Kaye KS, Gold HS, Schwaber MJ, Venkataraman L, D.G.P. Qi Y, Samore MH, Anderson G, Rasheed JK, and T. FC, *Variety of beta-lactamases produced by amoxicillin-clavulanate-resistant Escherichia coli isolated in the northeastern United States*. Antimicrob Agents Chemother, 2004. **48**(5): p. 1520-2525.
177. Robin F, Delmas J, Archambaud M, Schweitzer C, Chanal C, and B. R, *CMT-type beta-lactamase TEM-125, an emerging problem for extended-spectrum beta-lactamase detection*. Antimicrob Agents Chemother, 2006. **50**(7): p. 2403-2408.
178. Decré D, Burghoffer B, Gautier V, Petit JC, and A. G, *Outbreak of multi-resistant Klebsiella oxytoca involving strains with extended-spectrum beta-lactamases and strains with extended-spectrum activity of the chromosomal beta-lactamase*. J Antimicrob Chemother, 2004. **54**(5): p. 881-888.
179. Kruger T, Szabo D, Keddy KH, Deeley K, Marsh JW, Hujer AM, Bonomo RA, and P. DL, *Infections with nontyphoidal Salmonella species producing TEM-63 or a novel TEM enzyme, TEM-131, in South Africa*. Antimicrob Agents Chemother, 2004. **48**(11): p. 4263-4270.
180. Martina Zarnayová, Eliane Siebor, André Péchinot, Jean-Marie Duez, Helena Bujdaková, Roger Labia, and C. Neuwirth, *Survey of Enterobacteriaceae Producing Extended-Spectrum  $\beta$ -Lactamases in a Slovak Hospital: Dominance of SHV-2a and Characterization of TEM-132*. Antimicrob Agents Chemother, 2005. **49**(7): p. 3066–3069.
181. Hernández JR, Martínez-Martínez L, Cantón R, Coque TM, P. A., and S.G.f.N.I. (GEIH), *Nationwide study of Escherichia coli and Klebsiella pneumoniae producing extended-spectrum beta-lactamases in Spain*. Antimicrob Agents Chemother, 2005. **49**(5): p. 2122-2125.
182. Perilli M, Mugnaioli C, Luzzaro F, Fiore M, Stefani S, Rossolini GM, and A. G, *Novel TEM-type extended-spectrum beta-lactamase, TEM-134, in a Citrobacter koseri clinical isolate*. Antimicrob Agents Chemother, 2005. **49**(4): p. 1564-1566.
183. Pasquali F, Kehrenberg C, Manfreda G, and S. S, *Physical linkage of Tn3 and part of Tn1721 in a tetracycline and ampicillin resistance plasmid from Salmonella Typhimurium*. J Antimicrob Chemother, 2005. **55**(4): p. 562-565.
184. Bagattini M, Crivaro V, Di Popolo A, Gentile F, Scarcella A, Triassi M, Villari P, and Z. R, *Molecular epidemiology of extended-spectrum beta-lactamase-producing Klebsiella pneumoniae in a neonatal intensive care unit*. J Antimicrob Chemother, 2006. **57**(5): p. 979-982.

185. Agnes Lefort, Guillaume Arlet, Olivier F. Join-Lambert, Marc Lecuit, and O. Lortholary, *Novel Extended-spectrum  $\beta$ -Lactamase in Shigella sonnei*. *Emerg Infect Dis*, 2007. **13**(4): p. 653–654.
186. Chedly Chouchani, Renaud Berlemont, Afef Masmoudi, Moreno Galleni, Jean-Marie Frere, Omrane Belhadj, and K. Ben-Mahrez, *A Novel Extended-Spectrum TEM-Type  $\beta$ -Lactamase, TEM-138, from Salmonella enterica Serovar Infantis*. *Antimicrob Agents Chemother*, 2006. **50**(9): p. 3183–3185.
187. Schneider I, Markovska R, Keuleyan E, Sredkova M, Rachkova K, Mitov I, and B. A, *Dissemination and persistence of a plasmid-mediated TEM-3-like beta-lactamase, TEM-139, among Enterobacteriaceae in Bulgaria*. *Int J Antimicrob Agents*, 2007. **29**(6): p. 710-714.
188. Vignoli R, Cordeiro NF, García V, Mota MI, Betancor L, Power P, Chabalgoity JA, Schelotto F, Gutkind G, and A. JA, *New TEM-derived extended-spectrum beta-lactamase and its genomic context in plasmids from Salmonella enterica serovar derby isolates from Uruguay*. *Antimicrob Agents Chemother*, 2006. **50**(2): p. 781-784.
189. Perilli M, Celenza G, De Santis F, Pellegrini C, Forcella C, Rossolini GM, Stefani S, and A. G, *E240V substitution increases catalytic efficiency toward ceftazidime in a new natural TEM-type extended-spectrum beta-lactamase, TEM-149, from Enterobacter aerogenes and Serratia marcescens clinical isolates*. *Antimicrob Agents Chemother*, 2008. **52**(3): p. 915-919.
190. Robin F, Delmas J, Schweitzer C, Tournilhac O, Lesens O, Chanal C, and B. R, *Evolution of TEM-type enzymes: biochemical and genetic characterization of two new complex mutant TEM enzymes, TEM-151 and TEM-152, from a single patient*. *Antimicrob Agents Chemother*, 2007. **51**(4): p. 1304-1309.
191. Machado E, Coque TM, Cantón R, Novais A, Sousa JC, Baquero F, P. L., and P.R.S. Group, *High diversity of extended-spectrum  $\beta$ -lactamases among clinical isolates of Enterobacteriaceae from Portugal*. *J Antimicrob Chemother*, 2007. **60**(6): p. 1370-1374.
192. Jones CH, Ruzin A, Tuckman M, Visalli MA, Petersen PJ, and B. PA, *Pyrosequencing using the single-nucleotide polymorphism protocol for rapid determination of TEM- and SHV-type extended-spectrum  $\beta$ -lactamases in clinical isolates and identification of the novel  $\beta$ -lactamase genes blaSHV-48, blaSHV-105, and blaTEM-155*. *Antimicrob Agents Chemother*, 2009. **53**(3): p. 977-986.

193. Frédéric Robin, Julien Delmas, Amélie Brebion, Damien Dubois, Jean-Michel Constantin, and R. Bonnet, *TEM-158 (CMT-9), a new member of the CMT-type extended-spectrum  $\beta$ -lactamases*. *Antimicrob Agents Chemother*, 2007. **51**(11): p. 4181-4183.
194. Ben Achour N, Mercuri PS, Ben Moussa M, Galleni M, and B. O, *Characterization of a novel extended-spectrum TEM-type  $\beta$ -lactamase, TEM-164, in a clinical strain of Klebsiella pneumoniae in Tunisia*. *Microb Drug Resist*, 2009. **15**(3): p. 195-199.
195. Mulvey MR and B. DA, *TEM-168, a heretofore laboratory-derived TEM  $\beta$ -lactamase variant found in an Escherichia coli clinical isolate*. *Antimicrob Agents Chemother*, 2009. **53**(11): p. 4955-4956.
196. Adler A, Baraniak A, Izdebski R, Fiett J, Gniadkowski M, Hryniewicz W, Salvia A, Rossini A, Goossens H, Malhotra S, Lerman Y, Elenbogen M, C. Y., and M.W.W.s. groups, *A binational cohort study of intestinal colonization with ESBL-producing Proteus mirabilis in patients admitted to rehabilitation centers*. *Clinical Microbiology and Infection*, 2013. **19**(2): p. E51-E58.
197. Perilli M, Felici A, Franceschini N, De Santis A, Pagani L, Luzzaro F, Oratore A, Rossolini GM, Knox JR, and A. G, *Characterization of a new TEM-derived  $\beta$ -lactamase produced in a Serratia marcescens strain*. *Antimicrob Agents Chemother*, 1997. **41**(11): p. 2371-2382.
198. Shaheen BW, Nayak R, Foley SL, Kweon O, Deck J, Park M, Rafii F, and B. DM, *Molecular characterization of resistance to extended-spectrum cephalosporins in clinical Escherichia coli isolates from companion animals in the United States*. *Antimicrob Agents Chemother*, 2011. **55**(12): p. 5666-5675.
199. Geser N, Stephan R, and H. H, *Occurrence and characteristics of extended spectrum beta-lactamase (ESBL) producing Enterobacteriaceae in food producing animals, minced meat and raw milk*. *BMC Vet Res*, 2012. **8**(21).
200. Corvec S, Beyrouthy R, Crémet L, Aubin GG, Robin F, Bonnet R, and R. A, *TEM-187. a new extended-spectrum beta-lactamase with weak activity in a Proteus mirabilis clinical strain*. *Antimicrob Agents Chemother*, 2013. **57**(5): p. 2410-2412.
201. Bradford, P.A., *Automated thermal cycling is superior to traditional methods for nucleotide sequencing of blaSHV genes*. *Antimicrob Agents Chemother*, 1999. **43**(12): p. 2960-2963.

202. Nukaga M, Mayama K, Hujer AM, Bonomo RA, and K. JR, *Ultra-high resolution structure of a class A beta-lactamase: on the mechanism and specificity of the extended-spectrum SHV-2 enzyme*. J Mol Biol, 2003. **328**(1): p. 289-301.
203. Podbielski A, Schönling J, Melzer B, Warnatz K, and L. HG, *Molecular characterization of a new plasmid-encoded SHV-type  $\beta$ -lactamase (SHV-2 variant) conferring high-level cefotaxime resistance upon Klebsiella pneumoniae*. J Gen Microbiol, 1991. **137**(3): p. 569-578.
204. M H Nicolas, V Jarlier, N Honore, A Philippon, and S.T. Cole, *Molecular characterization of the gene encoding SHV-3  $\beta$ -lactamase responsible for transferable cefotaxime resistance in clinical isolates of Klebsiella pneumoniae*. Antimicrob Agents Chemother, 1989. **33**(12): p. 2096-2100.
205. Péduzzi J, Barthélémy M, Tiwari K, Mattioni D, and L. R, *Structural features related to hydrolytic activity against ceftazidime of plasmid-mediated SHV-type CAZ-5  $\beta$ -lactamase*. Antimicrob Agents Chemother, 1989. **33**(12): p. 2160-2163.
206. Gutmann L, Ferré B, Goldstein FW, Rizk N, Pinto-Schuster E, Acar JF, and C. E, *SHV-5, a novel SHV-type beta-lactamase that hydrolyzes broad-spectrum cephalosporins and monobactams*. Antimicrob Agents Chemother, 1989. **33**(6): p. 951-956.
207. Arlet G, Rouveau M, and P. A, *Substitution of alanine for aspartate at position 179 in the SHV-6 extended-spectrum  $\beta$ -lactamase*. FEMS Microbiol Lett, 1997. **152**(1): p. 163-167.
208. Bradford PA, Urban C, Jaiswal A, Mariano N, Rasmussen BA, Projan SJ, Rahal JJ, and B. K, *SHV-7, a novel cefotaxime-hydrolyzing  $\beta$ -lactamase, identified in Escherichia coli isolated from hospitalized nursing home patients*. Antimicrob Agents Chemother, 1995. **39**(4): p. 899-905.
209. Rasheed JK, Jay C, Metchock B, Berkowitz F, Weigel L, Crellin J, Steward C, Hill B, Medeiros AA, and T. FC, *Evolution of extended-spectrum  $\beta$ -lactam resistance (SHV-8) in a strain of Escherichia coli during multiple episodes of bacteremia*. Antimicrob Agents Chemother, 1997. **41**(3): p. 647-653.
210. Prinarakis EE, Tzelepi E, Gazouli M, Mentis AF, and T. LS, *Characterization of a novel SHV  $\beta$ -lactamase variant that resembles the SHV-5 enzyme*. FEMS Microbiol Lett, 1996. **139**(2-3): p. 229-234.

211. Prinarakis EE, Miriagou V, Tzelepi E, Gazouli M, and T. LS, *Emergence of an inhibitor-resistant  $\beta$ -lactamase (SHV-10) derived from an SHV-5 variant*. *Antimicrob Agents Chemother*, 1997. **41**(4): p. 838-840.
212. Nüesch-Inderbinen MT and H.H. Kayser FH, *Survey and molecular genetics of SHV  $\beta$ -lactamases in Enterobacteriaceae in Switzerland: two novel enzymes, SHV-11 and SHV-12*. *Antimicrob. Agents Chemother*, 1997. **41**(5): p. 943-949.
213. Yuan M, Hall LM, Savelkoul PH, Vandenbroucke-Grauls CM, and L. DM, *SHV-13, a novel extended-spectrum  $\beta$ -lactamase, in Klebsiella pneumoniae isolates from patients in an intensive care unit in Amsterdam*. *Antimicrob Agents Chemother*, 2000. **44**(4): p. 1081-1084.
214. Yuan M, Hall LM, Hoogkamp-Korstanje J, and L. DM, *SHV-14, a novel  $\beta$ -lactamase variant in Klebsiella pneumoniae form Nijmegen, The Netherlands*. *Antimicrob Agents Chemother*, 2001. **45**(1): p. 309-311.
215. Rasheed JK, Anderson GJ, Yigit H, Queenan AM, Doménech-Sánchez A, Swenson JM, Biddle JW, Ferraro MJ, Jacoby GA, and T. FC, *Characterization of the extended-spectrum  $\beta$ -lactamase reference strain, Klebsiella pneumoniae K6 (ATCC 700603), which produces the novel enzyme SHV-18*. *Antimicrob Agents Chemother*, 2000. **44**(9): p. 2382-2388.
216. Essack SY, Hall LM, and L. DM, *Klebsiella pneumoniae isolate from South Africa with multiple TEM, SHV and AmpC  $\beta$ -lactamases*. *Int J Antimicrob Agents*, 2004. **23**(4): p. 398-400.
217. Kurokawa H, Yagi T, Shibata N, Shibayama K, Kamachi K, and A. Y., *A new SHV-derived extended-spectrum  $\beta$ -lactamase (SHV-24) that hydrolyzed ceftazidime through a single-amino-acid substitution (D179G) in the omega-loop*. *Antimicrob Agents Chemother*, 2000. **44**(6): p. 1725-1727.
218. Chang FY, Siu LK, Fung CP, Huang MH, and H. M, *Diversity of SHV and TEM beta-lactamases in Klebsiella pneumoniae: gene evolution in Northern Taiwan and two novel beta-lactamases, SHV-25 and SHV-26*. *Antimicrob Agents Chemother*, 2001. **45**(9): p. 2407-2413.
219. Yigit H, Queenan AM, Anderson GJ, Domenech-Sanchez A, Biddle JW, Steward CD, Alberti S, Bush K, and T. FC, *Novel carbapenem-hydrolyzing  $\beta$ -lactamase KPC-I, from a carbapenem-resistant strain of Klebsiella pneumoniae*. *Antimicrob Agents Chemother*, 2001. **45**(4): p. 1151-1161.



220. Dóra Szabó, Melissa A. Melan, Andrea M. Hujer, Robert A. Bonomo, Kristine M. Hujer, Christopher R. Bethel, Katalin Kristóf, and D.L. Paterson, *Molecular analysis of the simultaneous production of two SHV-type extended-spectrum beta-lactamases in a clinical isolate of Enterobacter cloacae by using single-nucleotide polymorphism genotyping*. Antimicrob Agents Chemother, 2005. **49**(11): p. 4716–4720.
221. Mazzariol A, Roelofsen E, Koncan R, Voss A, and C. G, *Detection of a new SHV-type extended-spectrum  $\beta$ -lactamase, SHV-31, in a Klebsiella pneumoniae strain causing a large nosocomial outbreak in The Netherlands*. Antimicrob Agents Chemother, 2007. **51**(3): p. 1082-1084.
222. Chaves J, Ladona MG, Segura C, Coira A, Reig R, and A. C, *SHV-1  $\beta$ -lactamase is mainly a chromosomally encoded species-specific enzyme in Klebsiella pneumoniae*. Antimicrob Agents Chemother, 2001. **45**(10): p. 2856-2861.
223. Heritage J, Chambers PA, Tyndall C, and B. ES, *SHV-34: an extended-spectrum  $\beta$ -lactamase encoded by an epidemic plasmid*. J Antimicrob Chemother, 2003. **52**(6): p. 1015-1017.
224. Poirel L, Héritier C, Podglajen I, Sougakoff W, Gutmann L, and N. P, *Emergence in Klebsiella pneumoniae of a chromosome-encoded SHV  $\beta$ -lactamase that compromises the efficacy of imipenem*. . Antimicrob Agents Chemother, 2003. **47**(2): p. 755-758.
225. Wang H, Kelkar S, Wu W, Chen M, and Q. JP, *Clinical isolates of Enterobacteriaceae producing extended-spectrum  $\beta$ -lactamases: prevalence of CTX-M-3 at a hospital in China*. Antimicrob Agents Chemother, 2003. **47**(2): p. 790-793.
226. Arpin C, Dubois V, Coulange L, André C, Fischer I, Noury P, Grobost F, Brochet JP, Jullin J, Dutilh B, Larribet G, Lagrange I, and Q. C, *Extended-spectrum  $\beta$ -lactamase-producing Enterobacteriaceae in community and private health care centers*. Antimicrob Agents Chemother, 2003. **47**(11): p. 3506-3514.
227. Yigit H, Queenan AM, Rasheed JK, Biddle JW, Domenech-Sanchez A, Alberti S, Bush K, and T. FC, *Carbapenem-resistant strain of Klebsiella oxytoca harboring carbapenem-hydrolyzing  $\beta$ -lactamase KPC-2*. Antimicrob Agents Chemother, 2003. **47**(12): p. 3881-3889.
228. Dubois V, Poirel L, Arpin C, Coulange L, Bebear C, Nordmann P, and Q. C, *SHV-49, a novel inhibitor-resistant  $\beta$ -lactamase in a clinical isolate of Klebsiella pneumoniae*. Antimicrob Agents Chemother, 2004. **48**(11): p. 4466-4469.

229. Mendonça N, Ferreira E, and C. M, *Occurrence of a novel SHV-type enzyme (SHV-55) among isolates of Klebsiella pneumoniae from Portuguese origin in a comparison study for extended-spectrum  $\beta$ -lactamase-producing evaluation*. Diagn Microbiol Infect Dis, 2006. **56**(4): p. 415-420.
230. Dubois V, Poirel L, Demarthe F, Arpin C, Coulange L, Minarini LA, Beziau MC, Nordmann P, and Q. C, *Molecular and biochemical characterization of SHV-56, a novel inhibitor-resistant  $\beta$ -lactamase from Klebsiella pneumoniae*. Antimicrob Agents Chemother, 2008. **52**(10): p. 3792-3794.
231. Ma L, Alba J, Chang FY, Ishiguro M, Yamaguchi K, Siu LK, and I. Y, *Novel SHV-derived extended-spectrum  $\beta$ -lactamase, SHV-57, that confers resistance to ceftazidime but not ceftazolin*. Antimicrob Agents Chemother, 2005. **49**(2): p. 600-605.
232. Mendonça, N., E. Ferreira, D. Louro, A. Participants, and M. Caniça, *Molecular epidemiology and antimicrobial susceptibility of extended- and broad-spectrum  $\beta$ -lactamase-producing Klebsiella pneumoniae isolated in Portugal*. Int J Antimicrob Agents, 2009. **34**(1): p. 29-37.
233. Ling BD, Liu G, Xie YE, Zhou QX, Zhao TK, Li CQ, Yu X, and L. J, *Characterization of a novel extended-spectrum  $\beta$ -lactamase, SHV-70, from a clinical isolate of Enterobacter cloacae in China*. Int J Antimicrob Agents, 2006. **27**(4): p. 355-356.
234. de Oliveira Garcia D, Doi Y, Szabo D, Adams-Haduch JM, Vaz TM, Leite D, Padoveze MC, Freire MP, Silveira FP, and P. DL, *Multiclonal outbreak of Klebsiella pneumoniae producing extended-spectrum  $\beta$ -lactamase CTX-M-2 and novel variant CTX-M-59 in a neonatal intensive care unit in Brazil*. Antimicrob Agents Chemother, 2008. **52**(5): p. 1790-1793.
235. Li JB, Cheng J, Wang Q, Chen Y, Ye Y, and Z. XJ, *A novel SHV-type  $\beta$ -lactamase variant (SHV-89) in clinical isolates in China*. Mol Bio Rep, 2009. **36**(5): p. 1141-1148.
236. Lavilla S, González-López JJ, Sabaté M, García-Fernández A, Larrosa MN, Bartolomé RM, Carattoli A, and P. G, *Prevalence of qnr genes among extended-spectrum  $\beta$ -lactamase-producing enterobacterial isolates in Barcelona, Spain*. J Antimicrob Chemother, 2008. **61**(2): p. 291-295.
237. Nadjia Ramdani-Bouguessa, Vera Manageiro, Daniela Jones-Dias, Eugénia Ferreira, Mohamed Tazir, and M. Caniça, *Role of SHV  $\beta$ -lactamase variants in resistance of clinical Klebsiella pneumoniae strains to  $\beta$ -lactams in an Algerian hospital*. J Med Microbiol, 2011. **60**(7): p. 983-987.

238. Brasme L, Nordmann P, Fidel F, Lartigue MF, Bajolet O, Poirel L, Forte D, Vernet-Garnier V, Madoux J, Reveil JC, Alba-Sauviat C, Baudinat I, Bineau P, Bouquigny-Saison C, Eloy C, Lafaurie C, Siméon D, Verquin JP, Noël F, Strady C, and D.C. C, *Incidence of class A extended-spectrum  $\beta$ -lactamases in Champagne-Ardenne (France): a 1 year prospective study*. J Antimicrob Chemother, 2007. **60**(5): p. 956-964.
239. Vinué L, Lantero M, Sáenz Y, Somalo S, de Diego I, Pérez F, Ruiz-Larrea F, Zarazaga M, and T. C, *Characterization of extended-spectrum  $\beta$ -lactamases and integrons in Escherichia coli isolates in a Spanish hospital*. J Med Microbiol, 2008. **57**(7): p. 916-920.
240. Abbassi MS, Torres C, Achour W, Vinué L, Sáenz Y, Costa D, Bouchami O, and B.H. A, *Genetic characterisation of CTX-M-15-producing Klebsiella pneumoniae and Escherichia coli strains isolated from stem cell transplant patients in Tunisia*. Int J Antimicrob Agents, 2008. **32**(4): p. 308-314.
241. Zong Z, Partridge SR, Thomas L, and I. JR, *Dominance of blaCTX-M within an Australian extended-spectrum  $\beta$ -lactamase gene pool*. Antimicrob Agents Chemother, 2008. **52**(11): p. 4198-4202.
242. Hammad AM, Ishida Y, and S. T, *Prevalence and molecular characterization of ampicillin-resistant Enterobacteriaceae isolated from traditional Egyptian Domiati cheese*. J Food Prot, 2009. **72**(3): p. 624-630.
243. Lascols C, Hackel M, Hujer AM, Marshall SH, Bouchillon SK, Hoban DJ, Hawser SP, Badal RE, and B. RA, *Using nucleic acid microarrays to perform molecular epidemiology and detect novel  $\beta$ -lactamases: a snapshot of extended-spectrum  $\beta$ -lactamases throughout the world*. J Clin Microbiol, 2012. **50**(5): p. 1632-1639.
244. An S, Chen J, Wang Z, Wang X, Yan X, Li J, Chen Y, Wang Q, Xu X, Li J, Yang J, Wang H, and G. Z, *Predominant characteristics of CTX-M-producing Klebsiella pneumoniae isolates from patients with lower respiratory tract infection in multiple medical centers in China*. FEMS Microbiol Lett, 2012. **332**(2): p. 137-145.
245. Castanheira M, Farrell SE, Deshpande LM, Mendes RE, and J. RN, *Prevalence of Beta-Lactamase-Encoding Genes among Enterobacteriaceae Bacteremia Isolates Collected in 26 U.S. Hospitals: Report from the SENTRY Antimicrobial Surveillance Program*. Antimicrob Agents Chemother, 2013. **57**(7): p. 3012-3020.

246. Datta S, Mitra S, Viswanathan R, Saha A, and B. S, *Characterization of novel plasmid-mediated beta-lactamases (SHV-167) and ACT-16 associated with New Delhi Metallo-beta-lactamase 1-harboring isolates from neonates in India.* J Med Microbiol, 2014. **63**(3): p. 480-482.
247. Gilliane Guillaume, Marc Vanhove, Josette Lamotte-Brasseur, Philippe Ledent, Marc Jamin, Bernard Joris, and J.-M. Fre`re, *Site-directed Mutagenesis of Glutamate 166 in Two  $\beta$ -Lactamases.* J Biol Chem., 1997. **272**(9): p. 5438–5444.
248. R M Gibson, H Christensen, and S.G. Waley, *Site-directed mutagenesis of beta-lactamase I. Single and double mutants of Glu-166 and Lys-73.* Biochem J., 1990. **272**(3): p. 613–619.
249. Strynadka NCJ, Adachi H, Jensen SE, Johns K, Sielecki A, Betzel C, Sutoh K, and J. MNG, *Molecular structure of the acyl-enzyme intermediate in  $\beta$ -lactam hydrolysis at 1.7 Å resolution.* Nature, 1992. **359**: p. 700-705.
250. Knox JR, Moews PC, Escobar WA, and F. AL., *A catalytically-impaired class A beta-lactamase: 2 A crystal structure and kinetics of the Bacillus licheniformis E166A mutant.* Protein Eng., 1993. **6**(1): p. 11-18.
251. Samy O. Meroueh, Jed F. Fisher, H. Bernhard Schlegel, and S. Mobashery, *Ab Initio QM/MM Study of Class A b-Lactamase Acylation: Dual Participation of Glu166 and Lys73 in a Concerted Base Promotion of Ser70.* J. Am. Chem. Soc., 2005. **127**: p. 15397-15407.

## ACKNOWLEDGEMENTS

First and foremost, I would like to express my deepest appreciation to my supervisor, Prof. Sung Haeng Lee, Doctor of Philosophy, who has taught me the science, given me the inspiration in the research, conducted and advised me to complete this dissertation. The most important lesson I have learned from Him is the invaluable perception of how to become a true scientist.

My dissertation would not be completed without the considerations and reviews from the Committee of my dissertation defense, therefore,

I would like to thank Prof. Bang Iel Soo, Chairman of Committee, who has considered and straightly given the critical comments to improve my dissertation.

I would like to thank Prof. Changwook Lee, Member of Committee, who has considered and traveled a long way to attend my dissertation defense, and given me the valuable comments for structural analysis.

I would like to thank Prof. Eunae Kim, Member of Committee, who has considered and given me precious pieces of advice about the molecular dynamics simulation data.

I would like to thank Prof. Kwangho Nam, Member of Committee, who though could not attend my dissertation defense, yet has considered and advised me for the analysis of enzyme kinetics and molecular dynamics simulation data, and warmly given me valuable comments to improve my writing.

Furthermore, I would like to thank Dr. Jin Myung Choi, my senior, for his teaching and helping when we worked together in our lab. I would like to thank Dr. Immanuel Dhanasingh, who has been working with me for five years. He helped me to the final presentation with his excellent skills.

I would like to thank my friends, Võ Thị Phương Huyền and Jung Sung Kim, who helped me to read and translate the abstract in Korean version. A special thanks to my friend, Nguyễn Duy Quang, who gave me his precious time in my final defense.

My family, my wife and my daughters, and our parents are where I always can find my happiness and motivations for all my efforts.

## DEDICATION

To

My wife, Nguyễn Thị Đài Trang, to her sacrifices in this hard life for my  
achievements,

And to

The future of our beloved daughter, Cao Nhật Tuệ.